

The Role of the Substantia Nigra in Goal Directed Behavior

by

Joseph William Barter

Department of Psychology and Neuroscience

Duke University

Date: \_\_\_\_\_

Approved:

\_\_\_\_\_  
Henry H. Yin, Supervisor

\_\_\_\_\_  
Staci D. Bilbo

\_\_\_\_\_  
Elizabeth M. Brannon

\_\_\_\_\_  
Marc A. Sommer

Dissertation submitted in partial fulfillment of  
the requirements for the degree of Doctor  
of Philosophy in the Department of  
Psychology and Neuroscience in the Graduate School  
of Duke University

2015

ABSTRACT

The Role of the Substantia Nigra in Goal Directed Behavior

by

Joseph William Barter

Department of Psychology and Neuroscience

Duke University

Date: \_\_\_\_\_

Approved:

\_\_\_\_\_  
Henry H. Yin, Supervisor

\_\_\_\_\_  
Staci D. Bilbo

\_\_\_\_\_  
Elizabeth M. Brannon

\_\_\_\_\_  
Marc A. Sommer

Dissertation submitted in partial fulfillment of  
the requirements for the degree of Doctor  
of Philosophy in the Department of  
Psychology and Neuroscience in the Graduate School  
of Duke University

2015

Copyright by  
Joseph William Barter  
2015

## **Abstract**

Animals must continuously move through the environment in pursuit of the goals required to maintain homeostasis. In vertebrates, this is accomplished through an ever-changing pattern of muscle contraction in a complex body, and coordinated by a hierarchy of neural circuits acting in parallel. At the lower levels of this hierarchy, spinal circuits control muscle force and length. One level above that, brainstem, midbrain and cortical circuits control various aspects of body configuration as well as a number of self-contained motor functions including locomotion and orientation. A still-higher level of organization is controlled by the basal ganglia, a set of subcortical nuclei that appear to be responsible for continuously orchestrating the extent and direction of various motor programs and body configurations for the sake of controlling a still higher level of perceptual variable, such as proximity to food. In this way, the basal ganglia orchestrate the performance of motor functions to achieve a single goal in the same way that a conductor orchestrates the performance of musicians in a symphony to achieve a single song.

Despite the continuous and graded nature of animal behavior, researchers have traditionally studied the basal ganglia in the context of highly controlled experimental tasks or neglected to record continuous measures of behavioral outputs. To address this gap, the following experiments were designed investigate role of the basal ganglia in continuously modulating unconstrained goal directed movements. In the first set of

experiments (chapter 2), mice stood on a small covered perch which was continuously tipped left and right along the roll plane while neural activity was recorded wirelessly. During each recording session, mice were exposed to slow and fast speeds of postural disturbance. Pressure pads were mounted in the left and right floor of the perch to monitor mouse movement. In both putative dopamine and GABA neurons, we found two basic patterns of neural activity; one class of cell increased firing with tip to the left and decreased with tip to the right while the other class decreased firing with tip to the left and increased with tip to right. This correlation between neural firing rate and instantaneous postural disturbance is continuous and very high. The correlation is seen for both slow and fast disturbances. The majority of cells recorded fell into one of these two categories. Pressure pad readout, as expected, revealed paw forces on the left pad to increase with tilt to the left and decrease with tilt to the right while the opposite pattern was observed on the right pad. These results show continuous and graded modulation of activity in the substantia nigra during performance of an ongoing motor task and suggest that BG outputs, rather than monolithically disinhibiting brainstem motor structures, instead coordinate behavior by continuously specifying desired states of lower motor systems.

In the second set of experiments (chapter 3), we employed continuous motion tracking of the head in parallel with neural recording from the substantia nigra pars reticulata during a simple goal-directed task. In this study, mice were water deprived and then positioned on a perch equipped with a movable drinking spout. During each

session, mice performed a simple reward-guided task in which sucrose solution was delivered in small quantities after the presentation a cue. The purpose of this task was to elicit voluntary head movements and to investigate the continuous relationship between these movements and the activity of GABA output neurons.

A typical reward-directed behavior involved the movement of the whole head and body to collect the sucrose solution following its delivery. However, movements during each individual trial were unique. For all movements, the majority of GABA cells were found to either positively or negatively correlate with either X or Y axis vector components of head position. These correlations were very high, and not due to averaging artifacts as trial-by-trial correlation between movement and neural activity can be clearly observed. These correlations were also independent of the presence of a reward. These data show for the first time a continuous and quantitative relationship between basal ganglia output and body posture. It is hypothesized that these signals represent reference signals sent to downstream postural and orientation controllers. In this case a baseline level of GABA activity would represent neutral reference position, and changes in activity above and below this level represent increased or decreased reference positions.

In the third set of experiments (chapter 4), we recorded from dopamine neurons in the substantia nigra pars compacta during the same task as in chapter 3. The purpose of this task was to investigate the correlation between dopamine activity and movement kinematics during goal-directed behavior. Animals were found to produce

movements at the onset of the cue and also at reward delivery. Dopamine-classified cells show phasic firing or pausing at the onset of each of these movements. When compared to head movement kinematics, these patterns of neural activity correlate highly with different vector components of head acceleration and velocity; up, down, left and right. Importantly, these correlations are continuous and exist throughout the entire recording session. These correlations are also independent of the presence of reward. To test the 'causality' of these observed patterns, we also employed optogenetics to stimulate substantia nigra dopamine neurons expressing channelrhodopsin 2 (Chr2) while head movements were recorded and quantified. We found that stimulation of Chr2-expressing animals could elicit head movement while stimulation of control animals had no effect. Combined, these data suggest that dopamine is responsible for controlling the velocity of transitions between different body postures.

## **Dedication**

This thesis is dedicated to William T. Powers

August 29, 1926-May 23, 2013

## Contents

Abstract.....	iv
List of Tables .....	xiv
List of Figures .....	xv
1. Introduction .....	1
1.1. Homeostasis and motor behavior.....	1
1.1.1. Motor behavior and homeostatic control .....	2
1.2. Motor coordination and the basal ganglia .....	4
1.3. Review of basic motor functions .....	5
1.3.1. Control of locomotor rhythm and joint angle by central pattern generators .....	5
1.3.2. Brainstem control of central pattern generator circuits .....	7
1.3.2.1. Control of locomotor speed.....	9
1.3.2.2. Control of turning .....	9
1.3.2.3. Control of posture.....	10
1.3.3. Descending control of reticulospinal system.....	12
1.3.3.1. Brainstem locomotor regions .....	13
1.3.3.2. Tectum .....	14
1.3.3.3. Pedunculopontine nucleus .....	15
1.3.3.4. Motor cortex.....	16
1.3.4. The importance of the basal ganglia.....	17
1.4. Functional anatomy of the basal ganglia .....	18
1.4.1. Outputs of the basal ganglia .....	19
1.4.2. Inputs of the basal ganglia .....	20
1.4.3. Intrinsic connections of the basal ganglia.....	21
1.4.4. Thalamic closed loops.....	23
1.5. Movement disorders of the basal ganglia .....	24
1.5.1. Hypokinetic disorders: Parkinson's disease .....	25
1.5.2. Hyperkinetic disorders: Huntington's .....	26
1.6. Open questions regarding the functions of the basal ganglia .....	27
1.6.1. Graded modulation of basal ganglia output.....	27

1.6.2. Antiphase signaling of basal ganglia outputs.....	28
1.6.3. Reward prediction and motor control .....	28
1.6.4. Summary of experiments.....	30
2. The Role of the Substantia Nigra in Posture Control .....	31
2.1. Introduction .....	31
2.2. Materials and Methods.....	33
2.2.1. Subjects and Surgery.....	33
2.2.2. Behavioral Apparatus.....	35
2.2.3. Recording and spike sorting.....	39
2.2.4. Classifying single units .....	39
2.2.5. Data analysis .....	40
2.3. Results.....	40
2.3.1. Postural disturbance and behavior.....	40
2.3.2. Neural correlates of postural disturbance.....	43
2.4. Discussion.....	48
2.4.1. Summary .....	48
2.4.2. Reticulospinal cells and postural control .....	49
2.4.3. Closed loop control of posture .....	50
2.4.4. DA-GABA interactions .....	54
2.4.5. Classical model in need of revision.....	55
3. Basal ganglia outputs map instantaneous position coordinates during behavior .....	57
3.1. Introduction .....	57
3.2. Materials and Methods.....	59
3.2.1. Subjects and Surgery.....	59
3.2.2. Behavioral task.....	60
3.2.3. Video tracking .....	63
3.2.4. Neural recording and data analysis .....	64
3.3. Results.....	65
3.3.1. Histology and single unit classification of putative GABAergic neurons .....	65
3.3.2. Behavior .....	65

3.3.3. Neural activity reflects position coordinates .....	66
3.3.4. Normalization of neural activity .....	71
3.3.5. Dissociation from reward expectancy .....	71
3.3.6. Topographical distribution.....	74
3.3.7. Egocentric reference frame and movement direction .....	77
3.4. Discussion.....	78
3.4.1. Summary .....	78
3.4.2. Problems with current models of BG function .....	79
3.4.3. The meaning of transition control .....	88
3.4.4. The basal ganglia and transition control.....	91
3.4.5. Significance .....	94
4. Beyond Reward Prediction Errors: the Role of Dopamine in Movement Kinematics .....	95
4.1. Introduction .....	95
4.2. Methods.....	97
4.2.1. Subjects.....	97
4.2.2. Behavior .....	97
4.2.3. Neural recording and data analysis .....	100
4.2.4. Kinematic variables .....	101
4.2.5. Optogenetic stimulation .....	102
4.3. Results.....	104
4.3.1. Video tracking .....	104
4.3.2. Classification of DA neurons .....	104
4.3.3. Correlation between DA activity and kinematics .....	105
4.3.4. Appetitive vs. aversive behavioral tasks .....	110
4.3.5. Summary of correlation analysis.....	111
4.3.6. Lateralization of the DA response.....	111
4.3.7. Optogenetic stimulation of DA neurons .....	113
4.3.8. Comparing DA and GABA neurons.....	115
4.4. Discussion.....	120
4.4.1. Summary .....	120

4.4.2. Caveats.....	125
4.4.3. Reward prediction error .....	127
4.4.4. Nigrostriatal DA and direction specificity .....	129
4.4.5. Transition control.....	130
4.4.6. Above transition control .....	135
4.4.7. Control of input.....	137
4.4.8. DA and adaptive gain control.....	138
4.4.9. Relationship between BG output and DA activity .....	139
4.4.10. Clinical implications .....	142
4.4.11. Implications for motor control.....	144
4.4.12. Rewards and other goals .....	145
4.4.13. Conclusions .....	148
5. General Discussion.....	150
5.1. Summary .....	150
5.1.1. Summary, Chapter 2 .....	150
5.1.2. Summary, Chapter 3 .....	151
5.1.3. Summary, Chapter 4 .....	153
5.2. The role of BG in behavior .....	154
5.3. Control of sensory input .....	154
5.3.1. Motor control as control of sensory input.....	156
5.3.2. Goal directed behavior as control of sensory input.....	157
5.4. Model of the motor control hierarchy.....	159
5.4.1. Muscle force control .....	160
5.4.2. Muscle length control .....	161
5.4.3. Body configuration control .....	163
5.4.4. Transition control.....	165
5.4.5. Control of higher sensory variables .....	166
5.4.6. Learning.....	168
5.5. The role of SN in behavior.....	169
5.6. Limitations and future directions .....	171

References .....	173
Biography .....	188

## List of Tables

Table 1. Summary of different types of dopamine neurons.....	123
--	-----

## List of Figures

Figure 1. Apparatus for generating postural disturbance and illustration of in vivo wireless multi-electrode recording in freely behaving mice. (A) Miniaturized 16 channel wireless headstage (1.5x1 x 1.5cm) weighing about 3.8 g. (B) Illustration of the postural disturbance task. Up to 7 degrees of tilt were introduced in either direction along the roll axis of the mouse. (C) A mouse perched on an elevated tilting platform housed in a tube. The layout of the perch prevented mice from moving excessively or changing orientation while still allowing free standing postural adjustment and head movement. (D) Pressure pad readout traces during continuous postural disturbance of 30rpm. Data show overlay of 44 individual session averages. Forces on the left (red) and right (blue) pressure pads were generated by contact with the mouse's left and right paws, respectively. Time 0 on the x-axis indicates the point of the greatest disturbance to the left (7 degrees tilting to the left side); times -2 and +2s show the point of greatest disturbance to the right. At time 0 the force exerted by the left paws on the left pressure pad is greatest and force exerted by the right paws on the right pressure pad is least; at times -2 and +2 the opposite pattern can be seen. (E) Pressure pad readout (Z score) traces during continuous postural disturbance of 60rpm. Traces are from the same sessions shown in D. Time 0 indicates the point of the greatest disturbance to the left (7 degrees tilting to the left side); times -1 and +1 show the point of greatest disturbance to the right. The same basic pattern shown in D may also be seen here. (F) Pressure pad readout (Z score) during rest, in the absence of any tilt. Traces are from same sessions shown in D and E and represent peri-event averages around arbitrary points spaced 2s apart. No clear pattern of force change is demonstrated. Grooming behavior was often observed during this period.....34

Figure 2. Classification of GABA and DA neurons. (A) Representative spike waveform recorded with wireless technology, with a high signal-to-noise ratio. Three examples of typical action waveforms are shown for each cell type. The duration of action potentials in GABA neurons is much shorter than in DA neurons (Ungless and Grace, 2012). (B) Cell type classification. Putative DA neurons (red) have significantly wider waveforms. FWHM, full width half maximum (spike duration at half maximum). DA neurons have lower mean firing rate ( $7.8 \pm 0.92$  Hz,  $n=62$ ) than putative GABA neurons ( $19 \pm 0.94$  Hz,  $n=427$ ).....36

Figure 3. Coronal sections showing the location of electrode implants for all mice. Scale bars 0.5 mm.....38

Figure 4. Representative neural activity during postural disturbances. (A) Pattern of postural disturbance (B) GABA neuron activity throughout the slow tilt cycle (15 tilts to each side/minute). Top plot shows L+R- cell; bottom plot shows L-R+ cell. (C) Activity of the same cells shown to the left during the fast tilt cycle (30 tilts to each side/minute).

(D) Dopamine neuron activity during the slow tilt cycle. Top plot is L+R-; bottom plot is L-R+. (E) Activity of the same cells shown to the left during the fast tilt cycle.....41

Figure 5. Left substantia nigra summary. Spike density functions and averages of cell populations recorded from the substantia nigra whose activity was significantly correlated with tilt disturbance. Left column of all plots shows peri-tilt activity during 30rpm disturbance (15 tilts/side/minute). Right column shows activity during 60rpm disturbance (30 tilts/side/minute). Top spike density function of each pair shows L-R+ cells; bottom heatmap shows L+R- cells. Blue trace in each population average plot shows average firing of L-R+ cells shown in above heatmaps; red trace shows average firing of L+R- cells shown in above heatmaps. All plots are normalized by z-score (number of standard deviations from the mean). (A) Pattern of postural disturbance. (B) Spike density functions of peri-tilt activity in GABA neurons. (C) Population averages of peri-tilt activity in GABA neurons. (D) Spike density functions of peri-tilt activity in DA neurons. (E) Population averages of peri-tilt activity in DA neurons.....42

Figure 6. Relationship between mean firing rate and tilt angle in different populations of neurons. For each mouse, units significantly modulated by tilt were used in a regression analysis. For a mouse with sufficient number of recorded units, the mean firing rate of each population of dopamine '+' and '-', and GABA '+' and '-' units was calculated, and the coefficient of determination ( $R^2$  value) was calculated between tilt disturbance and mean firing rate. Each graph shows the line of best fit between tilt and firing rate in a given population. The corresponding colored dots show the mean firing rate of that population for different angles of tilt. For all regression analyses shown,  $P < 0.05$ . The corresponding  $R^2$  value is shown. (A) L+R- neurons. (B) L-R+ neurons.....46

Figure 7. Relationship between mean firing rate and pressure pad readings in different populations of neurons. For each mouse, units significantly modulated by tilt were used in a regression analysis. In two mice, the coefficient of determination ( $R^2$  value) was calculated between the pressure pad reading and mean firing rate in a representative session. The corresponding colored dots show the mean firing rate of that population at different angles of tilt. For all regression analyses shown,  $P < 0.05$ .....47

Figure 8. A hypothetical orientation control hierarchy showing how two axes of postural control can share the same motor output. Green arrows represent perceptual inputs; blue arrows represent output reference signals; red arrows represent error signals. (A) Level 4 of the control hierarchy. There are two systems at this level; one for roll control and one for pitch control. (B) Level 3. There are two systems at this level; one for controlling the foot pressure difference between the left and the right side of the body and one for controlling the front-back difference. Perceptual inputs to these systems are derived from perceptual inputs from systems at level 1. Outputs to lower systems

represent the difference between reference signal and perceptual signal, sign switched so that the outputs are produced in the correct direction. (C) Level 2. There are 4 systems at this level; one controlling foot pressure at each individual foot. Each system receives a reference signal from both systems at level 2, which are added together. (D) Level 1. There are 4 systems at this level; one controlling perceived leg extension at each individual leg. Each system receives a reference signal from both the food pressure control system for the same leg.....53

Figure 9. *In vivo* electrophysiological recording and classification of single units. (A) Illustration of the representative placement of electrode array in the SNr. (B) Placement of the 4x4 electrode array as shown in representative coronal brain sections from three different mice. Red arrows indicate electrode tracks. Scale bar, 500µm. (C) Summary of electrode placements. The coronal sections are from the Allen Mouse Brain Atlas (Lein et al., 2007); <http://mouse.brain-map.org/>. (D) Four representative examples of putative GABAergic neurons, showing the waveforms and interspike interval distribution. (E) Plot of firing rate versus spike width. Neurons with wider action potentials are excluded (other).....61

Figure 10. Illustration of behavioral task and wireless recording. (A) Illustration of *in vivo* wireless multielectrode recording and the behavioral task. The mouse perches on a small platform, where it is free to move, but locomotion is not possible as the platform is elevated. On its head is a 16-channel wireless headstage (1.5 x 1.5cm) weighing 3.8g and connected to a chronically implanted multielectrode array targeting the SNr. Sucrose solution is delivered into the spout periodically, preceded by a brief tone. Position of the LED is defined on a Cartesian plot with the ordered pair (x, y). (B) Illustration of variability in movement trajectory. Each color represents position change during a single trial. (C) Diagram illustration of a typical movement initiated by the mouse to collect sucrose from the spout. (D) Representative illustration of LED position from 45 consecutive trials in a session. The x and y-coordinates are plotted separately.....62

Figure 11. Relationship between single-unit activity from SNr and raw position coordinates during movement. (A) The firing rate of SNr neurons exhibits high correlation with instantaneous position coordinates. The position is defined from the edge of the frame in the captured image. Higher x-coordinate values indicate positions to the left of the resting neutral position, whereas lower x-values indicate positions to the right. In each of the four panels, red raster plots and histograms illustrate the activity of a single neuron; blue plots illustrate the corresponding x or y-axis head position of the animal during the same session, as measured with LED tracking. The cartoon sequence at the bottom of each panel depicts the head movement. All plots are centered around reward delivery, which is marked with a light blue bar. The top left

panel shows a neuron with positive correlation with x-coordinates of the head (X+ neuron,  $p < 0.001$ ).; top right panel shows a neuron whose activity correlates positively with the y-coordinate of the head (Y+ neuron,  $p < 0.001$ ); bottom left shows a negative correlation with x-position (X- neuron,  $p < 0.001$ ); bottom right shows a negative correlation with y-position (Y- neuron,  $p < 0.001$ ). (B) Correlation between firing rate and instantaneous position coordinates.....67

Figure 12. Summary of different types of nigral neurons. (A) r values for the four types of neurons identified, showing high correlation between firing rate and either x or y-coordinate. (B) r values for the four types of neurons identified, showing much reduced correlation between firing rate and the alternative coordinate. For example, activity of X neurons is poorly correlated with the y-coordinate. C, Baseline firing rate during a 2s period before trial onset. (D) Timing of the neural activity (all four classes of neurons) in relation to movement. Cumulative probability distribution of the time it takes from reward delivery and the maximum or minimum value of the firing rates or position coordinates. For the position data, this is approximately the time it takes for the mouse to reach the farthest point from its resting position in either the x or y-axis.....68

Figure 13. Summary of baseline neural activity and movement. (A) Stability of position measure and firing rate. We extracted 10s time windows during rest periods from all sessions. The position signal and the neural activity are shown. There is no systematic change in these measures during the rest period over the course of a session. (B) Coefficient of variation (CV,  $SD/mean$ ) in the position measure during a trial and during the rest period. During the rest period between trials, there is little movement as indicated by much lower CV values in the position. (C) Correlation between firing rate and during the rest period, when there is little movement.....73

Figure 14. Normalization of firing rates in SNr neurons. (A) Each row includes raw firing rates and normalized firing rates from two neurons, and corresponding position change from a different mouse. Left column: raw firing rates of two neurons of a given type from a mouse. Middle column: normalized firing rates of the same neurons. The rates are normalized by dividing by the baseline rate of each neuron. Right column: position change. The relative change in position from baseline is shown, as absolute position values are defined by the edge of the camera frame. (B) The range of baseline firing rates in neurons from the four different classes. Each graph represents the range of baseline firing rates from a single session. Data from all mice with multiple neurons from a class are shown. There is considerable variability in baseline firing rates, although the correlation with position coordinates is highly similar. (C) Distribution of firing rate modulation (% of baseline) per millimeter. Most neurons show comparable degree of modulation relative to movement amplitude.....75

Figure 15. Relationship between firing rate and Cartesian coordinates is similar for both reward and air puff trials. (A) Left: firing rate of a Y+ neuron in relation to air puff/reward. The activity of the same neuron from both types of trials is shown. Right: example movement trajectory for air puff and reward trials. The correlation between neural activity and Cartesian coordinates is high on both sucrose reward trials and air puff trials. (B) Firing rate of a Y- neuron. Same as above. (C) Distribution of r values of all neurons recorded during both reward and air puff trials.....76

Figure 16. Single-unit activity from a single electrode compared with LFP signal from the same electrode. (A) Probability of co-occurring neurons recorded from the same electrode. (B) Illustration of the per-reward change in x and y-coordinates during a single session. (C) From the same session, 2 X+ neurons and 2 Y- neurons are shown with their waveforms. All cells show high correlation with position coordinates. Correlation analysis is performed on data from a 10s perireward time window (5s before and 5s after reward delivery). (D) LFP recorded from the same electrode as X cell #1. Correlation between LFP and position coordinates is much weaker. (E) The distribution of r values for all the recorded LFP channels. Of the 166 LFP channels analyzed, only 15 showed significant correlation with position coordinates (colored,  $p < 0.001$ ). Thus, when activity is summed from different types of neurons, the resulting correlation between neural activity and position is weaker. The relatively rare examples of LFP being highly correlated with position coordinates suggest that neurons belonging to a particular class (e.g., X+) might be located close to each other.....80

Figure 17. Schematic illustration of different types of neurons. (A) Illustration of hypothetical mouse movement in relation to the neural activity. The firing rates of the four types of neurons are shown. For this hypothetical example, 1 spike/s is equal to 1 unit of change in x or y-coordinate. The units are arbitrary. The starting position is (9, 9). (B) The mouse moves to its left and up. The LED position changes to (11, 11). (C) Right, The mouse moves to a new position (6, 7). Relative to its start position, the change is (3,2). (D) Schematic illustration of the relationship between neural activity in relation to movements in four directions. The illustration of neural activity does not represent actual data because we did not record all four types of neurons from a single animal during a session. Opponent activity was observed during movement in any direction. For example, Y+ (Up) neurons increase their activity during upward movements and decrease their activity during downward movements. The opposite is true of Y- (Down) neurons.....81

Figure 18. Left + (X+) neuron increases firing during leftward movement and decreases firing during rightward movement. (A) Detailed illustration of the correlation between firing rate and x-coordinates on a trial-by-trial basis. Neural activity and x-coordinates

from 10 consecutive trials are shown. Each row represents a single trial. (B) Neural and position data from a single trial are selected and compared. x-axis position changes during each movement are reflected in the firing rate of this neuron. The mouse moves to the right to consume sucrose. The activity of the neuron decreased during the rightward movement and then increased when the mouse moves left again to recover its initial starting position. (C) Average firing rate changes and changes in different movement parameters. In this example, the y-component of the movement is much smaller. The plots on the right show velocity and acceleration data for the same movements. (D) Using an egocentric reference frame, the direction of firing rate changes corresponds to the direction of movement. There was a positive correlation between neural activity and position change in a leftward direction ( $r=0.99$ ,  $p<0.001$ ). The correlation with the non-preferred Cartesian axis is also shown. The diagram on the right shows the gradient of firing rate in relation to position coordinates.....82

Figure 19. Right (X-) neuron increases firing during rightward movement and decreases firing during leftward movement. (A) Detailed illustration of the correlation between firing rate and x-coordinates on a trial-by-trial basis. Neural activity and x-coordinates from 9 consecutive trials are shown. Each row represents a single trial. (B) Neural and position data from a single trial are selected and compared. x-axis position changes during each movement are reflected in the firing rate of this neuron. (C) Average firing rate changes and changes in different movement parameters. The plots on the right show velocity and acceleration data for the same movements. (D) Using an egocentric reference frame, the direction of firing rate changes corresponds to the direction of movement. There was therefore a negative correlation between firing rate and raw x-coordinate value but a positive correlation between firing rate and distance in the rightward direction ( $p<0.001$ ). The correlation with the non-preferred Cartesian axis is also shown. The diagram on the right shows the gradient of firing rate in relation to position coordinates.....83

Figure 20. Up (Y+) neuron increases firing during upward movement and decreases firing during downward movement. (A) Detailed illustration of the correlation between firing rate and y-coordinates on a trial-by-trial basis. Neural activity and y-coordinates from 10 consecutive trials are shown. Each row represents a single trial. (B) Neural and position data from a single trial are selected and compared. (C) Average firing rate changes and changes in different movement parameters. The plots on the right show velocity and acceleration data for the same movements. (D) There is a positive correlation between firing rate and y-coordinates and distance in the upward direction ( $p<0.001$ ). Using an egocentric reference frame, the direction of firing rate changes corresponds to the direction of movement. The correlation with the non-preferred Cartesian axis is also shown. The diagram on the right shows the gradient of firing rate in relation to position coordinates.....84

Figure 21. Down(Y-) neuron increases firing during downward movement and decreases firing during upward movement. (A) Detailed illustration of the correlation between firing rate and y-coordinates on a trial-by-trial basis. Neural activity and y-coordinates from 10 consecutive trials are shown. Each row represents a single trial. (B) Neural and position data from a single trial are selected and compared. (C) Average firing rate changes and changes in different movement parameters. The plots on the right show velocity and acceleration data for the same movements. (D) Using an egocentric reference frame, the direction of firing rate changes corresponds to the direction of movement ( $p < 0.001$ ). There was therefore a negative correlation between firing rate and raw y-coordinate value but a positive correlation between firing rate and distance in the downward direction ( $p < 0.001$ ). The correlation with the nonpreferred Cartesian axis is also shown. In this case, the correlation with distance traveled in the leftward direction is also high because the movement is nearly diagonal, so that the x and y-position changes are similar. However, the correlation with y is still considerably higher, and trial-by-trial examination of the data confirms that this neuron is selective for the y component of the position vector. The diagram on the right shows the gradient of firing rate in relation to position coordinates.....85

Figure 22. Hypothetical BG circuit. SNr neurons receive projections from the striatum and external globus pallidus, via the direct (D, striatonigral) and indirect (I, striatopallidal) pathways. Although these projections are GABAergic, the net effect on the SNr can be either inhibitory or excitatory (disinhibitory), since changes can occur above or below baseline firing rate. In this model, outputs from both direct and indirect pathways of the striatum represent velocity error signals which are integrated in the SNr to generate a position reference signal. This SNr integrator is assumed to be leaky. Similar to reciprocal inhibition in the spinal cord, the proposed circuit generates opponent outputs for movement in any direction. Here we show an x and a y head position controller but in principle a similar circuit could underlie position control of any joint. The functional significance of this reciprocal innervation is to allow movements in both directions; without it—as with two muscles at a joint—the system could move quickly in one direction but not in the other. The striatum, especially the sensorimotor region, is hypothesized to contain at least four different modules, each responsible for movement in a specific direction. Because z-axis motion has not been measured, only four directions are illustrated here. Two of the four vector components are associated with any movement (e.g., upward and rightward), as movements usually have both horizontal and vertical components. The total output (number of spikes) from a particular striatal module represents the magnitude of the isolated position vector component, and the firing rate represents velocity (Kim et al., 2014). Using the outputs from different vector component modules, this circuit can perform vector addition to generate the resultant movement vector.....86

Figure 23. Illustration of a hierarchical ‘x-axis’ orientation control system with an output function consisting of two muscles. A-D comprise a schematic showing a perceptual control hierarchy with perceptual inputs in green, error signals in red and reference signals in blue. (A) Transition control. This is the level of the basal ganglia. The x-orientation reference signal is generated by output of ‘X+’ and ‘X-’ neurons of the SNr. (B) Configuration control. This level is controlled by brainstem motor regions and motor cortex via the pyramidal tract. (C) Muscle length control by the spinal cord. (D) Muscle force control by the spinal cord. (E) Diagram showing the relationship between muscle length and bend along the x-axis of the spinal joint.....92

Figure 24. Behavior and video tracking in unrestrained mice. (A) Mice perched on an elevated platform housed in a tube, wearing a miniaturized 16 channel wireless headstage (~3.8g). The camera (not shown) is facing the animal. (B) Illustration of movement trajectory. The mouse starts to move following presentation of the cue (CS), and moves again following the presentation of the reward (US, 13µl 20% sucrose solution). Each color illustrates the path on a single trial, showing variability from trial to trial. (C) Illustration of the Pavlovian trace conditioning task used (Barter et al., 2015). (D) Cartoon illustration of the movements. Top row illustrates movement toward the spout; bottom row illustrates movement back to the starting position. (E) Illustration of movement tracked by the head LED. Pressure pads were placed underneath the animal, so that changes in pressure exerted by the hind paws can be measured. Pressure pad measures as well as video tracking of the tail demonstrate that the movements were not restricted to the head. Position coordinates are mm from frame edge.....99

Figure 25. Identification of DA neurons in the substantia nigra. (A) Classification of a putative DA neuron and a non-DA neuron using principal component analysis (PCA). (B) Representative waveforms of putative DA neurons. (C) Summary of electrode placements shown in coronal brain sections take from the Allen Brain Atlas (Lein et al., 2006). (D) Average firing rate and spike width (FWHM, full width at half maximum) of putative DA neurons and non-DA neurons. DA neurons are characterized by lower firing rates and wider spike widths (unpaired t-tests,  $p < 0.0001$ ).....100

Figure 26. “Burst” DA neurons show positive correlation with kinematic variables. (A) Firing rate of representative neuron showing positive correlation with vector components of velocity and acceleration. Two major movements are detected during the trial, one in response to the cue and the other in response to reward delivery. These are displayed separately. “Velocity up” means velocity in the upward direction. Blue arrows indicate movement direction, but note that only the vector components are indicated. Actual movements would consist of both x and y-components. The correlation analysis uses data displayed in the raster plots below. A 1s peri-event

window (either cue or reward) was used. (B) Peri-event raster plots of the neurons and the correlated kinematic variables. (C) The major alternative kinematic variables are shown. These are not highly correlated with neural activity as determined by our unbiased cross-correlation analysis.....106

Figure 27. “Pause” DA neurons is negative correlated with kinematic variables. (A) Firing rate of representative neuron showing negative correlation with vector components of velocity and acceleration. Two major movements are detected during the trial, one in response to the cue and the other in response to reward delivery. These are displayed separately. (B) Peri-event raster plots of the neurons and the correlated kinematic variables. (C) The major alternative kinematic variables are shown.....107

Figure 28. Continuous correlation between neural activity and kinematics. Illustration of a representative neuron and its correlation with kinematics independent of task-related events such as cue and reward. To dissociate kinematic variables from these task events. Rather than selecting only data from the trial, we performed an unbiased correlation between firing rate and the kinematic variables for the entire session, including inter-trial-intervals. This unbiased analysis was used to classify the neurons.....108

Figure 29. Selectivity of DA responses. To illustrate the direction selectivity of DA neurons, we compared the session-wide cross-correlation between neural activity and velocity in opposite directions. Shown are two examples in which the cell is positive correlated with movement in one direction and negatively correlated with movement in the opposite direction. This pattern is similar to what we observed previously in SNr GABAergic output neurons (Barter et al., 2015).....112

Figure 30. Correlation between firing rate and acceleration is similar on appetitive (sucrose reward) and aversive (air puff) trials. (A) An example of a positively correlated DA neuron on reward trials. The red line represents average movement trajectory from the session. (B) The same neuron on air puff trials. Note that the actual trajectories differed significantly between reward and air puff trials, but the upward components of velocity are similar, as shown here. (C) An example of a negatively correlated DA neuron on reward trials. (D) The same neuron on air puff trials.....116

Figure 31. Population data for DA neurons on rewarded and air puff trials. (A) Different classes of DA neurons show comparable firing rates. (B) Using cross correlation analysis, we also found the lag is much longer for negatively correlated neurons, suggesting that, in these neurons, a pause in firing precedes some movement. (C) The proportion of positively and negatively correlated neurons is similar for aversive and rewarding sessions.....117

Figure 32. Lateralization of direction-specific neurons. Among velocity-related DA neurons, there are more rightward neurons in the left nigra, and more leftward neurons in the right nigra. There was no significant lateralization among acceleration-related neurons, though the sample size is much smaller.....117

Figure 33. Expression of channelrhodopsin 2 in dopamine neurons in Th::Ai32mice. (A) Locations of bilateral optic fibers based on histological verification of coronal brain slices. Representative GFP fluorescence, indicating ChR2 expression, is co localized with TH in the substantia nigra of Th::Ai32transgenic mice. Scale bar is 50 $\mu$ m (upper panels). Lower panels are zoomed in images from the box shown in the upper right panel (scale bar 5 $\mu$ m). (B) GFP fluorescence is absent in Th-Cre control mice. Same conventions as A. (C) Optic fiber placements for Th::Ai32(n=4; blackcircles) or Th-Cre (n=3; yellow circles) mice. Atlas images are from the Allen Brain Atlas (Lein et al., 2006). Available from: <http://mouse.brain-map.org/>.....118

Figure 34. Optogenetic stimulation of DA neurons can elicit movements.(A) To mimic burst firing of DA neurons, we selectively stimulated DA neurons using optogenetics. We generated a transgenic mouse line (Th-Cre $\times$ Ai32) to selectively express ChR2 in DA (tyrosine hydroxylase-positive) neurons. A brief stimulation at 40Hz (3ms pulse width,5 pulses) generated movement, in the ChR2 (Th::Ai32) mouse but not in a control mouse (Th-Cre) that also received the same light stimulation. Control mice were implanted with fibers and stimulated using identical procedures. Red trace represents movement trajectory. (B) Peak speed and distance forChR2 (Th::Ai32) and control (Th-Cre) mice.\*p<0.05. (C) Left, movement kinematics plotted for different stimulation frequencies(11, 15, and 25Hz,3ms pulse width, 1 s duration. (D) Peak speed during stimulation train and distance traveled (at the end of the train) at different stimulation frequencies.\*p<0.05.....119

Figure 35. Detailed movement kinematics during optogenetic stimulation. (A) Representative horizontal (x) and vertical (y) components of the movements in a control mouse (Th-Cre). Position, velocity, and acceleration are plotted separately. Red traces show movement trajectories produced by the stimulation. (B) Representative data from a Th::Ai32 mouse.....120

Figure 36. Comparison of putative nigral GABA and DA neurons from the same electrode array. (A) The activity of the GABA neuron reflects y-position coordinates, an example of representation of instantaneous position coordinates reported in our recent study (Barter et al., 2015). The activity of DA neuron reflects velocity in the upward direction. If we take the derivative of the GABA output, we can generate a mirror image of the DA activity. This result, then, is in support of disinhibition: the reduction in GABA output is

accompanied by an increase in DA firing. Note that these projections are mostly collaterals of fibers terminating in other areas such as the tectum and thalamus. Cross-correlogram shows the relationship between DA firing and the derivative of the GABA output from the entire session.(B) Another example illustrating the relationship between DA and GABA neurons from a different mouse.....124

Figure 37. Proposed model for DA modulation of striatal outputs. (A) SNr neurons receive projections from the striatum and external globus pallidus, via the direct (D, striatonigral) and indirect (I, striatopallidal) pathways. The net effect on the SNr could be either inhibitory (minus sign) or excitatory (disinhibitory, plus sign). Both types of signals represent velocity error signals from the velocity controller. The dorsal striatum is hypothesized to contain at least four different modules, each responsible for movement in a specific direction. Striatal neurons can signal velocity error signals (Kim et al.,2014), which is integrated by the SNr and converted into position reference signal to position controllers in the midbrain and diencephalon (Barter et al.,2015). Using the outputs from the different modules, this circuit can perform vector addition to generate the actual movement vector. The magnitude of the signal entering the integrator is proportional to the rate of change in the integrator output. (B) Illustration of activity in the BG circuit, using a square pulse to represent a transient burst of action potentials with constant firing rate from striatal projection neurons. Dotted lines indicate altered firing rates as a result of DA modulation. DA is known to exert opposite effects on striatonigral neurons and striatopallidal neurons. Striatonigral neurons, which express D1 receptors, are increased by D1 activation, whereas striatopallidal neurons are inhibited by D2 activation(Gerfen and Surmeier, 2011).Moreover, activation of D1 receptors can also potentiate GABA release at the striatonigral terminals (Chuhma et al., 2011), whereas activation of D2receptors can reduce GABA release at the pallidonigral terminals (Connelly et al., 2010; de Jesús Aceves et al., 2011). The net effect is consistent for the targets of SNr output. DA modulation has the net effect of potentiating the firing rate in a given position vector component, and further suppressing the antagonistic component. By increasing the rate of change in the position reference, the actual movement velocity is increased. As shown, both movement amplitude and speed are altered, but these variables can be independently controlled.....132

Figure 38. Model of cascade control hierarchy for velocity and position control of a single joint angle. The velocity control system is hierarchically higher than the position control system. There are multiple position controllers, including those for orientation and body configuration, which can command hierarchically lower controllers for joint angle, muscle length, and muscle tension (not shown here). The lowest level is the tension or force controller, with alpha motor neurons acting as the comparator and muscles as the output function (Yin, 2014a).....133

## **Acknowledgements**

This work was made possible with the help of guidance of many people. I thank the members of my thesis committee, Staci Bilbo, Marc Sommer and Elizabeth Brannon.

I also thank the past and present members of the Yin Lab at Duke University. In no particular order I thank Mark Rossi, Haofang Li, Kara Clissold, C. Tyler Shoemaker, Ryan Bartholomew, Nam Soo Kim, Vlad and Yedema Hayrapetyan, Chunxiu Yu, David Fan, Tatyana Sukharnikova, Erin Gaidis, Suellen Li, Daniel Salas-Meza and Dongye Lu. Without their countless hours of help none of this work would have been possible.

Finally, I thank my mentor, Henry Yin, for his tireless guidance, support and friendship. I am truly honored and extremely lucky to have had the opportunity to work with him during these past five years. There is nowhere else I would have rather been. The perspective that Henry has shared with me has changed my life, and I have no doubt that it will change the world.

# **1. Introduction**

## **1.1. Homeostasis and motor behavior**

A defining property of living things is that they actively defend their internal stability against a changing and unpredictable environment. When this internal stability is challenged by some changing environmental condition, energy-requiring protective mechanisms work to oppose the effects of that change. This state of internal stability is called homeostasis (Cannon, 1935), and the process of defending it is called homeostatic control.

Homeostatic control consists of the regulation a large number of interdependent internal variables including temperature, water, oxygen, energy stores, and physical integrity (Cannon, 1935). Depending on the species, these variables can be regulated through a diverse set of functions. For example, when exposed to cold temperature a mammal may contract surface blood vessels to reduce exposure of warm blood, increase metabolic activity, or shiver (Cannon, 1935). But the most generalizable and effective of functions for defending internal stability is motor behavior; rather than remaining stationary and being forced to defend against disturbances from a single spot, organisms with the capacity for movement can quickly improve their surrounding environment by moving through it.

In single-celled organisms this strategy is ubiquitous. Bacteria move constantly through the environment; seeking nutrients and avoiding injury by detecting relevant

chemical gradients and controlling patterns of rotation in flagella anchored to the cell membrane in such a way as to move up favorable gradients and down noxious gradients (Manson, 1998). Other single-celled organisms such as protozoa exhibit similar but even more complex motor behaviors owing to their relatively more elaborate sensory systems (Naitoh, 1974; Swanson, 2003). However, in multicellular organisms, motor behavior is a significantly more complex problem because it requires the fast coordination of a large body of individual cells. Of all multicellular organisms, this capacity is only found in animals and requires a nervous system, whose essential function is fast communication between cells. Several properties of neurons make them especially good at this task; they are sensitive, they communicate rapidly and over a long range, and their inputs and outputs are spatially restricted so that they can be highly localized at relevant parts of the body (Swanson, 2003). In vertebrates, the motor function of the nervous system is clearly evident in its basic architecture; a head with a condensation of specialized sensors pointed in the direction of movement contains the brain, which projects a nerve cord into the body for commanding muscles (Swanson, 2003).

### **1.1.1. Motor behavior and homeostatic control**

In computational terms, homeostatic regulation constitutes a biological negative feedback control system, continuously sensing deviations in variables from desired

levels and producing corrective outputs (Woods et al., 1998). First discovered in the 1930s (Black, 1934), tellingly, as a method to replace human operators of simple output systems, negative feedback control systems have three essential parts; an input function capable of sensing the environmental variable to be controlled, a comparator function which compares the perceived value with an internally specified reference value to calculate the error between them, and an output function which amplifies the error and turns it into a proportional command signal to an effector capable of acting through the environment to reduce the error (Powers, 1973). To use the classic example of a thermostat; the input function measures the current room temperature, the comparator function compares the current room temperature to the reference room temperature or 'set point' and generates an error, and the output function amplifies that error and, depending its sign, uses it as a command signal to engage either the air-conditioner or furnace proportionately to the error. A properly functioning thermostat holds the room constant at the reference temperature.

Thus, a more precise way to frame motor behavior is as the output function of a biological control system; in the same way that a thermostat adjusts outputs in a furnace or air-conditioner to control sensed room temperature; the brain adjusts outputs in the motor system to control internally sensed homeostatic variables. For example, an animal may move through space to pursue food as a means of regulating blood glucose, or to pursue warmth as a means of regulating body temperature. However, unlike temperature control by a thermostat in which errors are reduced

simply by increasing and decreasing monolithic output signals to dedicated heating and cooling devices, homeostatic control in an animal requires that certain errors be transformed into extremely complex and dynamic patterns of muscle output in a multipurpose body.

## **1.2. Motor coordination and the basal ganglia**

An animal must continuously achieve the changing goals that add up to homeostasis; a hungry animal must seek food and a cold animal must seek warmth, or else it will likely die. In an ever-changing environment the outputs required to achieve these goals must also change; the paths of escape taken by a prey animals, the exact distribution of food in the environment, and the terrain are all constantly changing and require constant adaptation of motor output if the animal is to remain successful. Thus, motor behavior consists of an ever-changing set of active motor functions, which are themselves continuously varying in extent and direction. Certain motor functions, such as locomotion and postural control, must occur together. Certain other motor functions, such as turning and forward-locomotion, can both occur at once or in close sequence without either one failing entirely. Certain other motor functions such as approach and escape, or forwards and backwards locomotion are completely incompatible. Motor functions can also occur with different intensities, such as speed of locomotion and degree of turning, which can affect the degree of conflict between them. An important

task of higher brain structures is therefore to coordinate the identities, directions and relative intensities of ongoing motor functions to minimize conflict while maximizing overall effectiveness in pursuit of a higher goal. The basal ganglia (BG), a set of subcortical nuclei which lie just above the brainstem are thought to be important in accomplishing this task.

### **1.3. Review of basic motor functions**

In order to understand the role of the BG in coordinating motor functions, it is first necessary to have an understanding of the motor functions themselves. In the following section, we review some of the most basic and common motor functions and their neural substrates: locomotion, postural control and orientation.

#### **1.3.1. Control of locomotor rhythm and joint angle by central pattern generators**

Locomotion is characterized by rhythmic patterns of whole body movement driven by underlying patterns of muscle contraction and relaxation. Animals may swim, crawl, hop, walk or fly at different speeds and through different media, but a common feature of all of these movements is their rhythmicity (Alexander, 2003). Neuronal circuits known as central pattern generators (CPGs) are responsible for producing the patterns of muscle contraction underlying locomotor movements (Delcomyn, 1980).

GPGs may also be employed non-rhythmically as simple joint-angle controllers, such as during turns and postural corrections (Fagerstedt and Ullen, 2001).

Some of the most well characterized CPGs are those of the lamprey, an order of eel-like jawless fish with all of the basic features of the mammalian nervous system but with orders of magnitude fewer cells (Grillner et al., 1995). Lamprey swimming is characterized by a lateral bending wave which travels anterior to posterior and pushes the animal forward in the water. This bending wave is produced by the sequential activation of 100 different segments along the length of body (Grillner and Wallen, 2002). Each segment contains a coupled oscillator circuit composed of two reciprocally inhibiting burst generators, each of which causes contraction of ipsilateral muscles when activated. Oscillation in the circuit therefore causes rhythmic left-right bending in the body segment, while stable activation of one burst generator causes stable bending of the body segment to one side. Sensory feedback from stretch receptors with contralateral inhibitory projections is thought to be important for coordinating the sequential activation of neighboring segments into a whole-body bending wave (Tresch and Kiehn, 2000), and in adapting muscle output to environmental conditions through forms of negative feedback (Ekeberg and Grillner, 1999).

In legged animals and particularly higher vertebrates, CPGs are much less well understood owing to the complexity of legged locomotion (Guerton et al., 2009). However, the underlying neural control of these patterns may not be significantly different from that of lamprey (Rauscent et al., 2006). The essential pattern of muscle

output seen in quadrupedal locomotion may be partially modeled by assuming that each limb behaves as an independent lamprey spinal cord in which each joint is analogous to a pair of coupled burst generators (Grillner, 2006). Different patterns of muscle contraction, such as those seen during different gaits, can also be simulated by slightly altering the reciprocal connectivity between different burst generator chains across the body (Grillner, 2006).

### **1.3.2. Brainstem control of central pattern generator circuits**

CPG circuits form the basic structure of locomotor movements and postures, but these are ineffective without a higher level of organization. If an animal cannot stay upright then locomotor movements will only serve disorient it further, and if an animal cannot steer then locomotion cannot be directed towards or away from anything relevant. This next level of locomotor organization is thought to be coordinated by descending influences from the brainstem. These descending influences can be divided into three major pathways controlling movement: vestibulospinal, reticulospinal, rubrospinal (Squire et al., 2003). Although these pathways normally work together at many levels (Mann, 1981), they are known to control different properties of movement. The rubrospinal tract preferentially innervates distal musculature and is thought to be less important for locomotor behavior. The vestibulospinal and reticulospinal (RS) tracts, in comparison, are essential for effective locomotor behavior. These tracts preferentially

innervate the proximal muscles of the trunk (Squire et al., 2003). Animals with lesions to this system show ataxia of proximal muscles and fall over when they attempt to locomote despite having in-tact fine motor control over extremities (Squire et al., 2003, Eidelberg, 1981).

In lamprey, the RS tract provides direct control and drive to spinal CPGs. RS cells are arranged in a bilaterally symmetric fashion (Brocard and Dubuc, 2003) and send the majority of their projections ipsilaterally (Fagerstedt et al., 2000). Together, these descending projections exert their influence over the entirety of the spine (Zelenin et al., 2001). The exact pattern of this influence on spinal motor neurons has been investigated and up to 20 different distinct patterns have been observed (Zelenin et al., 2001). In legged mammals, RS projections provide postural tone (Mori et al., 1982) and project widely and without strong somatotopic organization (Magoun, 1950). For example, microstimulation of RS cells in the resting cat elicits brief contractions of both extensors and flexors of multiple limbs (Drew and Rossignol, 1990). Recording from RS cells during locomotion in the cat has revealed that most exhibit either a strict correlation with EMG patterns recorded from various muscles throughout the body, or periodic activity related to the overall pattern and timing of locomotion (Drew et al., 1986). These patterns suggest that RS neurons may exert control over the spinal network both at the level of individual muscles and at the level of muscle synergies.

### **1.3.2.1. Control of locomotor speed**

In lamprey, because there is a constant phase delay between segment bursts, speed of locomotion is proportional to frequency of alternation which is controlled by descending RS inputs (Grillner et al., 1991). In RS neurons, both frequency of rhythmic antiphasic burst firing and corresponding frequency of locomotor behavior have been found to correlate positively with level of tonic input from mesencephalic locomotor region (MLR) (Brocard et al., 2010). Thus, although the exact mechanisms of speed control in lampreys remain unknown, one reasonable possibility is that RS neurons form an oscillatory network with spinal CPGs, and that the frequency of oscillation in this network is controlled by specialized locomotor regions. In legged animals, speed is determined by stride length multiplied by stride frequency (Alexander, 2003). Given the apparent parallels between mammalian CPGs and those of the lamprey, speed control in mammals likely depends upon a similar oscillating network which controls the frequency of spinal undulation, which in turn dictates step-cycle and gait.

### **1.3.2.2. Control of turning**

In Lamprey, left-right steering is accomplished by altering the basic pattern of locomotor undulation. During forward locomotion, the two halves of the animal generate alternating waves of contraction with symmetrical intensity and duration. During a turn these two patterns are made asymmetrical down the length of the fish

such that the side corresponding to the direction of turn is increased in intensity and duration over the other side (Fagerstedt and Ullen, 2001), which causes increased bending to that side. Thus, steering appears to be accomplished by temporarily breaking the pattern of symmetrical brainstem output and augmenting it to one side before returning it to normal. In legged mammals, steering can also be accomplished through spinal bending, as well as through adjustments to the relative amplitude or force of left and right stepping, or the relative angles of stepping (Grillner, 2011). Such steering movements can also occur in a stationary animal to accomplish orienting movements and various postural adjustments.

#### **1.3.2.3. Control of posture**

Animals must continuously defend body geometry and orientation in space against both environmental and internally generated disturbances. Lampreys, for example, swim with dorsal side up and must control stability in pitch roll and yaw planes. Disturbance along any one of these planes is neutralized through corrective 'postural reflexes', which are thought to operate in symmetrical and opposed pairs. Any deviation from normal orientation is sensed by the vestibular organs and transduced directly into the appropriate corrective movement; for example, tip to the left will elicit a movement that pushes the animal rightward and vice versa (Deliagnia et al., 2007). In

this way, postural reflexes form a closed loop negative feedback system to quickly correct posture and maintain it stably in the face of unpredictable disturbances.

Activity in RS neurons with direct inputs from the vestibular system has been found to respond to disturbance in pitch, roll and yaw planes (Zelenin et al., 2007) and correlate with both velocity of disturbance and absolute disturbance (Pavlova and Delaina, 2002). By examining the motor effects of recorded RS neurons, it was found that neurons produced movements which specifically counteracted the tip that elicited their activity (Zelenin et al., 2007). For each plane, two opposed populations of RS neurons were found to respond to opposite directions of tilt and to produce movements which counteracted those tilts. Interestingly, an increase in temperature was found to increase the ratio of up to down neurons and thus the tendency for the animal to turn downwards. In nature, this may function as the output of a temperature control system since deeper water tends to be colder. Thus, the reference setting of postural control systems can be altered by hierarchically higher systems as a means of accomplishing their own sensory goals.

In legged animals postural control is thought to depend primarily on somatosensory inputs, while vestibular input is more important for stabilizing the head (Deliagnia et al., 2006). Because decerebrate animals have largely intact postural control (Mori et al., 1987), the basic mechanisms of postural control are thought to exist in brainstem, cerebellum and spinal cord. Discrete postural disturbances during locomotion elicit corrective steps which are incorporated neatly into the locomotor

pattern; in response to a push from the side, the leg that is at the end of its stance phase will be directed inwards or outwards depending on the direction of push (Karayannidou et al., 2009). A continuous postural disturbance during locomotion, on the other hand, elicits a continuous postural correction. For example, when a cat walks on a tilted surface, the amplitude of various muscle contractions is altered to maintain trunk stability but typical locomotor phase relationships are preserved. RS neurons recorded during this task were found to correspondingly adjust their amplitude and pattern of firing during various tilts (Matsuyuma and Drew, 2000).

### **1.3.3. Descending control of reticulospinal system**

Control of movement by the brainstem and spinal cord is a continuous and hierarchical process; spinal circuits provide a basic pattern of movement which is then continuously shaped by descending RS projections in accordance with the higher goals of the animal. Like the strings of a marionette, different RS cells may be rhythmically 'tugged' to adjust speed, phasically tugged to produce a postural correction or turn, or tonically held at a certain height to stabilize locomotion over sloping terrain. These basic motor functions are an essential part of many goal directed behaviors, but they must be deployed differently to accomplish different behaviors requiring locomotion at different speeds, over different terrains, and in pursuit of stationary or moving targets. Thus, lower motor functions must be initiated as part of still higher motor functions. As we

have seen, spinal networks controlling locomotion are largely activated by RS neurons emanating from the brainstem. These descending RS projections which control basic aspects of posture, steering and locomotor drive are themselves controlled by descending commands from midbrain and diencephalic motor nuclei. In the same way that the strings of a marionette must be pulled in a meaningful pattern for the puppet to appear to walk, these descending commands are important in combining and organizing basic RS motor functions into coherent locomotor behaviors.

#### **1.3.3.1. Brainstem locomotor regions**

Two brain regions are thought to be responsible for issuing locomotor commands to RS nuclei: the mesencephalic locomotor region (MLR) and the diencephalic locomotor region (DLR). Both functionally and anatomically these two regions appear to be very similar; they both monosynaptically project to the same RS nuclei and stimulation of either is sufficient to initiate and then smoothly increase frequency and force of locomotion with increasing stimulation (Menard and Grillner, 2008). Although locomotor movements may be initiated at lower levels of brainstem and spinal cord, stimulation of DLR or MLR, or of specific subsets of RS neurons to which they project (Kinjo et al., 1990), appears to be required to elicit coordinated locomotor behavior.

In lamprey, left and right MLR both send symmetrical projections to left and right RS cells, and tonic input to either left or right MLR elicits the same antiphasic burst firing in both left and right populations of RS cells (Brocard et al., 2010). This firing excites motor neurons and contralaterally projecting inhibitory interneurons on one side of the body (Grillner et al., 1998), thus facilitating propagation of CPG-mediated bending wave along the body length. Because this excitatory RS output is antiphasic and rhythmic, its effect is to orchestrate the basic locomotor pattern of left-right alternation in CPG-mediated bending waves. Increasing stimulation from MLR has been found to increase speed of locomotion in all species tested to date (Dubuc, 2008). In salamanders, increasing MLR stimulation induces increasing frequency of rhythmic stepping until past a threshold the legs are held back against the body and swimming behavior is produced with increasing frequency (Cabelguen, 2003). In rats (Skinner and Garcia-rill, 1984), increasing stimulation of MLR causes walking, then trotting and finally running.

#### **1.3.3.2. Tectum**

Visual inputs are thought to exert a direct influence on locomotor behavior through the optic tectum, also called the superior colliculus, a midbrain structure that receives visual inputs in a retinotopic fashion and also functions as a motor map for controlling orientation movements of eye, neck and body with respect to a visual target (Sparks, 2002). In higher mammals, projections from SC to RS populations are thought to

control neck and body orientation in the horizontal axis while orienting in the vertical axis is controlled through a different population of neurons in the mesodiencephalic junction (Isa and Sasaki, 2002). The tectum is thought to project to both MLR (Saitoh et al., 2007) and DLR (El Manira et al., 1997) as well as directly to RS neurons, and stimulation of the tectum results in site-specific eye and body movements; brief pulses of stimulation results in just eye movement, while longer pulses result in corresponding body orientation movements and even longer pulses result in locomotor movements (Saitoh et al., 2007). These findings suggest that the tectum may function as an important control center for generating steering and postural corrections to maintain an object of interest centered in the visual field. If such corrections occur in parallel with forward locomotion and postural control, then the animal will effectively be locked into the pursuit of the target object even if the target object is also moving.

#### **1.3.3.3. Pedunculopontine nucleus**

The pedunculopontine nucleus (PPN) is a brainstem nucleus that has been implicated in controlling muscle tone. Stimulation of this region has been found to reduce muscle tone in both extensors and flexors, both at rest and during active movement (Takakusaki, 2003). Consequently, the PPN is believed to play an important role in patterning and adapting ongoing movements to changing behavioral requirements, such as speed of movement (Takakusaki, 2008).

#### **1.3.3.4. Motor cortex**

The motor cortex exerts a direct influence on brainstem motor regions including the reticular formation through the corticobulbar tract, as well as on spinal circuits at different levels through the corticospinal tract. These tracts together comprise the pyramidal tract (Mann, 1981). The pyramidal tract is believed to be most important for controlling precise and fractionated movements of distal musculature, such as precise limb placement when traveling across uneven terrain (Bretzner and Drew, 2005), or reaching to a particular point in space (Kakei et al., 2003). However, the cortex can still directly influence the activity of proximal musculature (Freund and Hummelsheim, 1984). Removal of the entire cortex has little effect on basic locomotor and goal directed behavior (Bjurston et al., 1976), implying that its function is mainly to produce learned movements requiring a high degree of motor flexibility. Although the functional logic of how pyramidal projections cooperate with lower levels of the motor hierarchy remains unknown (Miri et al., 2013), one possibility is that pyramidal influences are simply added into the existing reference signals and outputs at different levels in the motor hierarchy, like a president issuing direct orders to individual soldiers and commanders in a military hierarchy. By breaking the chain of command in this way, the pyramidal motor system can mobilize small groups of muscles in service of skilled behavior in the same way that a president can mobilize small groups of soldiers to

pursue specific goals relevant to his own office--but which the military as a whole has never been trained to pursue.

#### **1.3.4. The importance of the basal ganglia**

In vertebrates, motor behavior is accomplished by a hierarchy of neural circuits beginning with spinal GPGs, which provide the essential repeating pattern of locomotor movement and the lowest level of postural control. Descending commands from the brainstem, in turn, shape different aspects of this pattern to maintain posture and accomplish different maneuvers such as turning, which are themselves further organized into coherent motor functions by specialized higher structures such as the MLR, tectum, and motor cortex. A still-higher level of organization is controlled by the basal ganglia, a set of subcortical nuclei consisting of the striatum, globus pallidus, substantia nigra, and subthalamic nucleus (DeLong and Georgopoulos, 2011). These nuclei appear to be responsible for continuously orchestrating the pattern and intensity of various motor functions for the sake of accomplishing higher goals.

Free behavior is composed of multiple ongoing motor programs which are not only turned on and off in different overlapping patterns but also turned up or down in their intensity and direction. Even a simple lamprey searching for food must transition between forward swimming and turning, while simultaneously adjusting its speed and degree of turning in such a way that the overall pattern is coherent and functional with

respect to the goal of spotting and then catching food. In this way, the coordination of motor programs by the basal ganglia is like that of a conductor continuously controlling the identity and volume of different motor functions as though they were musicians in a symphony. As with music, the components of behavior must be harmonious; physically conflicting behaviors cannot occur at the same time, and slight turns and postural corrections must be compensated for by pauses and alterations in ongoing locomotor functions. Similarly, the relatively simple commands sent to motor programs by basal ganglia are independently transduced into complex and precisely coordinated rhythmic patterns of muscle contraction, like the notes and phrases played by individual musicians.

#### **1.4. Functional anatomy of the basal ganglia**

The basal ganglia are a set of functionally and anatomically related subcortical nuclei located in the mesencephalon, telencephalon and diencephalon (DeLong and Georgopoulos, 2011). As a rule, but with the exception of the STN whose projections are glutamatergic, the nuclei of the BG employ inhibitory GABA projection neurons (Yin, 2014). The basal ganglia receive inputs from areas of the entire cortex and thalamus, and send outputs to a number of brainstem motor nuclei as well as to diverse cortical regions via projections to thalamic nuclei (Alexander et al., 1986). Given their central location in the brain and strong connectivity with both cortex and brainstem motor

regions, the BG are believed to play important roles in shaping the higher levels of goal directed behavior. Indeed, damage to BG can result in a diverse array of severe behavioral and motor deficits, implying an important role in those processes (Albin et al., 1989).

#### **1.4.1. Outputs of the basal ganglia**

The major output nuclei of the BG are the substantia nigra pars reticulata (SNr) and the globus pallidus internal segment (GPi). In rodents, the entopeduncular nucleus is considered equivalent to the GPi (Carter and Fibiger, 1978). These outputs are GABAergic with a high (50-100Hz) baseline firing rate and project primarily to thalamus and brainstem motor areas (Hikosaka et al., 2000). Outputs from basal ganglia to brainstem areas are widely believed to coordinate the activity of motor functions by tonically inhibiting motor centers such as the MLR, (Garcia-Rill et al., 1986; Takakusaki et al., 2003 ), PPN (Takakusaki et al., 2004), motor cortex (Alexander & Crutcher, 1990) and tectum (Kaneda et al., 2008), and thus the motor functions specific to those regions. Release of this high tonic inhibition by the basal ganglia is thought to constitute the selection of a set of motor functions, and has been likened to a 'gate' which selectively frees a set of motor functions while inhibiting all others (Hikosaka, 2000; Grillner et al., 2013). There is also evidence that the behavior of a given motor region, such as the SC, can be modulated by BG outputs through disinhibition of different subpopulations in

that region. For example, SNr neurons recorded during a visually guided saccade task were found to pause around the time of saccade onset which corresponded with a burst in SC activity, but only when the saccade was directed towards a target placed in the contralateral visual field (Basso and Wurtz, 2002). Pharmacological inactivation of cells in the SNr can also cause irrepressible saccades towards the contralateral visual field (Hikosaka and Wurtz, 1985), presumably through exerting different effects on ipsilateral and contralateral halves of the SC.

Outputs from BG to thalamic nuclei are relayed by the thalamus to cortical regions, which in turn project back to the input nuclei of the basal ganglia. These circuits form sharply segregated closed loops through diverse regions of motor and prefrontal cortex (Alexander et al., 1986). These loops are discussed in greater detail below.

#### **1.4.2. Inputs of the basal ganglia**

The striatum is the input nucleus of the basal ganglia. Cells here have a high threshold for activation and receive extensive excitatory projections from diverse cortical regions including motor, premotor, associative, and entorhinal cortex (Alexander et al., 1986), as well as directly from thalamic nuclei (Grillner et al., 2008). 95% of the striatum consists of GABAergic projection neurons, which project to BG output nuclei, while the remaining 5% of the striatum includes cholinergic interneurons and a small population of GABAergic interneurons (Kreitzer, 2009). Striatal projection

neurons have a low baseline firing rate during resting conditions and a high threshold for activation (Kreitzer, 2009). However, dopamine input from substantia nigra pars compacta (SNc) to the striatum is thought to lower this typically high threshold and transition the cells to a more sensitive state. Striatal neurons are very difficult to activate without concurrent dopamine input (O'Donnel, 2003). Once sensitized by dopamine, striatal projection neurons can be more easily depolarized by cortical or thalamic inputs, and thus exert a greater influence on their targets. All vertebrates appear to have this basic organization: a striatum that is difficult to activate and serves as a relay for diverse cortical and thalamic inputs, and which depends critically on the presence dopamine to open (Grillner et al., 2008).

#### **1.4.3. Intrinsic connections of the basal ganglia**

The striatum projects directly to BG output nuclei through what is known as the 'direct pathway'. This pathway exerts a direct inhibitory influence on SNr/GPi. There also exist parallel 'indirect pathways' from the striatum which exert an opposite influence on the output nuclei. The first of these pathways projects from striatum to GPe, which in turn projects to SNr/GPi (Hikosaka et al., 2000). Because the projection neurons here are GABAergic, this additional stop compared to the direct pathway results in a sign change, such that increasing output through this pathway has an excitatory effect on the SNr/GPi. The second indirect pathway projects from striatum to

GPe to STN to SNr/GPi. Increasing striatal output to this pathway also results in increased SNr/GPi output because the STN is glutamatergic (Hikosaka et al., 2000). Within the striatum, projection neurons to the indirect pathway are spatially segregated from those of the direct pathway (Parent et al., 1984), and although still mediated by dopamine input these two populations are thought to respond in opposite directions to dopamine input because they express different types of dopamine receptor. Striatal neurons in the indirect pathway express D2 receptors while those in the direct pathway express D1 receptors (Gerfin et al., 1990). These two receptor types have opposite effects; D2 receptors inhibit production of adenylyl cyclase while D1 receptors stimulate its production (Stoof and Kebabian, 1981). However, because it has been shown that a proportion of striatal projection neurons co-express D1 and D2 receptors (Surmier et al., 1996), then the exact effect of dopamine input to a particular region will depend on the relative expression of receptor subtypes and whether cells project to direct or indirect pathways. Dopamine neurons project to the striatum from the SNc, a region sharing an indistinct border with the SNr, and the ventral tegmental area (VTA), a region dorsomedial to and continuous with the SNc (Beckstead et al, 1979). DA projections to the striatum exhibit a high degree of topographic organization (Fallon and Moore, 1978; Palidini and Roeper, 2014).

The functional significance of these different intrinsic pathways is still unclear; however one attractive possibility is that the direct and indirect pathways act in opposition to modulate BG outputs for various channels up and down. According to the

classical perspective, increasing or decreasing BG outputs simply increases or decreases tonic inhibition of various motor functions and thus constitutes 'action selection'.

However, an alternate possibility is that increasing or decreasing firing rate in SNr/GPi neurons above or below their baseline could encode an analog value with a positive or negative sign, respectively. Such signals could be used in diverse ways to perform a variety of analog computations beyond simply inhibiting and disinhibiting their targets.

#### **1.4.4. Thalamic closed loops**

In addition to their influence on brainstem motor structures, BG outputs influence cortical activity via projections to thalamus. These thalamic projections form a canonical 'closed loop' circuit which retains the same basic design features regardless of the striatal or cortical regions involved (Alexander et al., 1986). The basic circuit is as follows: SNr/GPi to thalamus to cortex to striatum and back to SNr/GPi through direct and indirect pathways. Although this essential circuit design does not vary significantly from region to region, it does segregate different regions into different parallel loops carrying distinct types of information. For example, there is a dedicated 'motor' loop through thalamic nuclei which projects primarily to motor cortex, and in turn to striatal and SNr/GPi regions which project back to the same thalamic nuclei (Alexander and Crutcher, 1990). Even within this motor loop there are thought to be circuits dedicated to the movement of different body parts in different directions; the striatum exhibits

topographic organization, with representation of orofacial movements located ventromedially, and upper and then lower extremities represented more dorsolaterally (Alexander et al., 1986). Additional loops include one passing through the frontal eye fields, as well as a number of 'associative loops' passing through dorsolateral prefrontal and orbitofrontal cortices which are thought to be involved in hierarchically higher properties of behavior (Alexander et al., 1986). Because these diverse circuits share a highly stereotypical organization, it is hypothesized that they share the same basic function which is simply applied to different types of information arising from different cortical regions (Alexander et al., 1986).

Compared to BG-brainstem projections, the function of these BG-thalamic loops remains unclear (Grillner et al., 2013). Because decorticate animals exhibit goal-directed behavior which is largely in-tact (Bjursten et al., 1976), these loops are likely most important in higher aspects of behavior requiring complex perceptions, hierarchically sequenced learned behaviors, or fine motor control of brainstem and spinal circuits via the pyramidal motor tract as mentioned earlier.

### **1.5. Movement disorders of the basal ganglia**

Much of what we know about the basal ganglia comes from observing clinical symptoms resulting from damage to its different parts. Below we summarize clinical

findings related to the two main classes of motor disorder associated with BG damage; hypokinetic disorders and hyperkinetic disorders.

### **1.5.1. Hypokinetic disorders: Parkinson's disease**

Hypokinetic movement disorders are characterized by impairments in initiating movements as well as a reduction in both speed and amplitude of movements. The most well characterized hypokinetic movement disorder is Parkinson's disease (PD), which is caused by death of dopaminergic neurons in the SNc. PD patients exhibit difficulty initiating voluntary movements but can still respond to environmental disturbances. For example, PD patients can be induced through visual stimulation—but not voluntarily—to walk up and down stairs, catch a ball, jog, and ride a bicycle almost normally (Glickstein and Stein, 1991). PD patients can also make postural corrections but have difficulty shifting their postural control strategy in response to altered disturbance patterns (Visser and Bloem, 2005), and generally show deficits in smoothly transitioning between the motor tasks that constitute a behavior (Stern et al., 1983). These observations suggest impairment in the ability of higher systems to transition between which motor functions are online, likely due to chronic low levels of striatal output caused by DA depletion. This interpretation is in agreement with the observed role of the basal ganglia in transitioning between motor functions within a sequence (Kermadi and Joseph, 1995).

Another striking feature of Parkinson's disease is bradykinesia or slowness of movement (Albin et al., 1989), which implies a lower-level deficit in transitioning between different reference settings within a given motor function. This deficit is also clearly seen in postural control tasks in which subjects are asked to voluntarily 'resist' or 'yield' to a disturbance. In these tasks, the gain of postural control is relatively fixed and unaffected by voluntary modulation in PD patients compared to control subjects (Bloem et al., 1994). By setting a reference state to 'zero', such a mechanism for continuous modulation of motor functions could also effectively turn off certain motor functions, and thus carry out second order motor transitions. Indeed, it is hypothesized that akinesia or inability to move in PD is just an extreme form of bradykinesia (DeLong, 1990). Combined, the deficits in Parkinson's disease imply a role for dopamine and the basal ganglia in transitioning and coordinating motor functions at multiple levels in the behavioral hierarchy.

### **1.5.2. Hyperkinetic disorders: Huntington's**

A different class of basal ganglia motor disorders, the hyperkinetic disorders, is characterized by ballistic and involuntary movements. The most well-known of these disorders is Huntington's disease (HD), which exhibits uncontrolled writhing and dancelike movements, and which is caused by death in striatal neurons (DeLong, 1990). Given that striatal damage does not always result in HD, that administration of D2

agonists alleviates symptoms in HD (Albin et al., 1989), and that selective damage to indirect pathway striatal projection neurons has been reported in HD patients (Reiner et al., 1988), the disease is thought to result primarily from damage to the striatal neurons that comprise the indirect pathways. However, striatal damage is rarely confined to only the indirect pathways; with severe HD both direct and indirect pathways are severely damaged (Reiner et al., 1988). Given that excessive dopamine activity can also elicit similar symptoms to HD, (DeLong, 1990) one way to interpret HD is as a disorder of striatal output in which striatal signaling to BG output nuclei is generally uncontrolled, ultimately resulting in complex patterns of motor hyperactivity and conflict.

## **1.6. Open questions regarding the functions of the basal ganglia**

### **1.6.1. Graded modulation of basal ganglia output**

As discussed previously, natural behavior requires the continuous modulation of the direction and extent of online motor programs by the basal ganglia; an animal must be able to adjust speed of locomotion, postural control and degree of turning. However, this observation is at odds with the classical perspective of the basal ganglia as a gate which must sustain output at a steady level to function properly (Hikosaka et al., 2000). Given that the strength of BG outputs is known to be graded by the presence of food reward (Rossi et al., 2013; Sato and Hikosaka, 2002; Hikosaka, 2007), there may be a common and yet undescribed neural mechanism for adjusting the intensity of BG output in service of higher behavioral goals.

### **1.6.2. Antiphase signaling of basal ganglia outputs**

According to the classical account of BG function, outputs of the SNr exert tonic inhibition on motor functions and coordinate them by releasing this tonic inhibition. However, it is commonly observed that SNr neurons will both increase and decrease their activity at the time of movement (Chevalier et al., 1984; Gulley et. al., 1999; Kaneda et al., 2008; Rossi et al., 2013; Fan et al., 2012; Sato and Hikosaka, 2002). It has been proposed that this represents a mechanism for ‘action selection’ whereby the desired actions are disinhibited while all others are inhibited. However, the exact meaning of action is rarely clearly defined, and given that even actions directed at the same end are constantly varying with changing environmental and muscular conditions, this account is problematic. The exact function of these antiphase outputs from the BG thus remains an open question.

### **1.6.3. Reward prediction and motor control**

An important principle for organizing motor functions into a coherent behavior is the higher goal or purpose of that behavior. As mentioned previously, another way to frame this is as a control system producing motor outputs to defend internal variables against change from their reference settings. For example a hungry animal may search for food to regulate blood sugar, or a territorial animal may seek to drive away an

intruder to regulate an internally defined social variable. Such goals for behavior are typically termed 'rewards'. A number of well-known studies have demonstrated SNc dopamine burst firing in response to delivery of a reward and in response to cues which reliably predict reward delivery (Glimcher et al., 2011), and that SNc activity prior to reward is strongly modulated by the size of the upcoming reward (Roesch et al., 2007). Striatal activity in monkeys (Kawagoe et al., 1998) and humans (Knutson et al., 2001) also exhibits sustained activity prior to delivery of an expected reward which is correlated with the expected value of that reward. As previously discussed, changes in striatal activity are thought to facilitate activation of motor functions. One could thus argue that a reward, and the perceptions that predict it, act as stimuli to 'switch on' the motor functions required to obtain it. However, it is clear that other stimuli which are not ostensibly rewarding may also elicit such a switch in ongoing behavior, such as when an animal is surprised or attacked. In accordance with this observation, experimenters have found similar patterns of activity in the basal ganglia in response to both rewards and unexpected or salient stimuli (Horvitz, 2000; Zink et al., 2003; 2008).

Because behavior is defined by movement, then such simple correlations between the presence of rewarding or salient stimuli and neural activity may be misinterpreted if movement is not carefully observed. This possibility has been suggested previously on the grounds that DA responses occur too quickly to underlie value assessment; DA response to a visual reward cue commonly occurs before the animal has time to foveate on the cue (Redgrave and Gurny, 2006). It is also known an

animal will by definition work harder for a more valued reward (Schultz et al., 1997).

Thus, the relationship between such reward-related events and movement kinematics remains an important unknown in our understanding of the BG.

#### **1.6.4. Summary of experiments**

The experiments in the following three chapters were performed to address the open questions regarding the function of the BG outlined above. In the first set of experiments, we recorded wirelessly from the SNr and SNc while mice were subjected to a continuous postural disturbance along the roll plane. This study was designed to address the role of antiphasic BG output in continuously adjusting motor functions. In the second and third sets of experiments we recorded wirelessly from the SNr and SNc respectively, in combination with video tracking of the head while mice performed a cued reward task. These studies were performed to further elucidate the role of antiphasic BG output in controlling the extent and direction of motor output, and the relationship of that role with reward processing.

## 2. The Role of the Substantia Nigra in Posture Control<sup>1</sup>

### 2.1. Introduction

Postural control is a continuous and integral part of all behavior. Proper execution of any movement requires continuous defense of body geometry and orientation in space against both environmental and self-generated disturbances. The neural mechanisms underlying postural control have been investigated in a number of species (Deliagina, 2007), but previous work has focused primarily on the role of brainstem and spinal networks, in particular the reticulospinal pathway (Deliagina et al., 2012). Because decorticate animals still show effective postural control (Bjursten et al., 1976), the cortex is thought not to play an important role in this process. However, patients with focal damage to the basal ganglia or its targets, such as the pedunculo-pontine or thalamus, have severe postural deficits (Visser and Bloem, 2005). Patients with Parkinson's disease also have postural deficits including a stooped neutral posture and difficulty adapting movements to postural disturbance (Dimitrova et al., 2003). Combined with the fact that the basal ganglia also exert direct influences over such regions as PPN and tectum which are known to play important roles in the control of posture and body configuration (Takakusaki et al., 2003; Takakusaki et al., 2008;

---

<sup>1</sup> This chapter is a modified version of a previously published article: Barter JW, Castro S, Sukharnikova T, Rossi MA, Yin HH (2014) The role of the substantia nigra in posture control. *Eur J Neurosci* 39:1465–1473.

Saitoh et al., 2007), these results suggest that BG outputs may serve an important function in adapting behavior to ongoing postural disturbances.

The basal ganglia have traditionally been implicated in learning and generation of actions (Graybiel, 1998; Wise et al., 1996, Grillner et al.,2013 ). However, little is known about the exact functional role of basal ganglia outputs in generating behavior. A prominent output nucleus of the basal ganglia, the SNr, sends projections to brainstem and midbrain structures including the PPN (Takakusaki et al., 2003) and tectum (Hikosaka et al., 2000), as well as to diverse regions of the cortex via thalamic projections (Alexander et al., 1986). Neural activity in the SNr has been found to correlate with a number of behavioral processes, including movement initiation and termination (Jin and Costa, 2010) and duration (Fan et al., 2012). A large body of classic work has suggested that projections from the SNr, particularly those to PPN and tectum, exert their effects on behavior by tonically inhibiting and disinhibiting—and thus turning off and on—various brainstem motor regions (Grillner et al.,2013, Hikosaka, 2007). While this model shows how SNr outputs could be capable of determining which motor functions are online at a given moment, it fails to explain how SNr outputs modulate the continuous and antagonistic properties of lower systems, such as the extent and direction of orienting turns or postural corrections made during locomotion.

Here we examined the role of basal ganglia outputs in posture control. We recorded from both DA and GABA neurons in a region bridging the SNr and SNc in unrestrained mice during continuous and cyclical postural disturbance along the roll

plane. To defend their upright posture during this task, mice were required to produce continuous corrective motor outputs to oppose the effects of roll disturbance. We found strong correlations between postural disturbance and neural activity: in both putative DA and GABA cell populations, one group of neurons was inhibited with tilt in one direction and excited with tilt in the other direction, and another group of neurons exhibited the exact opposite pattern of activity.

## **2.2. Materials and Methods**

### **2.2.1. Subjects and Surgery**

All procedures were conducted in accordance with the guidelines laid down by the National Institutes of Health regarding the care and use of animals for experimental procedure, and were approved by the Duke University Animal Care and Use Committee. Eight adult male C57BL/6J mice (4–12 months old, 28–35g) were used. Surgical

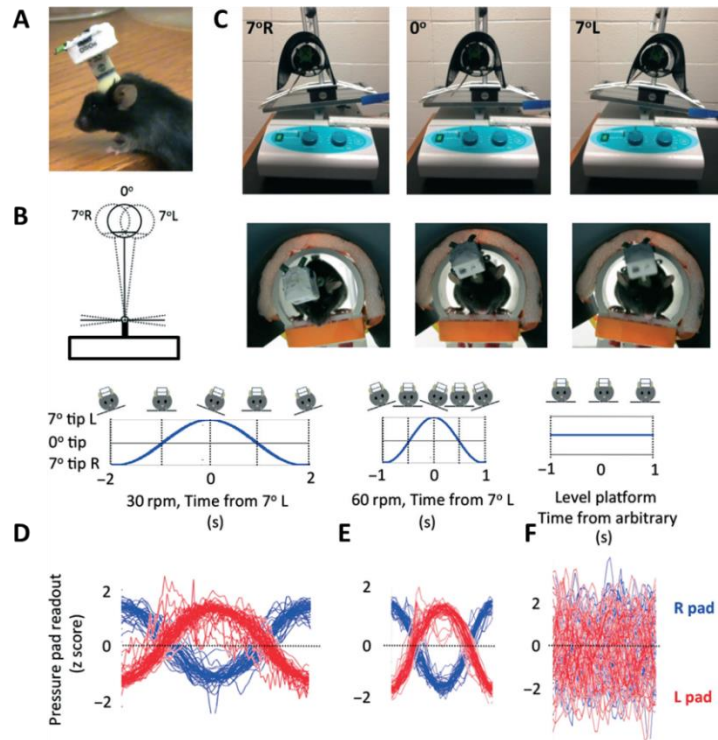


Figure 1. Apparatus for generating postural disturbance and illustration of in vivo wireless multi-electrode recording in freely behaving mice. (A) Miniaturized 16 channel wireless headstage (1.5x1x1.5cm) weighing about 3.8 g. (B) Illustration of the postural disturbance task. Up to 7 degrees of tilt were introduced in either direction along the roll axis of the mouse. (C) A mouse perched on an elevated tilting platform housed in a tube. The layout of the perch prevented mice from moving excessively or changing orientation while still allowing free standing postural adjustment and head movement. (D) Pressure pad readout traces during continuous postural disturbance of 30rpm. Data show overlay of 44 individual session averages. Forces on the left (red) and right (blue) pressure pads were generated by contact with the mouse's left and right paws, respectively. Time 0 on the x-axis indicates the point of the greatest disturbance to the left (7 degrees tilting to the left side); times -2 and +2 s show the point of greatest disturbance to the right. At time 0 the force exerted by the left paws on the left pressure pad is greatest and force exerted by the right paws on the right pressure pad is least; at times -2 and +2 the opposite pattern can be seen. (E) Pressure pad readout (Z score) traces during continuous postural disturbance of 60rpm. Traces are from the same sessions shown in D. Time 0 indicates the point of the greatest disturbance to the left (7 degrees tilting to the left side); times -1 and +1 show the point of greatest disturbance to the right. The same basic pattern shown in D may also be seen here. (F) Pressure pad readout (Z score) during rest, in the absence of any tilt. Traces are from same sessions shown in D and E and represent peri-event averages around arbitrary points spaced 2s apart. No clear pattern of force change is demonstrated. Grooming behavior was often observed during this period.

procedures for chronic electrode implants were as described previously (Fan et al., 2012; Rossi et al., 2013). Briefly, after creating a craniotomy, electrode arrays were lowered at the following stereotaxic coordinates in relation to bregma: 3.0mm posterior, 1.2mm lateral and 4.7mm below brain surface. In all experiments, 16-channel electrode arrays (Innovative Neurophysiology, Durham, NC, USA) were used. Seven of the arrays consisted of micro-polished tungsten wires, 35 $\mu$ m in diameter and 7mm in length, arranged in a 4x 4 configuration. One implanted array contains 35 $\mu$ m diameter tungsten wires 5mm in length and arranged in a 2x8 configuration. In all arrays row spacing was 200 $\mu$ m and electrode spacing was 150 $\mu$ m. All arrays were attached to an Omnetics connector (Omnetics Connector Corporation, Minneapolis, MN, USA) and firmly fixed to the skull with dental acrylic, allowing neural activity to be recorded chronically for up to 6 months. Following completion of the experiments, all mice were perfused and their brains sliced with a Vibratome 1000 into 100 $\mu$ m coronal sections. The sections were stained with thionin and examined under a microscope for electrode tracks to verify placement.

### **2.2.2. Behavioral Apparatus**

Mice perched on an elevated platform positioned within a tube (5cm diameter, 3.8cm length) and covered with a bonnet. Typical posture was characterized by a slightly

downward head angle with wireless transmitter balanced directly above the nose and outside the tube. Although the added height of the headstage prevented them

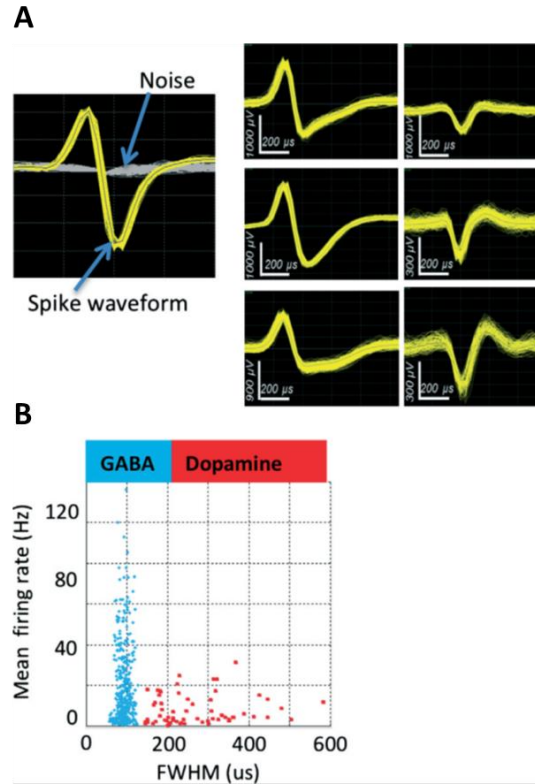


Figure 2. Classification of GABA and DA neurons. (A) Representative spike waveform recorded with wireless technology, with a high signal-to-noise ratio. Three examples of typical action waveforms are shown for each cell type. The duration of action potentials in GABA neurons is much shorter than in DA neurons (Ungless and Grace, 2012). (B) Cell type classification. Putative DA neurons (red) have significantly wider waveforms. FWHM, full width half maximum (spike duration at half maximum). DA neurons have lower mean firing rate ( $7.8 \pm 0.92 \text{ Hz}$ ,  $n=62$ ) than putative GABA neurons ( $19 \pm 0.94 \text{ Hz}$ ,  $n=427$ ).

from turning around easily on the platform, all mice could still freely move and groom.

The perch platform was suspended by a custom built rigid 'T'-shaped structure formed of 1cm-diameter aluminum rod. The horizontal section was 40cm in length and fixed at

its center to the top of an 18cm vertical rod. The perch was fixed to the underside of one end of this horizontal section and a 200g counterweight was fixed to the opposite end. The vertical rod was fixed at its bottom to the plate of a standard laboratory shaker (Lab-net Rocker 25) which generated postural disturbance in the form of continuous tilt to 7° in either direction along the roll axis of the mouse (Fig. 1). The platform was elevated (13cm) from the shaker plate. All mice were exposed to two speeds of continuous tilt disturbance in 10-min blocks with a 2-min break between blocks. During the first block there were 15 tilts to each side per minute, and during the second block there were 30 tilts per side per minute. At the beginning of each session and prior to onset of tilt disturbance mice were acclimated to the level platform for 2 min. Mouse movement was measured with custom-built pressure pads on the floor. These pads consisted of left and right rectangular floor pieces, each 1.9x3.8cm, with a 0.65cm diameter aluminum piston attached to the bottom center. Each piston rests on a 1.3 cm length of soft silicone tubing, 0.58cm o.d. 90.3cm wall (Cole-Parmer part # EW-96150-02, London, UK) connected to a pressure sensor at one end (Omron part # 2SMPP-02, Kyoto, Japan) and sealed at the other end. The signals from the pressure sensors were amplified and sent to the Black Rock Cerebrus data acquisition system via analog inputs at 2000 Hz. Timestamps were generated by the movement of the platform through an optical interrupter circuit (Fairchild model# H21A1, San Jose, CA, USA) and sent directly to the data acquisition system. These timestamps were used for correlating neural activity with tilt.

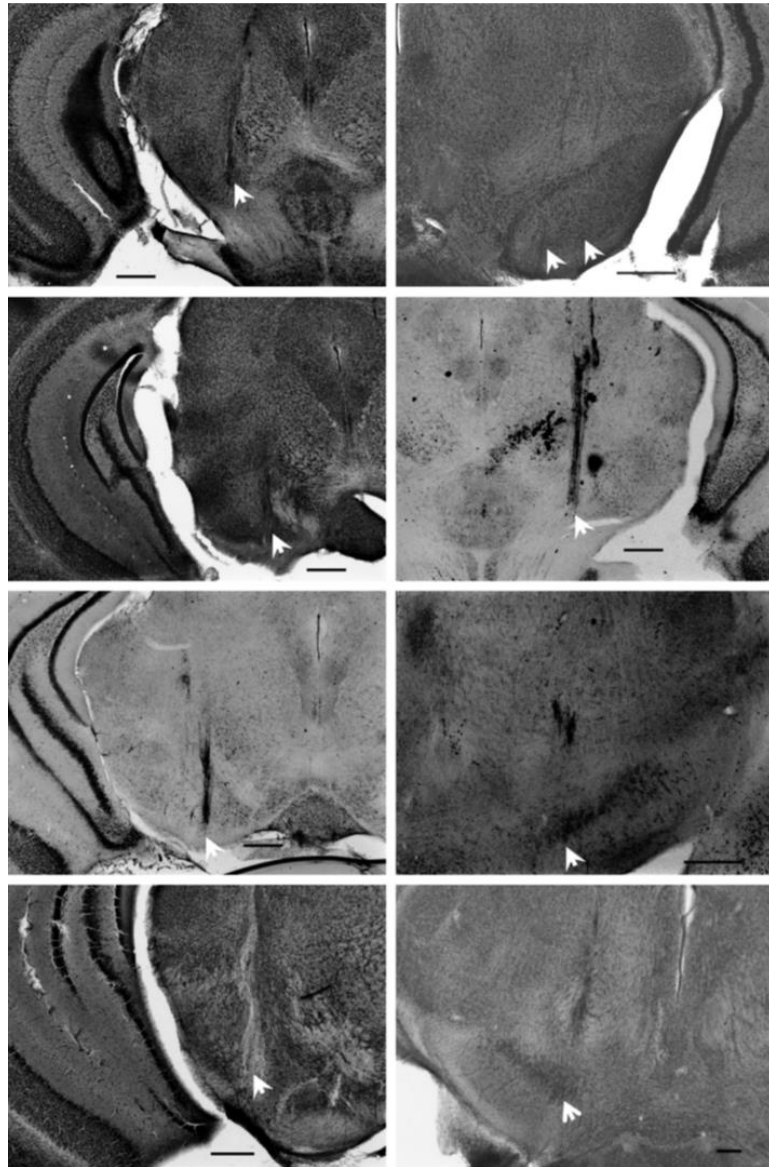


Figure 3. Coronal sections showing the location of electrode implants for all mice. Scale bars 0.5mm

### **2.2.3. Recording and spike sorting**

Single-unit activity was recorded with miniaturized wireless head-stages (Triangle Biosystems, Durham, NC, USA) using Cerebrus data acquisition systems (Blackrock Microsystems, Salt Lake City, UT, USA). Data were sampled after filtering with both analog and digital bandpass filters (analog high pass 1st order butterworth filter at 0.3Hz, analog low pass third order butterworth filter at 7.5kHz, digital high pass fourth order butterworth filter at 250Hz) and sampled at 30kS/s (Fan et al., 2011). In five mice electrodes were implanted in the left nigra; in three mice electrodes were implanted in the right nigra. Spike sorting for each unit was performed using Offline Sorter (Plexon, Dallas, TX, USA). Waveforms were classified as single units as previously described (Nicolelis, 2007; Fan et al., 2012; Yu et al., 2012). The following criteria were used: (i) a signal-to-noise ratio of at least 4:1; (ii) consistent waveforms throughout the recording session; and (iii) refractory period of at least 1200 $\mu$ s. Units were classified as either putative dopamine or putative GABA on the basis of mean firing rate and waveform duration and shape (Fan et al., 2012; Ungless & Grace, 2012; Rossi et al., 2013).

### **2.2.4. Classifying single units**

We identified neurons that significantly changed their firing rate in response to posture disturbance generated by the tilt. Time intervals were defined to categorize cells based on their firing rate changes in response to different directions of postural

disturbance: 0° to 7°L to 0°, and 0° to 7°R to 0°. As full tip to one side occurred at a rate of either once every 4 s or once every 2 s, the time windows for comparison were as follows: 7°L±1s and 7°R±1s (30 r.p.m.), 7°L±0.5s and 7°R±0.5s (60 r.p.m.).

### **2.2.5. Data analysis**

The behavioral and electrophysiological data were recorded with a Blackrock data acquisition system and analysed with Matlab and Graphpad Prism. Peri-event raster plots were generated using Neuroexplorer.

## **2.3. Results**

### **2.3.1. Postural disturbance and behavior**

Eight adult male C57 BL/6J mice were exposed to 2 different speeds of continuous postural disturbance along the roll plane: 30rpm (15 tips/side/minute) and 60rpm (30 tips/side/minute). Typically, after a single session mice stopped trying to turn around on the platform or escape and adopted a consistent head-forward stance (Figure 1C). Pressure pad readout was recorded for four mice during 44 sessions of postural disturbance. Pressure on the left and right pads continuously changed as the animal's weight was shifted during postural disturbance; as the platform tilts to the animal's right, the force generated by its paws is greater on the right pad than the left pad and vice versa. During postural disturbance, forces exerted on left and right pads were at

baseline average when the platform was level (Figure 1D-E). During the 2m break period between blocks, force readouts on the left and right pads were comparable (Figure 1F).

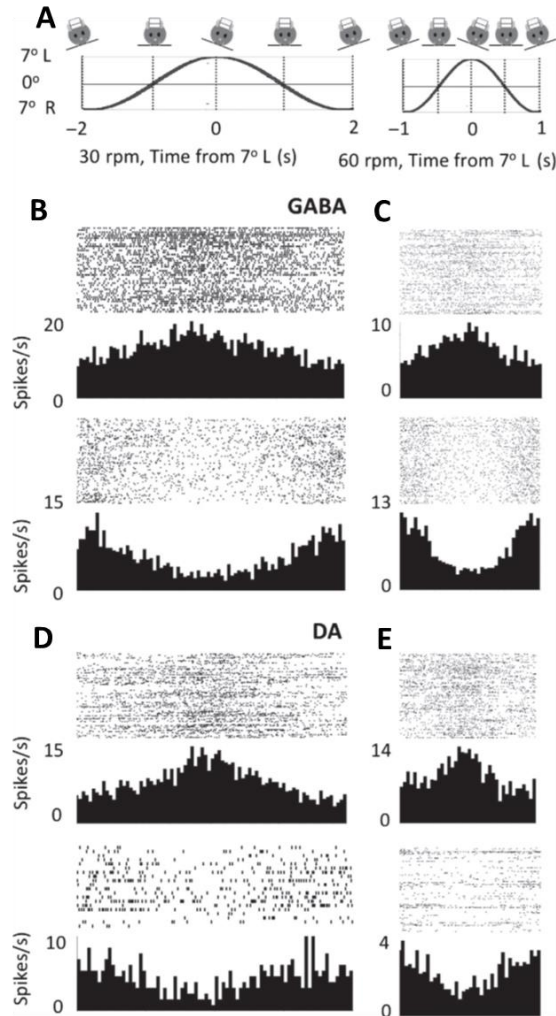


Figure 4. Representative neural activity during postural disturbances. (A) Pattern of postural disturbance. (B) GABA neuron activity throughout the slow tilt cycle (15 tilts to each side/minute). Top plot shows L+R- cell; bottom plot shows L-R+ cell. (C) Activity of the same cells shown to the left during the fast tilt cycle (30 tilts to each side/minute). (D) Dopamine neuron activity during the slow tilt cycle. Top plot is L+R-; bottom plot is L-R+. (E) Activity of the same cells shown to the left during the fast tilt cycle.

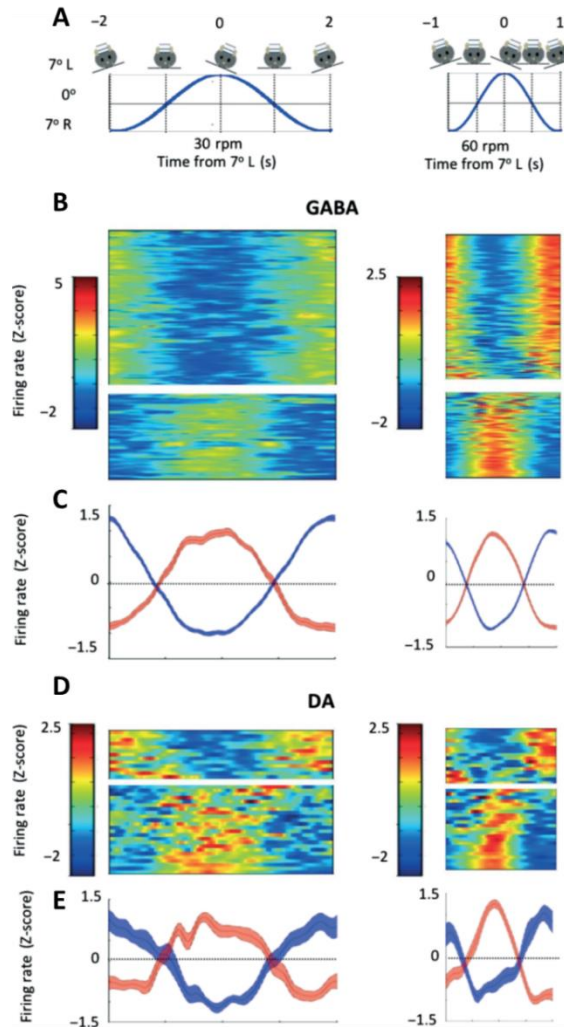


Figure 5. Left substantia nigra summary. Spike density functions and averages of cell populations recorded from the substantia nigra whose activity was significantly correlated with tilt disturbance. Left column of all plots shows peri-tilt activity during 30rpm disturbance (15 tilts/side/minute). Right column shows activity during 60rpm disturbance (30 tilts/side/minute). Top spike density function of each pair shows L-R+ cells; bottom heatmap shows L-R- cells. Blue trace in each population average plot shows average firing of L-R+ cells shown in above heatmaps; red trace shows average firing of L-R- cells shown in above heatmaps. All plots are normalized by z-score (number of standard deviations from the mean). (A) Pattern of postural disturbance. (B) Spike density functions of peri-tilt activity in GABA neurons. (C) Population averages of peri-tilt activity in GABA neurons. (D) Spike density functions of peri-tilt activity in DA neurons. (E) Population averages of peri-tilt activity in DA neurons.

### 2.3.2. Neural correlates of postural disturbance

Neural activity was recorded from DA (n=62) and GABA (n=427) neurons in the substantia nigra of 8 mice over a period of roughly 4 months per animal. Waveforms were manually classified as single units on the basis of appearance and clear separation from noise. The same electrode could pick up signals from multiple distinct single units at a time. The range of single units recorded during a single session on all channels combined was 3 to 31. Waveforms changed significantly over the course of recording sessions in a given animal, suggesting the detection of new units over time. After the experiments were completed, mice were perfused and electrode placement was verified. All electrodes were located in the substantia nigra pars reticulata and pars compacta.

As shown in Figure 2, the isolated single units were classified as putative GABAergic or dopaminergic (hereafter referred to as GABA and DA) on the basis of spike duration and mean firing rate, as established by previous work (Grace and Bunney, 1983; Ungless and Grace, 2012). As shown in Fig. 2, waveforms with longer durations (full width at half maximum) and lower firing rates (mean  $7.8 \pm 0.92$  Hz) were classified as DA neurons and those with short spike duration and higher firing rates (mean  $19 \pm 0.94$  Hz) classified as GABA neurons (Fan et al., 2012; Rossi et al., 2013). Although the mean firing rates of DA neurons are often higher than that reported in previous work, such differences may in part be attributed to the use of anesthetized preparations in

previous work (Brown et al., 2009). Of course, the use of awake-behaving mice in the present study precludes labeling and histological confirmation of cell type, which unfortunately remains a major limitation in studies of freely moving animals. It is important to note that many recorded putative DA and GABA neurons have comparable firing rates, but their spike durations are still significantly different. Cells with ambiguous classification based on the above criteria were excluded from all further analysis. The locations of all electrode arrays are shown in Fig. 3. All arrays targeted the substantia nigra, with electrode tracks in the pars reticulata and pars compacta.

Two clear patterns of neural activity were observed during postural disturbance: 'L+R-' cells continuously increased activity with increasing tilt to the left and continuously decreased activity with increasing tilt to the right; 'L-R+' cells exhibited the opposite pattern (Figures 4-5). These two patterns of activity were observed in both DA and GABA cells, during both fast and slow disturbance, and in both left and right nigra. Although more recorded neurons were classified as L-R+, an examination of the data from individual animals shows no consistent pattern, as some mice had more L+R- neurons.

To quantify the relationship between neural activity and postural disturbance, we performed a regression analysis with degree of tilt (7 to +7°) as the independent variable and firing rate as the dependent variable. Strikingly, as shown in Fig. 6, in 14 cases, the coefficient of determination ( $R^2$ ) was >0.9, with over 90% of the variability in firing rate accounted for by the variation in the degree of tilt ( $R^2$  values range from 0.33

to 0.98). Neurons were considered to show significant tuning to postural disturbance if the regression analysis reached statistical significance ( $P < 0.05$ ). Among 427 putative GABA neurons, there were 119 L+R cells (28%, mean firing rate =  $22.3 \pm 1.77$  Hz) and 202 LR+ cells (47%, mean firing rate =  $20.0 \pm 1.37$  Hz). Among 62 putative DA neurons, there were 23 L+R cells (37%, mean firing rate =  $9.24 \pm 1.83$  Hz) and 16 LR + cells (26%, mean firing rate =  $5.23 \pm 0.76$  Hz). By contrast, we did not find any systematic relationship between L+R–and LR+ neurons during the rest period, suggesting that these patterns of neural activity are task-related rather than due to intrinsic reciprocal inhibition between these different cell types.

We also performed a regression analysis to investigate the relationship between neural activity and pressure pad readout (Figure 7). Because pressure pad data were often noisy due to subtle movements and urination into the pressure pad mechanism, only data from two mice were included in the analysis. We again found very high  $R^2$  values during postural disturbance, indicating that the neural patterns described above reflect a behavioral variable which is closely related to foot ground force.

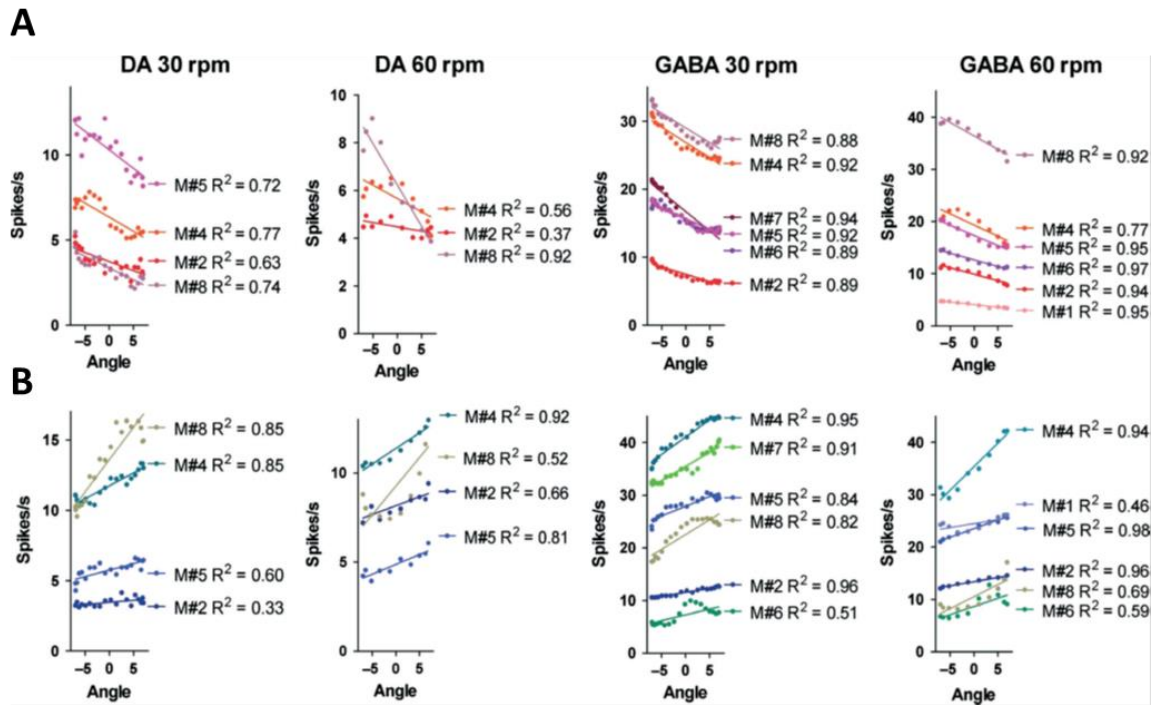


Figure 6. Relationship between mean firing rate and tilt angle in different populations of neurons. For each mouse, units significantly modulated by tilt were used in a regression analysis. For a mouse with sufficient number of recorded units, the mean firing rate of each population of dopamine '+' and '-', and GABA '+' and '-' units was calculated, and the coefficient of determination ( $R^2$  value) was calculated between tilt disturbance and mean firing rate. Each graph shows the line of best fit between tilt and firing rate in a given population. The corresponding colored dots show the mean firing rate of that population for different angles of tilt. For all regression analyses shown,  $P < 0.05$ . The corresponding  $R^2$  value is shown. (A) L+R- neurons. (B) L-R+ neurons.

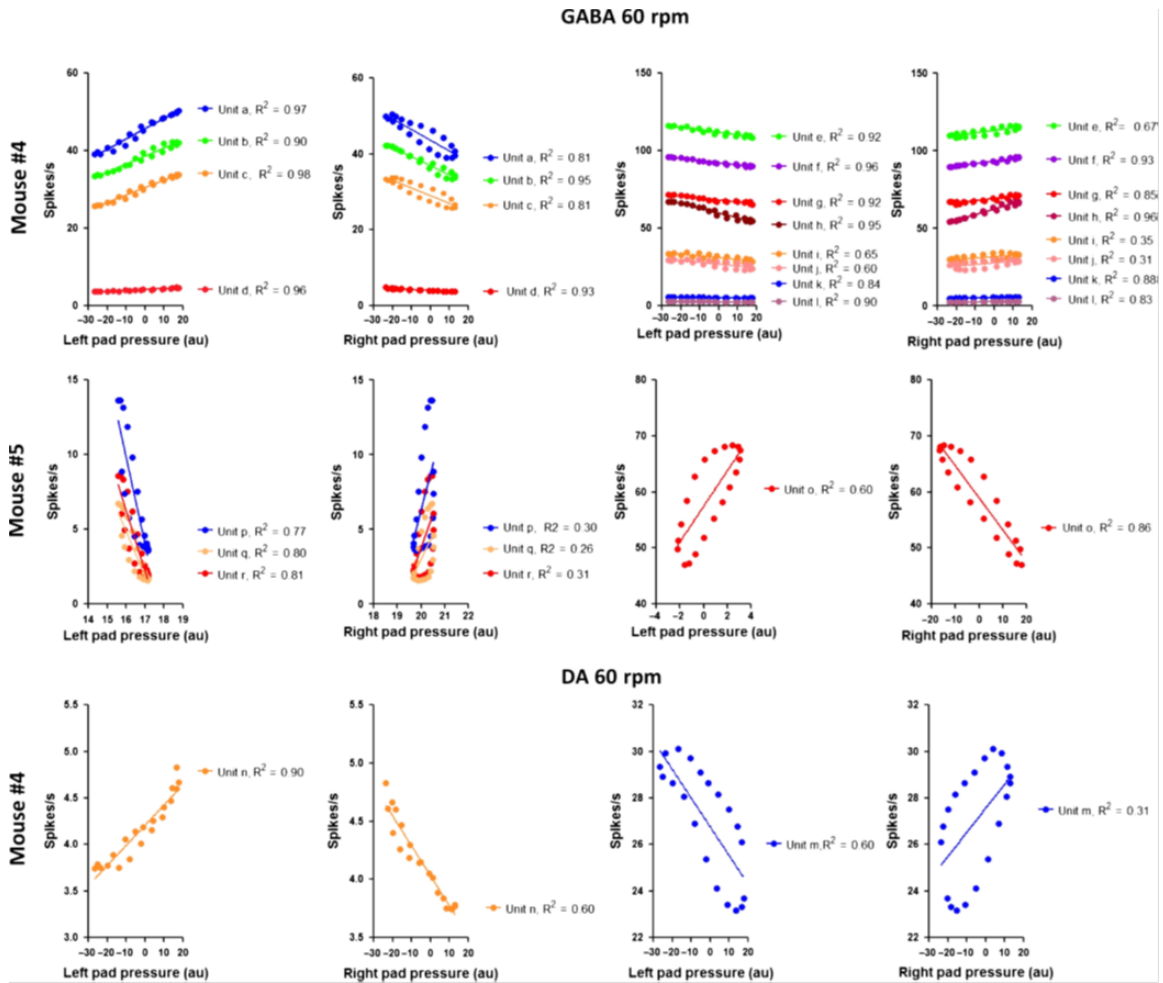


Figure 7. Relationship between mean firing rate and pressure pad readings in different populations of neurons. For each mouse, units significantly modulated by tilt were used in a regression analysis. In two mice, the coefficient of determination ( $R^2$  value) was calculated between the pressure pad reading and mean firing rate in a representative session. The corresponding colored dots show the mean firing rate of that population at different angles of tilt. For all regression analyses shown,  $P < 0.05$ .

## **2.4. Discussion**

### **2.4.1. Summary**

Here we exposed freely standing mice to two speeds of continuous postural disturbance along the roll plane while recording wirelessly from the substantia nigra. We found two clear patterns of neural activity during postural disturbance: L+R- cells that increased activity as the animal was tilted to the left and decreased activity as the animal was tilted to the right, and L-R+ cells that exhibited the opposite pattern of activity. These two cell types were seen in both putative DA and putative GABA cells, and in both left and right substantia nigra. In agreement with clinical observations (Bloem et al., 1995; Miller, 1968), these results suggest an important role for outputs of the basal ganglia in controlling posture.

Although the exact destinations of the signal reported here is unclear, it is known that the substantia nigra sends strong projections to a number of brainstem motor nuclei which are involved in different aspects of postural control. For example, the SNr has prominent projections to the PPN and MLR, which are thought to orchestrate motor sequences and transitions during locomotion (Garcia-Rill, 1986; Grillner et al., 2008, Takakusaki et al., 2003). The SN also projects to the tectum (Hikisaka, 2000), which controls orienting movements of the eyes, head and body (Saitoh et al., 2007). All of these target regions of the SNr exert an effect through the reticulospinal system, the system which has classically been most directly implicated in postural control.

#### **2.4.2. Reticulospinal cells and postural control**

Previous work has shown that the reticulospinal system can generate movements which resist the effects of postural disturbances (Zelenin et al., 2007). In lamprey, reticulospinal neurons are known to receive inputs from the vestibular nuclei and send projections to motor neurons. For each axis of postural control investigated, two complimentary types of reticulospinal neurons were found; each was activated by rotation in the opposite direction and produced movements that counteracted the effect of that rotation on body position (Pavlova et al., 2004; Zelenin et al., 2007). There are thus obvious parallels between reticulospinal activity and the nigral activity during postural disturbance. Given the known anatomical connections, such similarities are not surprising (Takakusaki, 2003; Takakusaki al., 2008). Our results suggest that the basal ganglia may represent a hierarchically higher level for the control of posture. The opponent outputs we observed may indeed ultimately influence distinct reticulospinal pathways responsible for the control of distinct muscle groups (Peterson, 1979; Peterson et al., 1979), via projections to tectum and PPN.

Interestingly, the opponent activity observed in this study is also similar to what has been observed in mice performing timed instrumental behaviors (Fan et al., 2012). When the mice were required to hold down a lever for a minimum time duration to earn a food reward, both GABA and DA neurons were found to exhibit opponent activity, one population increasing while another decreases its firing rate. Thus, for both posture control and reward-guided instrumental behavior the basal ganglia output can

be similar, generating a pair of opponent signals sent to downstream structures. These antiphase output signals appear to be a general feature of BG outputs.

### **2.4.3. Closed loop control of posture**

Posture control appears to operate as a closed loop negative feedback control system (Lacquaniti & Maioli, 1994). According to this interpretation, posture along a particular axis of body orientation is continuously restored to an equilibrium point through a sensorimotor transformation from vestibular input to a pair of competing spinal reflexes (Deliagina et al., 2006; Zelenin et al., 2007). However, because the internal equilibrium 'set point' for posture can change (Deliagina et al., 1998; Deliagina et al., 2006), then postural control cannot operate as simple sensorimotor transformation, but must instead operate through a comparison of sensory input to an internal reference signal (Yin, 2014a). Thus, a more computationally precise way of describing this function is as a perceptual control system (Powers, 1973), in which desired posture is represented as a set of controlled perceptual variables with internally specified reference values. The current state of each perceptual variable is continuously compared against its reference value to calculate an instantaneous error representing the difference between current state and desired state. The error is then continuously sent as a reference signal to lower systems in the control hierarchy that are capable of reducing it.

For example, orientation along the roll axis may be perceived in a quadruped as a single perceptual variable generated through a weighted combination of somatosensory (i.e. pressure distribution on the feet), vestibular and visual inputs (Figure 8). If an animal is tilted along the roll axis, the value of this perceptual variable will change compared to the reference value and generate an error of a particular sign. Depending on magnitude of this error, the animal may produce a corrective output ranging from reciprocal extension and retraction or sway of limbs across the body, to rapid leftward or rightward locomotor sequences. The sign of the error will determine whether the corrective responses are generated in the left or right directions.

According to this model, body orientation is controlled through a shared motor hierarchy in which a number of variables may be controlled at once as long as their outputs do not cancel each other. For example, an animal may control orientation along roll and pitch planes simultaneously by sharing the same four leg posture control systems as an output function to reduce the error (Figure 8). If the animal tips left, reference pressure to the left feet is increased; if the animal tips forward, reference pressure to the front feet is increased; if the animal is tipped left and forward then the same commands are simply added together. The same basic principle holds true if the animal is walking across a tilted surface; the outputs of locomotor and orientation control systems are added together to achieve simultaneous control of both variables.

An important property of such a hierarchy is that higher systems controlling 'voluntary' actions, such as the basal ganglia, will need to adapt to the necessary and

ongoing behavior of lower systems. If an animal is standing on a rightward tilted platform, then in order to remain upright it will need to modify its body configuration by extending the limbs on the right side of its body and retracting the limbs on the left side. While the platform remains tilted, the performance of certain higher systems likely depend on this altered configuration being treated as the new neutral baseline from which voluntary movements must leave from, and return to; to control a motor sequence on this tilted platform would require that this altered baseline be maintained by 'adding' it into the outputs, or else the outputs will likely fail, or the animal will fall over, or both. Thus, regardless of whether the postural correction itself is a function of lower brainstem regions, outputs of the basal ganglia must adapt accordingly. The patterns reported here could reflect such a shifting baseline for the effective neutral position of lower reference signals.

However, as previously mentioned, the correlations between neural activity and postural disturbance reported in the current study could also represent voluntary changes in the reference states of lower systems by the BG. In the same way that a passenger must produce voluntary movements and postural adjustments to succeed in drinking a cup of coffee in a moving car, a mouse must produce voluntary movements and postural adjustments to succeed in its own ongoing behavior on a tilting perch. In both of these cases, the voluntary movements and their neural substrates are expected to correlate in time, extent and direction with disturbances.

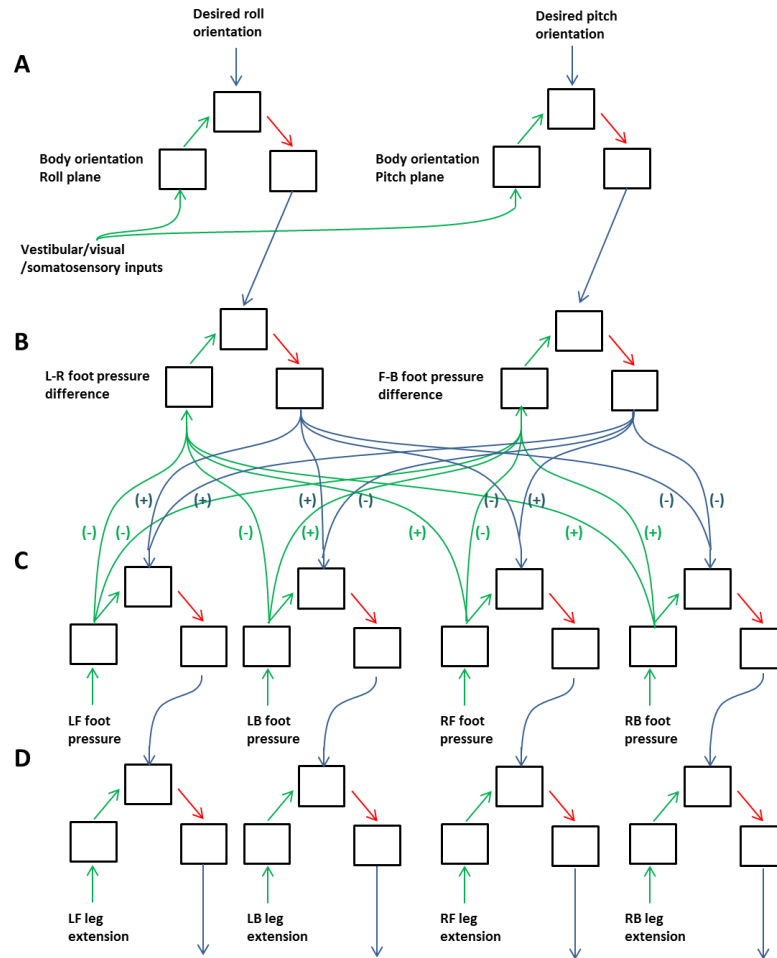


Figure 8. A hypothetical orientation control hierarchy showing how two axes of postural control can share the same motor output. Green arrows represent perceptual inputs; blue arrows represent output reference signals; red arrows represent error signals. (A) Level 4 of the control hierarchy. There are two systems at this level; one for roll control and one for pitch control. (B) Level 3. There are two systems at this level; one for controlling the foot pressure difference between the left and the right side of the body and one for controlling the front-back difference. Perceptual inputs to these systems are derived from perceptual inputs from systems at level 1. Outputs to lower systems represent the difference between reference signal and perceptual signal, sign switched so that the outputs are produced in the correct direction. (C) Level 2. There are 4 systems at this level; one controlling foot pressure at each individual foot. Each system receives a reference signal from both systems at level 2, which are added together. (D) Level 1. There are 4 systems at this level; one controlling perceived leg extension at each individual leg. Each system receives a reference signal from both the food pressure control system for the same leg

#### **2.4.4. DA-GABA interactions**

Our results support a model of postural control, and motor control in general, as a closed loop perceptual control system. However, the exact functions performed in this system by SNc DA and SNr GABA neurons remain unclear. It also remains unclear which input channels are responsible for the graded and continuous modulation of neural activity by postural disturbances observed here. While the GABA neurons are known to inhibit DA neurons, they are also known to be excited by DA. The activation of D1 receptors in SNr, through a TRPC3 mechanism, may be responsible for tonic depolarization and sustained spiking in the GABAergic projection neurons (Zhou, 2010). Because the basal ganglia have access to higher-order sensory information, which combines proprioceptive, visual, and vestibular inputs, the GABAergic outputs from the SNr can represent error signals in higher order control systems. Through connections to brainstem motor regions, these GABA signals can specify reference perceptions for lower levels, such as speed of locomotion at the MLR or orientation relative to target at the tectum. Through thalamic projections and the pyramidal tract, SNr GABA signaling may specify the body configurations and control sequences required to execute complex learned behavior. SNc DA output, on the other hand, targets a different set of brain regions primarily in the striatum. Because of its function as a neuromodulator that can adjust sensitivity in basal ganglia circuits, it is possible that dopamine performs a critical adaptive control process, such as gain adjustment in striatal outputs, and thus BG outputs, in response to signal velocity. The similarity in activity between dopamine and

GABA activity seen during postural disturbance could thus be due to the fact that adaptive gain control and movement are tightly coupled, or due to the fact that we used a continuous sinusoidal disturbance which makes it difficult to differentiate between signals representing velocity and those representing position.

It should also be noted that although the regions of the SN we recorded from (Figure 3) contain mostly GABA and DA neurons, we cannot ascertain the type of neurotransmitter used by the recorded neurons. Nor do the present results tell us how different types of tilt-activated neurons are related to the known heterogeneous cell groups in the substantia nigra (Henny et al., 2012). Thus, any reference to nigral GABAergic output or to nigrostriatal DA transmission is provisional. Future studies using direct and selective manipulations of these neuronal populations, e.g. with optogenetic techniques, are needed to confirm their functional roles

#### **2.4.5. Classical model in need of revision**

This continuous modulation of output shown here is at odds with the classical perspective of the basal ganglia as a gate which must sustain output at a steady level to function properly (Hikosaka, 2007). According to this model, the basal ganglia function as a gate by tonically inhibiting tectal and brainstem nuclei before behavior and transiently disinhibiting these target nuclei when a particular behavior is selected. It assumes that during a baseline period of no apparent behavior, the neural outputs of

those nuclei are suppressed by the basal ganglia. But this assumption is unrealistic, as behavior is rarely all or none. This fact becomes more apparent when one considers the importance of smoothly modulating the extent of various aspects of movement during natural behavior, such as speed of locomotion and degree of turning. Another finding which is at odds with the classical literature is the observation of two populations of SN GABA cells with reciprocal patterns of activity. This bidirectional modulation has been reported previously (Fan et al., 2012), and, combined with the current findings, suggests a scenario in which the high baseline firing rate of SNr GABA represents a 'zero' from which deviations above and below can act as specific positive and negative signals sent to command lower systems in different directions and to different degrees.

### **3. Basal ganglia outputs map instantaneous position coordinates during behavior<sup>1</sup>**

#### **3.1. Introduction**

As discussed in the previous chapter, the prevailing model of BG function assumes that a decrease in inhibitory output enables movements, whereas an increase prevents movements (Albin et al., 1989; DeLong, 1990; Hikosaka et al., 2000). Although this model is supported by a number of classic studies (Hikosaka et al., 2000), it is also incompatible with a number of behavioral and neural observations. For example, it is clear that behavior is rarely all or none but instead consists of a number of overlapping motor programs with graded intensity; an animal may speed up or slow down, turn more or less, and maintain upright posture all at once. It has also been observed that neurons in the SNr both increase and decrease their firing rates in relation to movement (Gulley et al., 1999; Basso and Wurtz, 2002; Fan et al., 2012; Freeze et al., 2013). As an attempt to fit these opponent outputs to the classic model framework, it has been proposed that the BG outputs disinhibit some actions while inhibiting all competing actions (Mink, 1996; Cui et al., 2013). However, this ‘focused selection’ model does not clearly define the meaning of ‘action’, and implies a scenario in which behavior consists of a set of motor programs which are simply ‘on’. This model makes no attempt to

---

<sup>1</sup> This chapter is a modified version of a previously published article: Barter JW, Li S, Sukharnikova T, Rossi MA, Bartholomew RA, Yin HH (2015b) Basal ganglia outputs map instantaneous position coordinates during behavior. *J Neurosci* 35:2703–2716.

explain the role of basal ganglia outputs in generating the complexity or graded nature of the kinematic outputs seen during natural behavior.

In the experiments of the previous chapter we demonstrated continuous and graded modulation of substantia nigra activity during a postural control task. The reported correlations between neural activity and tilt angle are thought to reflect adjustments in the parameters and reference states of motor systems required to maintain body stability on a tilting platform. However, because we did not directly record kinematic outputs in this study then the exact relationship between neural changes and postural changes remained unknown. The current experiment was designed to address this unknown through the use of continuous motion tracking of the head in parallel with neural recording from the substantia nigra during a simple goal-directed task.

In this study, mice (n=10) were water deprived and then positioned in the same perch used in experiment 1. However, in this study, the perch was kept stationary and modified by the addition of a movable drinking spout (Figure 10 A and C). During each session, mice performed a simple reward-guided task in which sucrose solution was delivered in small quantities ~2s after the presentation a cue. The purpose of this task was to elicit reward-directed head movements (recorded and tracked with the use of a head-mounted LED and a front-facing video camera), and to correlate these continuous movements with the activity of GABA output neurons in the SNr. Z axis movement, locomotion and body rotation were prevented by the small size of the perch so that

head tracking data largely represent x and y-movements of the head along the frontal plane (Figure 10A).

## **3.2. Materials and Methods**

### **3.2.1. Subjects and Surgery**

All procedures were approved by the Duke University Institutional Animal Care and Use Committee. Ten male C57BL6/J mice (25-31g) were used in the experiments. Detailed procedures for surgeries have been described previously (Fan et al., 2011; Fan et al., 2012; Rossi et al., 2013a). Sixteen-channel electrode arrays (Innovative Neurophysiology) were lowered at the following stereotaxic coordinates in relation to bregma: 2.9-3.0mm posterior, 1.2mm lateral, and 4.6-4.7mm below brain surface (5 mice were implanted in the left SNr; 5 in the right SNr). The arrays consisted of micro-polished tungsten wires, 35 $\mu$ m in diameter and 7mm in length, arranged in a 4 by 4 configuration. All arrays were attached to an Omnetics connector and fixed to the skull with dental acrylic. Row spacing was 200 $\mu$ m and electrode spacing was 150 $\mu$ m. Following the completion of the experiments, all mice were perfused and their brains sliced with a Vibratome into 100 $\mu$ m coronal sections, stained with thionin, and examined under a microscope to verify electrode placement.

### 3.2.2. Behavioral task

To induce mice to perform reliable movements repeatedly, we gave them limited access to water. After the recording session each day, they had free access to water for 1 hour. Each mouse received about 0.5ml to 1.3ml of 10% sucrose during the experimental session. When they had free access to water afterwards, they consumed ~2ml. The health of the mice was monitored daily by the laboratory staff and veterinarians from the Division of Laboratory Animal Resources at Duke University. On weekends, all mice were given continuous free access to water.

During the session, mice could obtain 10% sucrose solution from a spout located next to the platform. They perched on a platform positioned within a tube (5cm diameter, 3.8cm length, elevated 40cm). The platform (13cm) was suspended by a custom built rigid 'T' shaped structure formed of 1cm diameter aluminum rod. Mice were first exposed to the elevated platform for at least 1 hr before the start of the experiments, allowing them to acclimate to the experimental setup.

In most experiments we used a simple reward-guided task, in which sucrose solution was periodically delivered into a spout just below the platform. Each trial began with the presentation of a tone (21.6dB) followed by the delivery of 13 $\mu$ l 10% sucrose solution dispensed by a Valvelink 8.2 (AutoMate Scientific, click of the solenoid: 34.7 dB) and delivered through a rubber tube terminating in a metal spout. On some sessions, the spout was moved laterally to different positions along the front bottom of the platform. The approximate locations of the spout (distance from the edge of the frame

in mm) were: 40, 66, and 86 (x-axis), and 19 (y-axis).

On some sessions, a 100ms tone was used as a cue, and the sucrose was delivered ~2s after the termination of the tone (trace conditioning). On other sessions, a 2s tone was used, and the sucrose was delivered immediately after cue termination. Each session contained 30-250 trials, with an inter-trial-interval of 20-50s. Because the variation in the cue duration did not have any effect on the relationship between position coordinates and neural activity, the data were combined in the analysis.

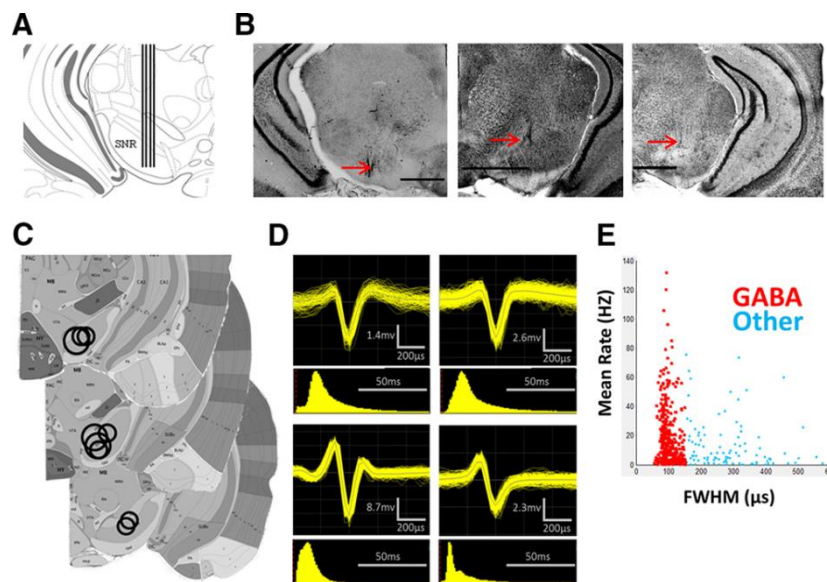


Figure 9. *In vivo* electrophysiological recording and classification of single units. (A) Illustration of the representative placement of electrode array in the SNr. (B) Placement of the 4x4 electrode array as shown in representative coronal brain sections from three different mice. Red arrows indicate electrode tracks. Scale bar, 500μm. (C) Summary of electrode placements. The coronal sections are from the Allen Mouse Brain Atlas (Lein et al., 2007); <http://mouse.brain-map.org/>. (D) Four representative examples of putative GABAergic neurons, showing the waveforms and interspike interval distribution. (E) Plot of firing rate versus spike width. Neurons with wider action potentials are excluded (other).

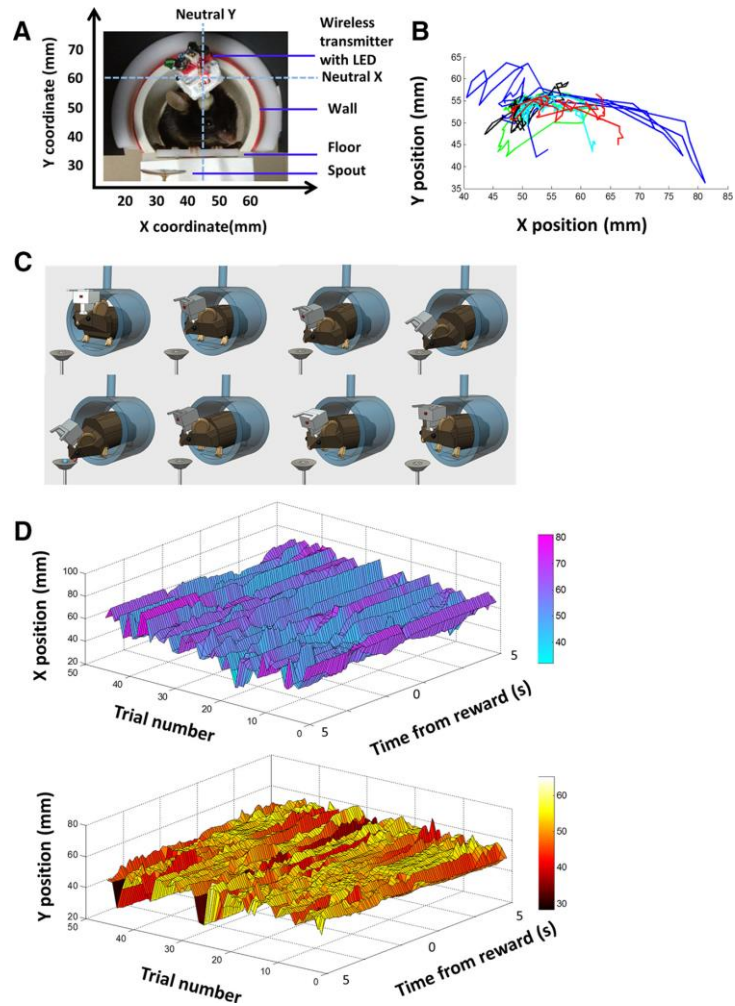


Figure 10. Illustration of behavioral task and wireless recording. (A) Illustration of in vivo wireless multielectrode recording and the behavioral task. The mouse perches on a small platform, where it is free to move, but locomotion is not possible as the platform is elevated. On its head is a 16-channel wireless headstage (1.5 x 1.5cm) weighing 3.8g and connected to a chronically implanted multielectrode array targeting the SNr. Sucrose solution is delivered into the spout periodically, preceded by a brief tone. Position of the LED is defined on a Cartesian plot with the ordered pair (x, y). (B) Illustration of variability in movement trajectory. Each color represents position change during a single trial. (C) Diagram illustration of a typical movement initiated by the mouse to collect sucrose from the spout. (D) Representative illustration of LED position from 45 consecutive trials in a session. The x- and y-coordinates are plotted separately.

Typically a mouse would move its entire body after the cue presentation and upon reward delivery. Its body was not restrained, but the size of the tube prevented it from turning around. The mouse could readily move towards the spout to collect sucrose reward and move back to resume its resting position. In some experiments (4 mice), we used both sucrose and air puff trials. The introduction of aversive air puff trials is designed to test whether the observed correlation between neural activity and movement kinematics is independent of the valence of the outcome. For sessions comparing reward trials and air puff trials, either an ABAB design was used, in which reward trials and air puff trials were presented in alternate blocks, or an AB design was used, in which reward trials were followed by air puff trials. The cue duration for these sessions was always 100ms. Air puffs (82.7kPa) were 200ms in duration and delivered from a computer-controlled 1500 series dispenser (EFD) from 10cm below the animal.

### **3.2.3. Video tracking**

Mouse movement was recorded with a steady-frame rate camera (Sony Handicam HRD-XR160) at 30frames/s. Video and neural datasets were aligned with an LED flash at the start of each session which generated a video time-marker in synchrony with a transistor-transistor logic (TTL) pulse in the Cerebus data acquisition system (Blackrock). Mouse movement was digitized offline using Optimap (Triangle BioSystems International), which tracked LED position in each frame in pixel coordinates. Because of

the orientation of the camera and the fact that the mouse is prevented from significantly changing orientation, these pixel coordinates accurately reflect head position in the frontal plane.

#### **3.2.4. Neural recording and data analysis**

Single unit activity was recorded with miniaturized wireless headstages (Triangle BioSystems International) using the Cerebus data acquisition system (Fan et al., 2011). The chronically implanted electrode array was connected to a wireless transmitter cap (~3.8g). Attached to the front end are miniature LEDs (2mm, Osram, powered by 2 Energizer 379-type batteries). During recording sessions, single units were selected using online sorting. Before data analysis, using Offline Sorter (Plexon) the waveforms were sorted again to eliminate noise and multi-unit waveforms (Fan et al., 2011; Rossi et al., 2013a). Only single-unit activity with a clear separation from noise (at least 5 to 1 compared to the noise band) was used for the data analysis (Nicoletis, 2007). The behavioral and electrophysiological data were recorded with a Cerebus data acquisition system and analyzed with Matlab, Neuroexplorer, and Graphpad Prism.

### **3.3. Results**

#### **3.3.1. Histology and single unit classification of putative GABAergic neurons**

Using chronically implanted 16-electrode arrays, we recorded from putative GABAergic output neurons in the SNr (Figure 9). The nissl stained brain slices showed that the electrode arrays in all mice were placed in the medial SNr, which receives projections primarily from the dorsal striatum (Bolam et al., 1993; Parent and Hazrati, 1995).

The putative GABAergic output neurons, which constitute the majority of neurons in the SNr, are known to inhibit downstream structures (Chevalier et al., 1984; Hikosaka, 2007; Zhou and Lee, 2011). They are characterized by high firing rates and narrow spike waveforms (Hikosaka, 2007; Jin and Costa, 2010; Zhou and Lee, 2011; Fan et al., 2012; Rossi et al., 2013a; Barter et al., 2014). For cell type classification, we used a criterion of 160  $\mu$ s for the full width half maximum measure (FWHM). As shown in Figure 1E, the FWHM of all neurons classified as putative GABAergic output neurons is less than 160 $\mu$ s.

#### **3.3.2. Behavior**

We tracked the position of the LED on the head of the mouse at 30frames/s. From the video recording we were able to obtain the xy Cartesian coordinates of the head position over time (Figure 10A-B). Because our camera is facing the animal, an

increase in the x-value indicates movement to the left of the mouse, whereas a decrease indicates movement to the right. An increase in the y-value indicates upward movement, whereas a decrease indicates downward movement.

All mice reliably moved following the tone to consume sucrose solution from the spout. Given the use of a single LED for video tracking, we cannot rule out the movement included head or eye rotation, or extension along the z-axis. However, unlike in primates, rodents rarely make eye or head rotations independently of the rest of the body. As illustrated in Figure 2C, a typical movement involved configuration changes throughout the entire body. Each movement in a session was also unique (Figure 10D), resulting in significant variability in movement kinematics throughout a single session. The variability in movement kinematics in unrestrained animals is in agreement with classic studies of human movements (Bernstein, 1967).

### **3.3.3. Neural activity reflects position coordinates**

From the motion tracking data we obtained x and y-coordinates of the head LED position at 30frames/s. When these are compared to the single unit activity, we observed a striking correlation between the firing rate and the Cartesian coordinates of head position (Figure 11).

The activity of 76% (243 of 318) of all putative GABAergic neurons is significantly correlated with the Cartesian coordinates of head position ( $p < 0.001$  for Pearson

correlation). Because each movement involves a change in both x and y-coordinates (Figure 10B), these measures can be correlated with each other. Because no movements are perfectly diagonal, however, x and y-coordinates do not change equally (Figure 10B). We classified a neuron as being correlated with x or y-coordinates only when

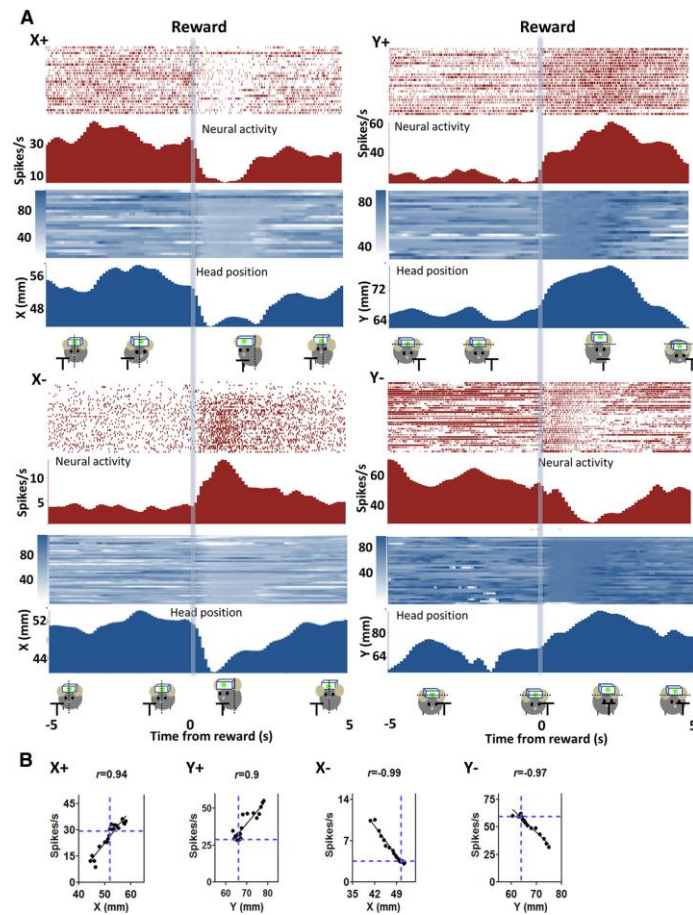


Figure 11. Relationship between single-unit activity from SNr and raw position coordinates during movement. (A) The firing rate of SNr neurons exhibits high correlation with instantaneous position coordinates. The position is defined from the edge of the frame in the captured image. Higher x-coordinate values indicate positions to the left of the resting neutral position, whereas lower x-values indicate positions to the right. In each of the four panels, red raster plots and histograms illustrate the activity of a single neuron; blue plots illustrate the corresponding x or y-axis head

position of the animal during the same session, as measured with LED tracking. The cartoon sequence at the bottom of each panel depicts the head movement. All plots are centered around reward delivery, which is marked with a light blue bar. The top left panel shows a neuron with positive correlation with x-coordinates of the head (X+ neuron,  $p < 0.001$ ); top right panel shows a neuron whose activity correlates positively with the y-coordinate of the head (Y+ neuron,  $p < 0.001$ ); bottom left shows a negative correlation with X position (X- neuron,  $p < 0.001$ ); bottom right shows a negative correlation with y-position (Y- neuron,  $p < 0.001$ ). (B) Correlation between firing rate and instantaneous position coordinates.

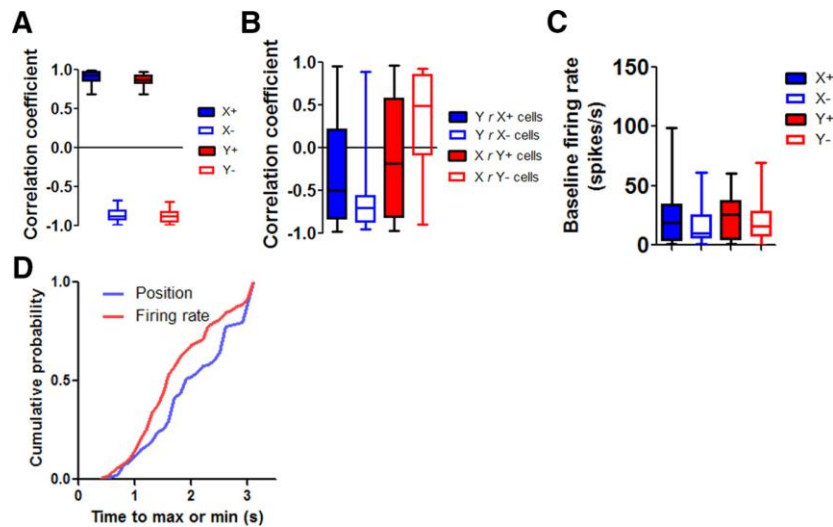


Figure 12. Summary of different types of nigral neurons. (A)  $r$  values for the four types of neurons identified, showing high correlation between firing rate and either x or y-coordinate. (B)  $r$  values for the four types of neurons identified, showing much reduced correlation between firing rate and the alternative coordinate. For example, activity of X+ neurons is poorly correlated with the y-coordinate. C, Baseline firing rate during a 2s period before trial onset. (D) Timing of the neural activity (all four classes of neurons) in relation to movement. Cumulative probability distribution of the time it takes from reward delivery and the maximum or minimum value of the firing rates or position coordinates. For the position data, this is approximately the time it takes for the mouse to reach the farthest point from its resting position in either the x or y-axis.

the correlation is very high ( $p < 0.001$ ). In this way we were able to identify neurons with activity reflecting either the x-coordinates or the y-coordinates of the instantaneous position.

For movement in any direction, single unit activity over time was either positively or negatively correlated with head position values (Figure 11). Among the x-correlated neurons, one class increases firing when the animal moves to its left side (X+) and decreases firing rate when moving to the right. The firing rate is positively correlated with the x-coordinates of the LED position ( $n=100$ , mean firing rate= $23.0 \pm 2.1$ Hz, mean  $r=0.91 \pm 0.008$ ,  $p < 0.001$ ), but poorly correlated with y-coordinates (mean  $r = -0.29 \pm 0.05$ ). Another class shows the opposite pattern, increasing firing rate when the animal moves to the right (“X- neurons”, negatively correlated with x-coordinates ( $n=39$ , mean firing rate= $17.5 \pm 2.6$ Hz, mean  $r=-0.84 \pm 0.01$ ,  $p < 0.001$ ), but less correlated with y-coordinates (mean  $r=-0.61 \pm 0.05$ ).

Among the y-correlated neurons, “Y+ neurons” are positively correlated with the y-coordinates: they increase firing with upward movement ( $n = 21$ , mean firing rate = $24.4 \pm 4.1$ Hz, mean  $r=-0.85 \pm 0.02$ ,  $p < 0.001$ ), but poorly correlated with x-coordinates (mean  $r=0.33 \pm 0.12$ ). “Y- neurons” (Down+) are negatively correlated with the y-coordinates: they increase firing with downward movement ( $n=83$ , mean firing rate =  $20.8 \pm 2.0$ Hz, mean  $r=0.87 \pm 0.009$ ,  $p < 0.001$ ), but poorly correlated with x-coordinates (mean  $r=-0.12 \pm 0.07$ ). Figure 4 shows the correlation coefficient ( $r$  values) for all 4 types of neurons. Neurons that are correlated with x-coordinates are poorly correlated with

the y-coordinates, and vice versa. On the other hand, these different types of neurons showed similar baseline firing rates.

One question we addressed is whether the change in neural activity precedes the change in head position. To assess the relative timing of these events, we measured the time it took for the firing rate or movement to reach the maximum value or minimum value (depending on the type of neuron) after the reward delivery (Figure 12D), which roughly corresponds to the time point at which the animal has reached the sucrose spout. We found that the neural changes typically preceded head position changes, suggesting that the nigral output could be used to generate the change in head position. It should be noted, however, that higher temporal resolution in video tracking will be needed to provide a better estimate of the lag between neural activity and movement.

Another question is whether the observed correlation during movement is still present in the absence of any overt movement. To address this, we compared the correlation between neural activity and position during trials with a comparable period between trials (a 10s window from the inter-trial-interval just before the onset of the trial). Not surprisingly, the coefficient of variation in position was much lower during the resting period (Figure 13), showing less movement during this period. As expected, since there was little variation in either the neural activity or position, the correlation was also much weaker.

### **3.3.4. Normalization of neural activity**

The mean firing rate of recorded neurons was highly variable. For all neurons in a particular class, the correlation with the position coordinate is highly similar, despite large variations in baseline firing rates (Figure 14). When the firing rate is normalized (divided by the baseline), the neurons show a remarkably uniform response in relation to changes in position coordinates. This is found in all 4 classes of neurons. Thus a given change in position coordinates is not accompanied by a certain amount of change in absolute firing rate, but rather in percent change in firing rate. For example, a neuron that fires at 30Hz at the onset of the movement can reduce its firing rate to 15Hz during a particular movement, whereas a neighboring neuron that fires at 14Hz will reduce its firing rate to 7Hz. When normalized both neurons show comparable proportional change from their baseline firing rate. In addition, as shown in Figure 6C, the firing rate modulation (% of baseline) needed to move a certain distance (1mm) is similar for most neurons.

### **3.3.5. Dissociation from reward expectancy**

The BG has long been implicated in reward-guided behavior (Kawagoe et al., 1998; Rossi et al., 2013b). Since our behavioral task used a food reward to elicit movement, one obvious question is whether the observed correlation is specific to reward-guided movements. Because the firing rate mirrored the position of the animal,

our results suggest that the SNr output may be necessary for all actions, not just reward-guided actions. If this is the case, then we would expect that in the absence of any rewards, or in response to an aversive stimulus, SNr activity should still be correlated with head position during movements. To address this question, we conducted an additional experiment in 4 mice, in which rewards were periodically replaced with an aversive air puff. In this experiment, a block of rewarded trials was followed by a block of air puff trials, or blocks of sucrose and air puff trials alternated in an ABAB design. On aversive trials, a brief air puff to the face is used as an aversive stimulus that reliably generates avoidance responses (Thompson et al., 1998; Matsumoto and Hikosaka, 2007). Using this technique, we were able to examine the response of the same neurons during sucrose and air puff trials. As shown in Figure 15, on both reward and air puff trials the mice reliably moved at the time of the cue and at the time of the air puff delivery. The movement trajectory, illustrated by the red trace in the cartoon, differed significantly between rewarded and aversive trials. On air puff trials, instead of approaching the spout, the animal moved its head up and away from the air puff. Yet the correlations between position coordinates and neural activity were comparable on both reward and air puff trials. This correlation is therefore independent of the presence of reward. These results suggest that the SNr output is crucial for controlling the kinematics of voluntary movements, regardless of the goal of the movements—whether to seek reward or to avoid harm. These results suggest that the SNr output is crucial for

controlling the kinematics of voluntary movements, regardless of the goal of the movements—whether to seek reward or to avoid harm.

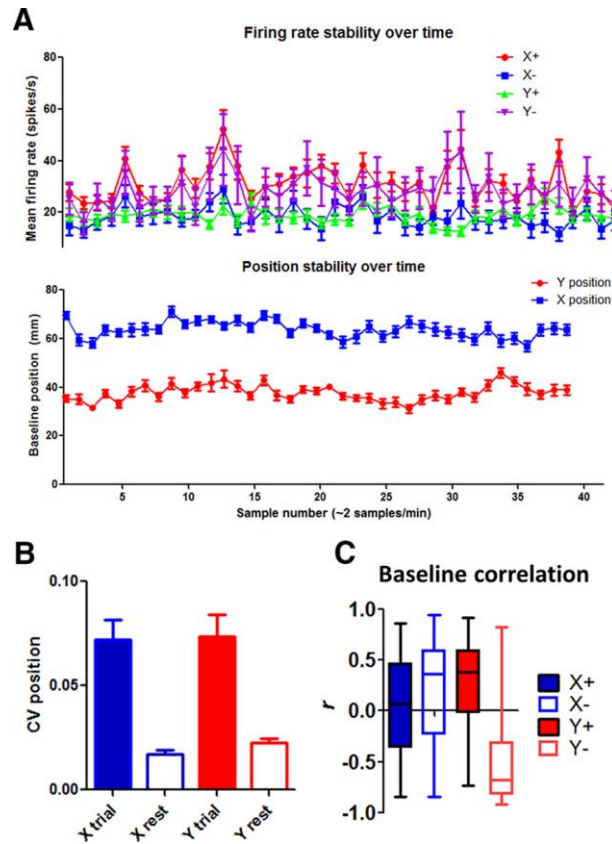


Figure 13. Summary of baseline neural activity and movement. (A) Stability of position measure and firing rate. We extracted 10 s time windows during rest periods from all sessions. The position signal and the neural activity are shown. There is no systematic change in these measures during the rest period over the course of a session. (B) Coefficient of variation (CV, SD/mean) in the position measure during a trial and during the rest period. During the rest period between trials, there is little movement as indicated by much lower CV values in the position. (C) Correlation between firing rate and during the rest period, when there is little movement.

### 3.3.6. Topographical distribution

Because each class of neurons classified in the present study is correlated with a unique set of position coordinates, then if their firing rates were averaged the resulting signal would not reflect any movement parameter accurately. We examined the relationship between local field potential (LFP), a measure of population activity in the SNr recorded using the same electrodes, and position coordinates. As expected, the LFP measure is not highly correlated with position coordinates. Of 166 LFP channels analyzed, only 15 show significant correlation with any of the 4 position variables (Figure 16). Thus more global measures of neural activity, such as LFP or the Blood-Oxygen-Level-Derived (BOLD) signal in fMRI, cannot accurately reveal the nigral representation of position coordinates during movement.

An additional important question is where these different classes of neurons are located in the SNr. It is plausible that there is regular spatial distribution of cell types, or even some form of somatotopic mapping. Unfortunately, with our *in vivo* recording techniques it is difficult to ascertain the precise location of recorded cells. However we were able to quantify the degree of ‘intermingling’ of recorded neurons by analyzing the co-occurrence of cell types on all electrodes that recorded activity from more than one neuron. This technique assumes that the co-occurrence of different neurons on a single electrode can serve as a measure of spatial proximity, and thus degree of

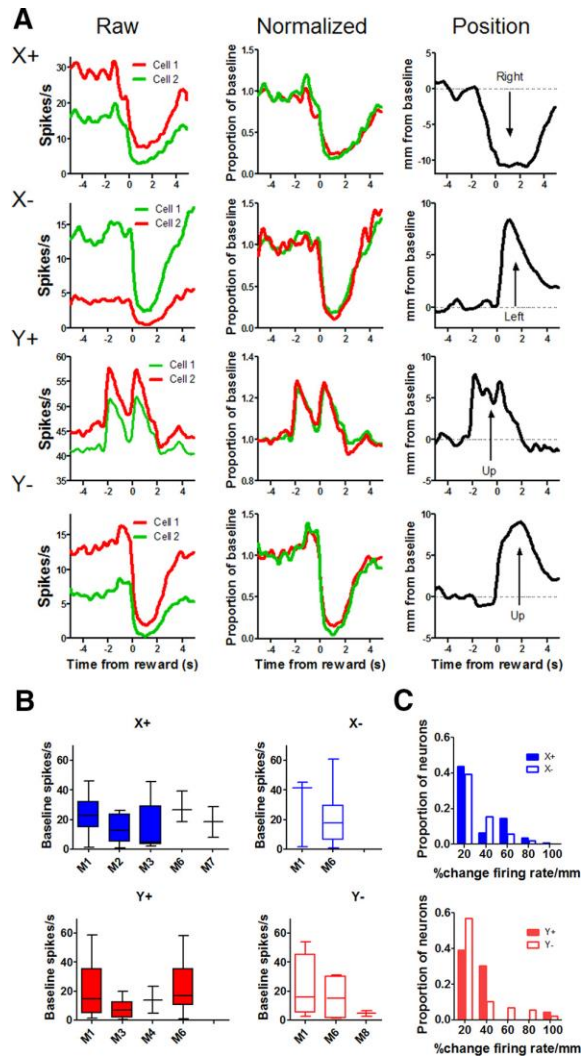


Figure 14. Normalization of firing rates in SNr neurons. (A) Each row includes raw firing rates and normalized firing rates from two neurons, and corresponding position change from a different mouse. Left column: raw firing rates of two neurons of a given type from a mouse. Middle column: normalized firing rates of the same neurons. The rates are normalized by dividing by the baseline rate of each neuron. Right column: position change. The relative change in position from baseline is shown, as absolute position values are defined by the edge of the camera frame. (B) The range of baseline firing rates in neurons from the four different classes. Each graph represents the range of baseline firing rates from a single session. Data from all mice with multiple neurons from a class are shown. There is considerable variability in baseline firing rates, although the correlation with position coordinates is highly similar. (C) Distribution of firing rate modulation (% of baseline) per millimeter. Most neurons show comparable degree of modulation relative to movement amplitude.

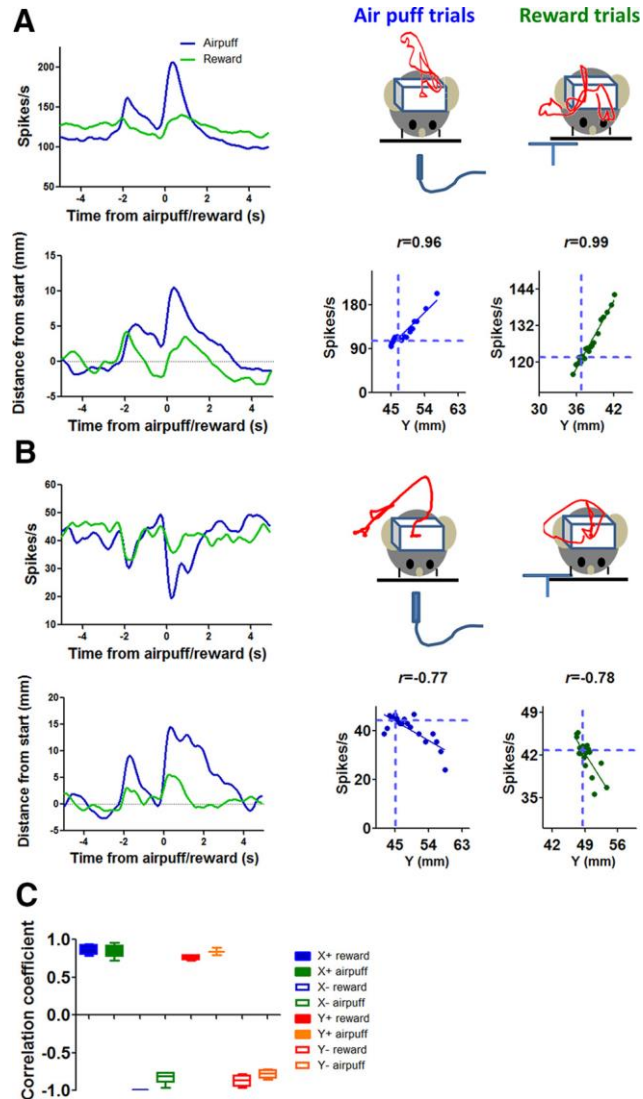


Figure 15. Relationship between firing rate and Cartesian coordinates is similar for both reward and air puff trials. (A) Left: firing rate of a Y+ neuron in relation to air puff/reward. The activity of the same neuron from both types of trials is shown. Right: example movement trajectory for air puff and reward trials. The correlation between neural activity and Cartesian coordinates is high on both sucrose reward trials and air puff trials. (B) Firing rate of a Y- neuron. Same as above. (C) Distribution of  $r$  values of all neurons recorded during both reward and air puff trials.

intermingling. As shown in Figure 16, it is common for a single electrode wire to detect signals from neurons from different classes, e.g. both X+ and Y+ neurons. Thus there appears to be significant intermingling of the different classes of neurons, though such a coarse analysis cannot reveal any fine spatial mapping of the neuronal classes. On the other hand, the possibility of topographic distribution of the respective functional cell classes is supported by the high proportions of simultaneous recordings of cells with similar properties, and by the few instances in which LFP was highly correlated with position coordinates (Figure 16E). It is also possible that mixed pairs recorded from a single electrode could result from recording in border zones.

### **3.3.7. Egocentric reference frame and movement direction**

The above results demonstrated that the firing rates of different SNr neurons reflect the Cartesian coordinates of the animal's instantaneous head position. However, the Cartesian mapping reflects the observer's view of the animal, as captured by the camera. From the perspective of the mouse, an egocentric frame of reference is appropriate. If we adopt an egocentric reference frame, then changes in position coordinates reflect movements in four directions: up, down, left, right (Figure 17). Thus, for movement in a particular direction, some neurons increase firing whereas others reduce firing. For example, when the mouse moves to its right, the firing rate of the "right+"(X-) neurons increases while that of a "left+" (X+) neuron decreases. Figures 10-

13 show that the observed correlation between neural activity and instantaneous position coordinates is found for every individual movement. The same neuron increases firing during movement in its “preferred” direction and reduces firing during movement in the opposite direction.

### **3.4. Discussion**

#### **3.4.1. Summary**

We found strong linear correlations between the firing rates of SNr GABA cells and the corresponding instantaneous head position of the animal in Cartesian space. Individual cells were correlated either positively or negatively with head position along either the x-axis or y-axis. Each class of neuron (X+, X-, Y+,Y-) represents the x or y-vector component of head-position. The combined output from both x and y-correlated cells is thus sufficient to recreate the animal’s head position over time.

It is important to note that we only recorded head position along x and y-axes of the frontal plane, so it is entirely possible that there could be similar populations in the SNr correlating with the position of other body parts, such as head extension along the z axis or aspects of limb configuration. To address this question we will need to employ 3D motion tracking. Despite this limitation, our results show for the first time a continuous and quantitative relationship between outputs of the basal ganglia and position coordinates during movement.

### **3.4.2. Problems with current models of BG function**

Current models of basal ganglia function assume that GABAergic outputs from the SNr, because of their high firing rates, are responsible for tonically inhibiting brainstem motor structures such as the tectum and MLR. According to these models, while these inhibitory signals are in place the motor structures are prevented from functioning and the animal does not move. By transiently pausing this inhibition to a particular motor region, that region is disinhibited by the BG and allowed to function; thus generating movement. (Hikosaka and Wurtz, 1983; Chevalier and Deniau, 1990; Hikosaka, 2007; Grillner et al., 2013). Although this model works to explain the discrete behavior of animals in certain highly controlled experimental tasks, it falls short in explaining the continuous changes in extent and direction of motor programs during free behavior. An additional difficulty with this model is in accounting for the experimental observations reported here; although we frequently found cells that were inhibited below baseline during movement in one direction, those same cells were found to be excited above baseline during movements in the other direction. Moreover, the signal is not monolithic but consists of at least 4 different components; two antiphase signals for each of the two axes of head movement (X+, X-, Y+, Y-). In spinal circuits, such opponent signaling is needed coordinate the activity of opponent muscles to change the angle of a joint. However the signals reported here do not reach the spinal cord but instead control a higher-level variable requiring the coordination of multiple muscles, such as joint angle itself or body orientation.

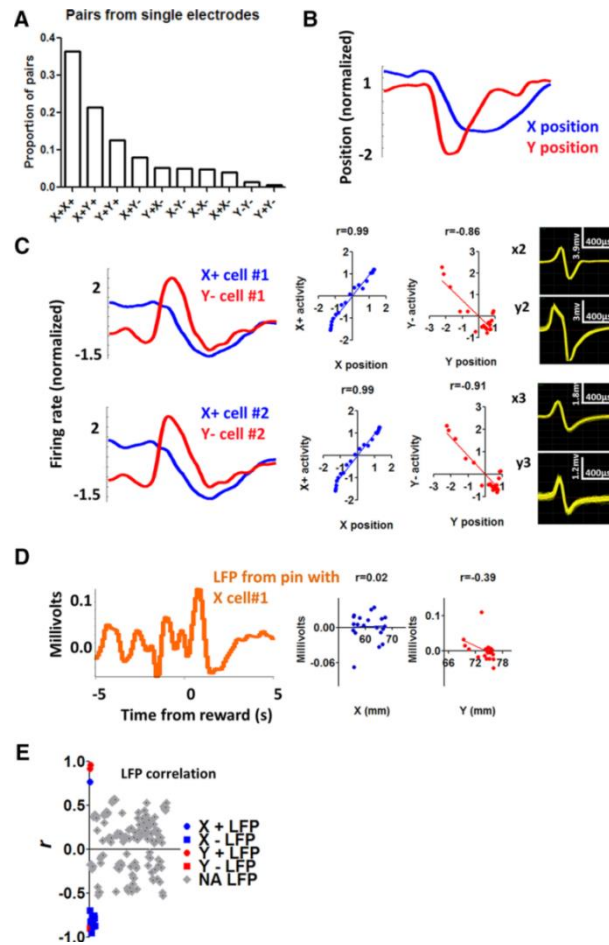


Figure 16. Single-unit activity from a single electrode compared with LFP signal from the same electrode. (A) Probability of co-occurring neurons recorded from the same electrode. (B) Illustration of the per-reward change in x and y-coordinates during a single session. (C) From the same session, 2 X+ neurons and 2 Y- neurons are shown with their waveforms. All cells show high correlation with position coordinates. Correlation analysis is performed on data from a 10 s perireward time window (5s before and 5s after reward delivery). (D) LFP recorded from the same electrode as X cell #1. Correlation between LFP and position coordinates is much weaker. (E) The distribution of r values for all the recorded LFP channels. Of the 166 LFP channels analyzed, only 15 showed significant correlation with position coordinates (colored,  $p < 0.001$ ). Thus, when activity is summed from different types of neurons, the resulting correlation between neural activity and position is weaker. The relatively rare examples of LFP being highly correlated with position coordinates suggest that neurons belonging to a particular class (e.g., X+) might be located close to each other.

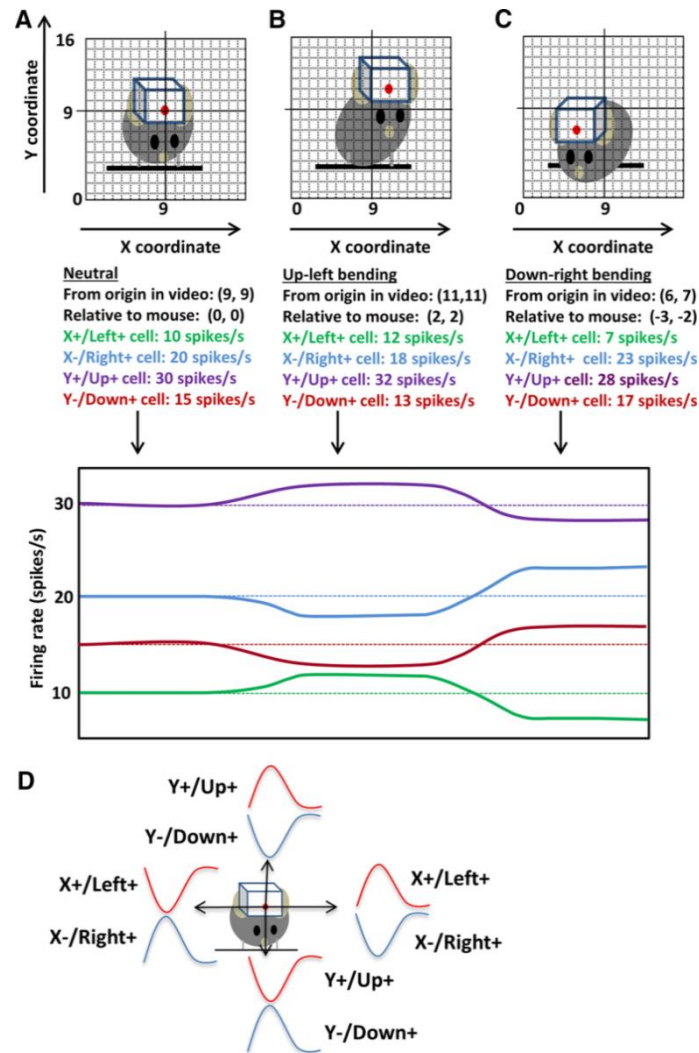


Figure 17. Schematic illustration of different types of neurons. (A) Illustration of hypothetical mouse movement in relation to the neural activity. The firing rates of the four types of neurons are shown. For this hypothetical example, 1 spike/s is equal to 1 unit of change in x or y-coordinate. The units are arbitrary. The starting position is (9, 9). (B) The mouse moves to its left and up. The LED position changes to (11, 11). (C) Right, The mouse moves to a new position (6, 7). Relative to its start position, the change is (3,2). (D) Schematic illustration of the relationship between neural activity in relation to movements in four directions. The illustration of neural activity does not represent actual data because we did not record all four types of neurons from a single animal during a session. Opponent activity was observed during movement in any direction. For example, Y+ (Up) neurons increase their activity during upward movements and decrease their activity during downward movements. The opposite is true of Y- (Down) neurons.

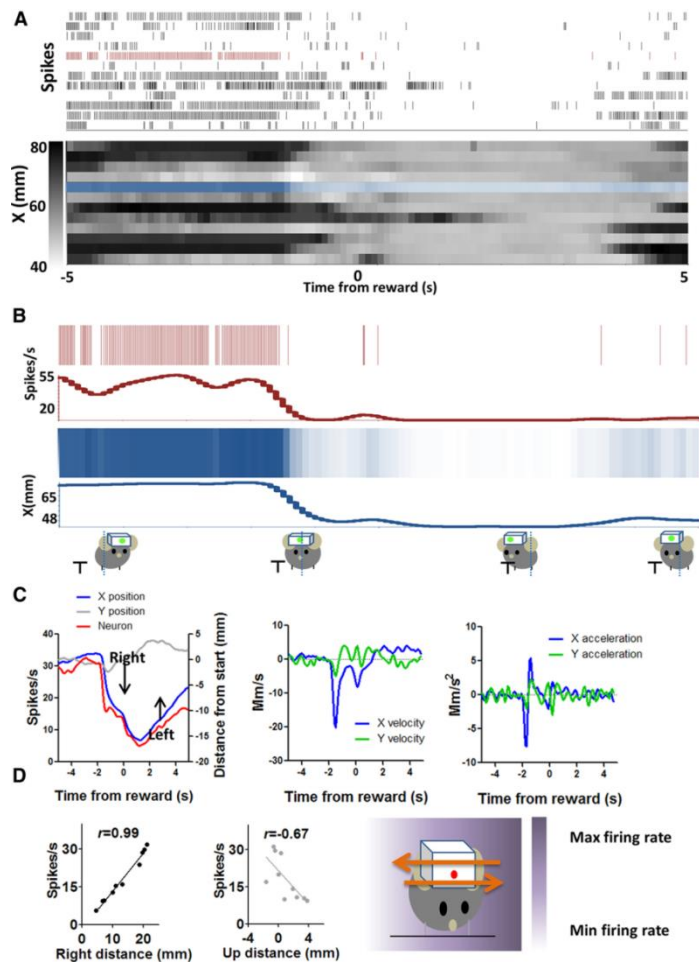


Figure 18. Left + (X+) neuron increases firing during leftward movement and decreases firing during rightward movement. (A) Detailed illustration of the correlation between firing rate and x-coordinates on a trial-by-trial basis. Neural activity and x-coordinates from 10 consecutive trials are shown. Each row represents a single trial. (B) Neural and position data from a single trial are selected and compared. x-axis position changes during each movement are reflected in the firing rate of this neuron. The mouse moves to the right to consume sucrose. The activity of the neuron decreased during the rightward movement and then increased when the mouse moves left again to recover its initial starting position. (C) Average firing rate changes and changes in different movement parameters. In this example, the y-component of the movement is much smaller. The plots on the right show velocity and acceleration data for the same movements. (D) Using an egocentric reference frame, the direction of firing rate changes corresponds to the direction of movement. There was a positive correlation between neural activity and position change in a leftward direction ( $r=0.99$ ,  $p<0.001$ ). The correlation with the non-preferred Cartesian axis is also shown. The diagram on the right shows the gradient of firing rate in relation to position coordinates.

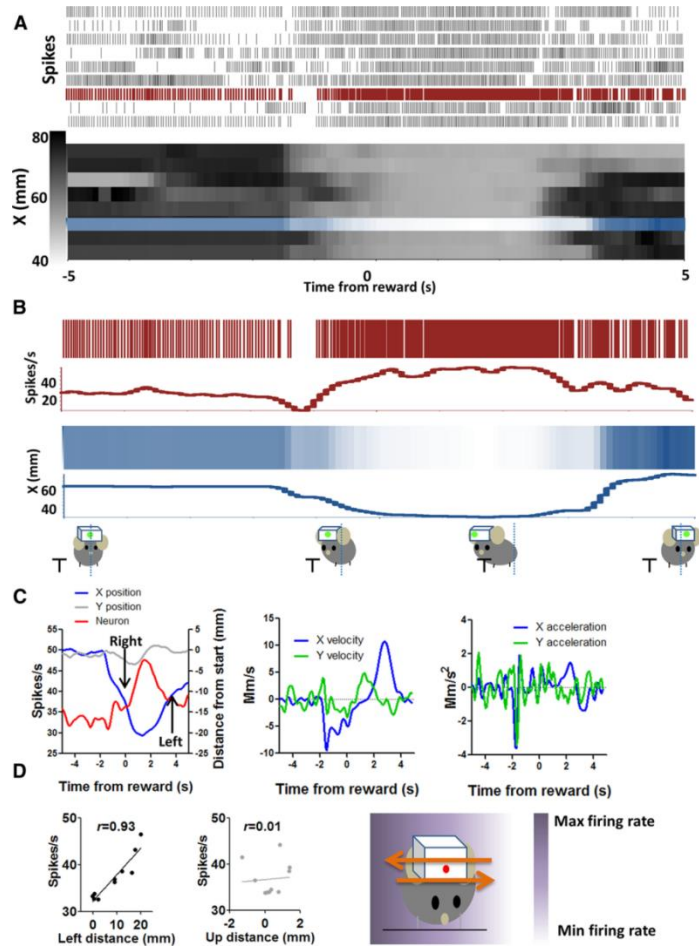


Figure 19. Right (X-) neuron increases firing during rightward movement and decreases firing during leftward movement. (A) Detailed illustration of the correlation between firing rate and x-coordinates on a trial-by-trial basis. Neural activity and x-coordinates from 9 consecutive trials are shown. Each row represents a single trial. (B) Neural and position data from a single trial are selected and compared. x-axis position changes during each movement are reflected in the firing rate of this neuron. (C) Average firing rate changes and changes in different movement parameters. The plots on the right show velocity and acceleration data for the same movements. (D) Using an egocentric reference frame, the direction of firing rate changes corresponds to the direction of movement. There was therefore a negative correlation between firing rate and raw x-coordinate value but a positive correlation between firing rate and distance in the rightward direction ( $p < 0.001$ ). The correlation with the nonpreferred Cartesian axis is also shown. The diagram on the right shows the gradient of firing rate in relation to position coordinates.

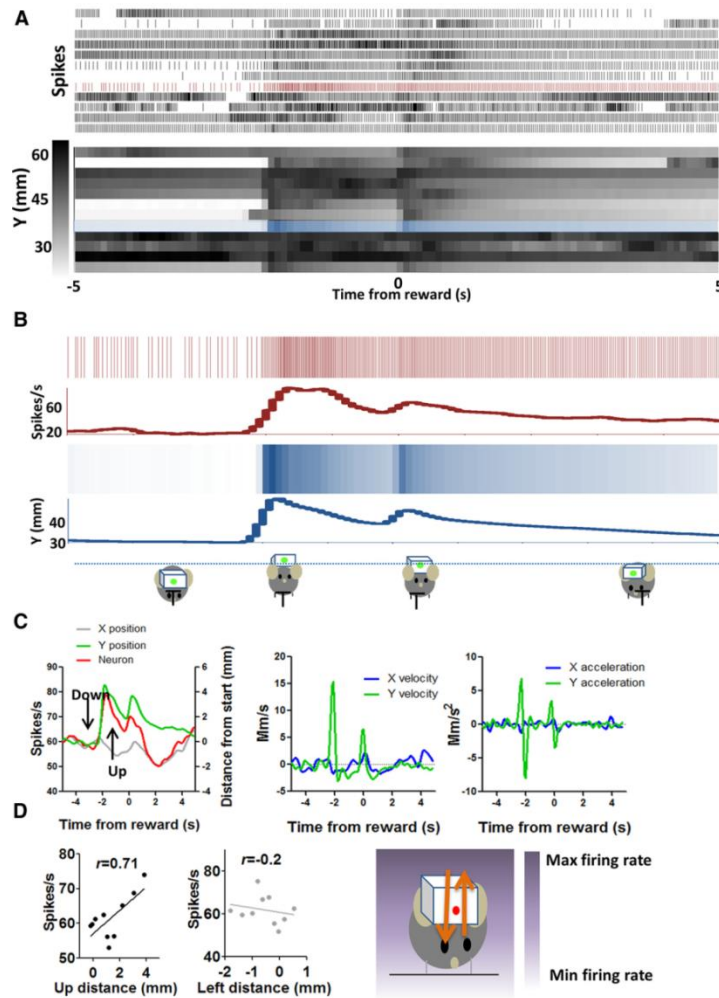


Figure 20. Up (Y+) neuron increases firing during upward movement and decreases firing during downward movement. (A) Detailed illustration of the correlation between firing rate and y-coordinates on a trial-by-trial basis. Neural activity and y-coordinates from 10 consecutive trials are shown. Each row represents a single trial. (B) Neural and position data from a single trial are selected and compared. (C) Average firing rate changes and changes in different movement parameters. The plots on the right show velocity and acceleration data for the same movements. (D) There is a positive correlation between firing rate and y-coordinates and distance in the upward direction ( $p < 0.001$ ). Using an egocentric reference frame, the direction of firing rate changes corresponds to the direction of movement. The correlation with the nonpreferred Cartesian axis is also shown. The diagram on the right shows the gradient of firing rate in relation to position coordinates.

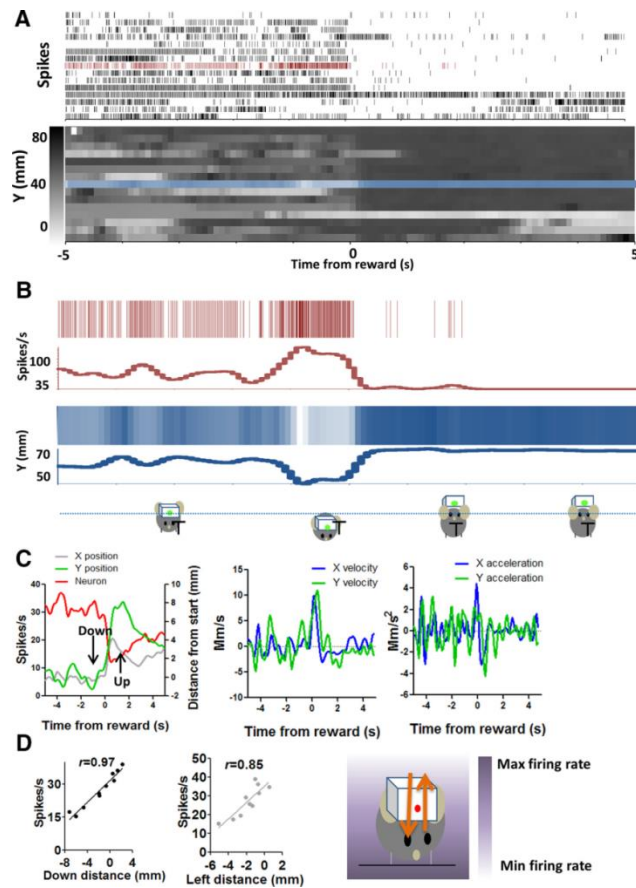


Figure 21. Down (Y-) neuron increases firing during downward movement and decreases firing during upward movement. (A) Detailed illustration of the correlation between firing rate and y-coordinates on a trial-by-trial basis. Neural activity and y-coordinates from 10 consecutive trials are shown. Each row represents a single trial. (B) Neural and position data from a single trial are selected and compared. (C) Average firing rate changes and changes in different movement parameters. The plots on the right show velocity and acceleration data for the same movements. (D) Using an egocentric reference frame, the direction of firing rate changes corresponds to the direction of movement ( $p < 0.001$ ). There was therefore a negative correlation between firing rate and raw y-coordinate value but a positive correlation between firing rate and distance in the downward direction ( $p < 0.001$ ). The correlation with the nonpreferred Cartesian axis is also shown. In this case, the correlation with distance traveled in the leftward direction is also high because the movement is nearly diagonal, so that the x and y-position changes are similar. However, the correlation with y is still considerably higher, and trial-by-trial examination of the data confirms that this neuron is selective for the y-component of the position vector. The diagram on the right shows the gradient of firing rate in relation to position coordinates.

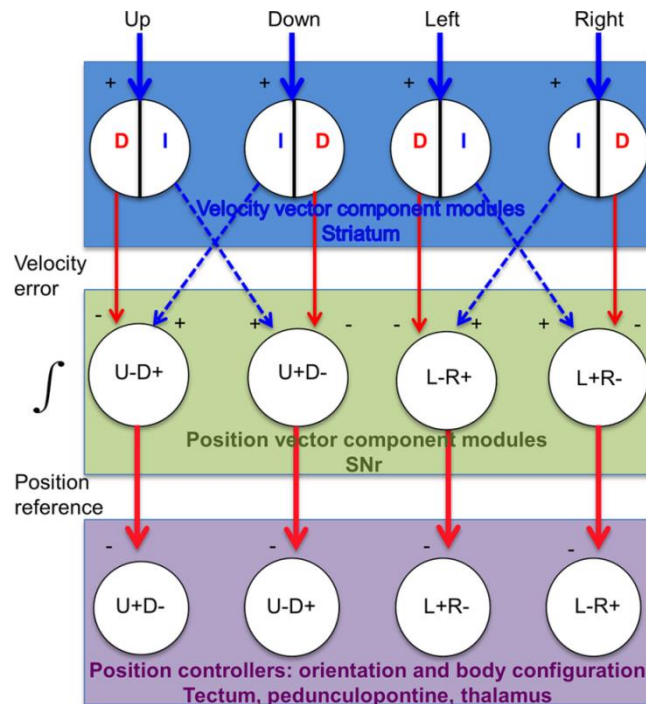


Figure 22. Hypothetical BG circuit. SNr neurons receive projections from the striatum and external globus pallidus, via the direct (D, striatonigral) and indirect (I, striatopallidal) pathways. Although these projections are GABAergic, the net effect on the SNr can be either inhibitory or excitatory (disinhibitory), since changes can occur above or below baseline firing rate. In this model, outputs from both direct and indirect pathways of the striatum represent velocity error signals which are integrated in the SNr to generate a position reference signal. This SNr integrator is assumed to be leaky.

Similar to reciprocal inhibition in the spinal cord, the proposed circuit generates opponent outputs for movement in any direction. Here we show an x and a y head position controller but in principle a similar circuit could underlie position control of any joint. The functional significance of this reciprocal innervation is to allow movements in both directions; without it—as with two muscles at a joint—the system could move quickly in one direction but not in the other. The striatum, especially the sensorimotor region, is hypothesized to contain at least four different modules, each responsible for movement in a specific direction. Because z-axis motion has not been measured, only four directions are illustrated here. Two of the four vector components are associated with any movement (e.g., upward and rightward), as movements usually have both horizontal and vertical components. The total output (number of spikes) from a particular striatal module represents the magnitude of the isolated position vector component, and the firing rate represents velocity (Kim et al., 2014). Using the outputs from different vector component modules, this circuit can perform vector addition to generate the resultant movement vector.

Previous models also assume that the basal ganglia are important for action selection, but the precise meaning of 'action' has never been made fully clear. Typically taken to mean an overt, 'all or none' task-related movement such as a saccade or lever press, the term implies that behavior consists of a series of pulse-like outputs when in reality it is a continuous and continuously graded process. For example, according to the 'focused selection' model (Mink, 1996), a pause in BG output disinhibits one action, such as reaching or locomotion, while inhibiting all other actions, such as postural corrections. As discussed previously, this account is at odds with the fact that postural control must occur in parallel with virtually all behaviors in order for those behaviors to occur successfully (it is difficult to reach for a lever if you have fallen down). This account is also at odds with the obvious reality of free behavior, which involves the continuous adjustment of multiple motor programs in parallel, such as running, jumping and orienting. By contrast, our results suggest that behavior must be studied as a continuous process, and neural activity as continuously varying. Another model of basal ganglia function that our results are at odds with is the 'rate model' (DeLong, 1990), according to which the direct and indirect pathways converge on the output nuclei of the basal ganglia where their influences are combined. This model assumes that monolithic output signal of the basal ganglia determines both the speed and amplitude of movements, with the direct pathway contributing to increase these variables and the indirect pathway contributing to decrease them. This model assumes that the amplitude and speed of movements are equally represented in the outputs of the BG, whereas our

data show that BG output signals are correlated with instantaneous head-position. It is thus the rate of change of these signals that represents velocity of movement, and the range of these signals that represents amplitude. While SNr output is affected by both direct and indirect pathways, which are known to be simultaneously active during movement (Cui et al., 2013), their exact contributions remains unknown. The role we hypothesize for the direct and indirect pathways in generating these signals is outlined in Figure 22.

### **3.4.3. The meaning of transition control**

All behavior involves movement, which can be described in terms of transitions between different body configurations. Bipedal locomotion, for example, is a repeating sequence of transitions between at least two body configurations; left foot stance and right foot stance. Orienting behavior, on the other hand, can be described as rotational transitions along the x and y axes of the trunk, neck and eyes. Learned behaviors, such as pressing a lever to obtain a food reward, can also be described as a sequence of transitions between whatever set of body configurations is required to meet a particular perceptual goal, such as the 'click' sound of a lever being depressed.

It has recently been proposed that the basal ganglia are responsible for transition control (Yin, 2014a; Yin, 2014b). According to this model, the basal ganglia function as a level in a perceptual control hierarchy and are responsible for setting and moving the

position of lower-level reference signals, such as those specifying velocity of locomotion, orientation relative to target, or body configuration itself. As previously mentioned, a perceptual control hierarchy is a form of cascade control hierarchy in which higher systems continuously specify the reference signals for lower systems as a means of controlling their own inputs (Powers, 1973). For example, a joint angle control system may perceive joint angle as the difference between extensor and flexor muscle length, and control that perception by sending its errors as reference signals of the appropriate signs to independent muscle length controllers at a lower level in the hierarchy (Figure 23). The lower systems, in turn, generate errors and produce their own corrective outputs by comparing incoming perceptions to reference signals issued from above. In this way, higher systems reduce their own errors not by telling lower systems what outputs to produce, but instead what inputs to sense. When such a hierarchy is working smoothly, all active systems are able to continuously maintain their perceptual signals very near to their desired levels. Such an arrangement is similar in many ways to a military hierarchy, in which commanders issue goals for their subordinates as opposed to commands for specific patterns of output.

According to this model, the controlled variable of the transition control system is velocity of a perceptual signal, such as the signal representing the angle of a joint or orientation relative to a target. Perceptual input for the velocity control system is generated by taking the derivative of the position perception, and controlled by sending

velocity errors to an integrator where they are added to generate a changing position reference signal (Figure 23).

Because it transitions the reference states of a number of lower motor systems, the transition control system is uniquely positioned to coordinate the outputs required of 'voluntary' goal directed behavior. Another way to state this is that the transition control system coordinates changes in the reference signals of lower systems as a means of reducing errors in still higher systems. For example, it is likely that in the current study one of the higher 'goals' or reference states of the animal is to achieve close proximity to the sucrose solution so that it can be consumed. Such a control system would depend on an accurate perceptual signal representing target proximity, and continuously generate an error representing the difference between desired proximity and current proximity. Assuming that the reference signal for proximity was set to 0, then this system would generate an error inversely proportional to perceived food proximity. For it to be reduced, this error would need to be split and converted into a set of velocity reference signals for the transition control system, describing particular directions and relative speeds of movement for the set of body parts used to reduce the proximity between the animal and the target. As the proximity is reduced, the error—and consequently the velocity reference signal being integrated to specify desired position—shrinks, causing the movement to slow as it reaches the target. This deceleration with decreasing proximity to target is a well-documented phenomenon in motor control (Shadmehar and

Krakauer, 2008). The vast majority of animal behavior can be modeled by this form of hierarchical perceptual control, from control of simple proximity to food and temperature gradients to social variables. In all cases, such perceptual variables can only be controlled through motor transitions of the body.

#### **3.4.4. The basal ganglia and transition control**

The high and continuous correlation between SNr activity and head position, combined with the fact that SNr neurons are known to exert direct control over downstream motor structures, suggests that the firing rate of these cells functions as the reference signal for lower-level position and orientation controllers via projections to the tectum and other brainstem regions such as the PPN (Robinson, 1972; Goodale and Murison, 1975; Waitzman et al., 1991; Takakusaki et al., 2004), as well as the cortex via thalamic projections (Alexander and Crutcher, 1990; Alexander et al., 1986). These structures, in turn, ultimately influence spinal pathways to activate functionally relevant muscles.

In accordance with our experimental findings, the high tonic baseline firing rate of these neurons could represent baseline position—neutral posture—and changes above or below this baseline could represent positions in one or the other direction from baseline. SNr cells receive direct and indirect inputs from the striatum. It has recently been shown that activity in these striatal output neurons reflect head

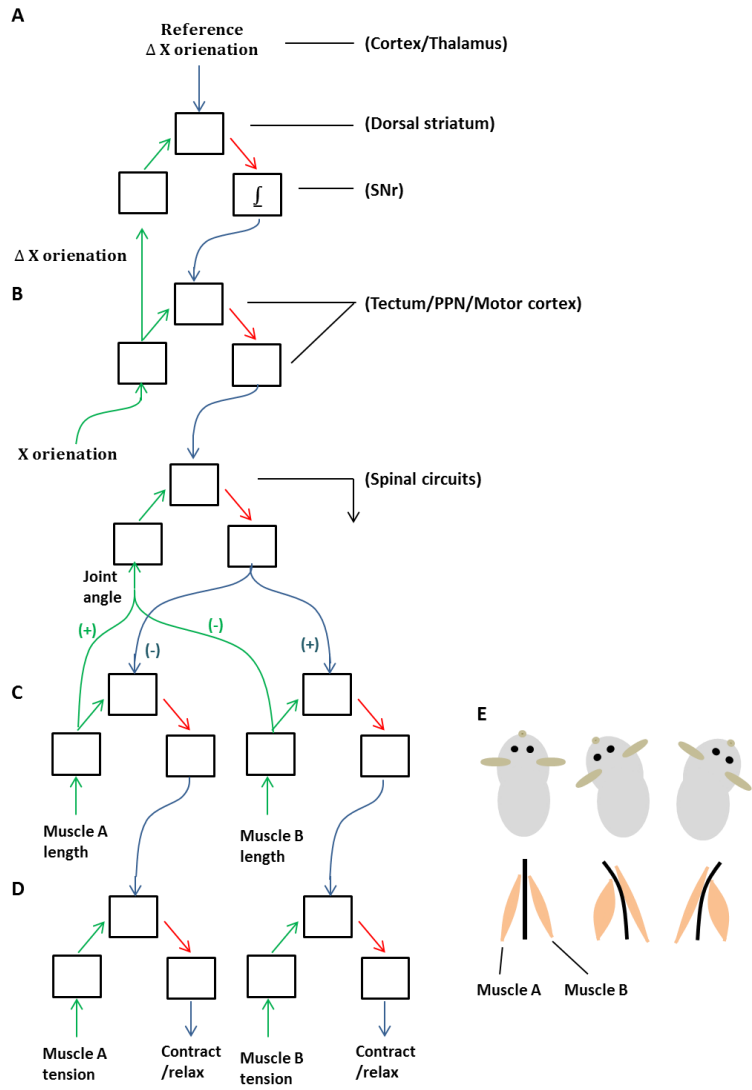


Figure 23. Illustration of a hierarchical 'x-axis' orientation control system with an output function consisting of two muscles. A-D comprise a schematic showing a perceptual control hierarchy with perceptual inputs in green, error signals in red and reference signals in blue. (A) Transition control. This is the level of the basal ganglia. The x orientation reference signal is generated by output of 'X+' and 'X-' neurons of the SNr. (B) Configuration control. This level is controlled by brainstem motor regions and motor cortex via the pyramidal tract. (C) Muscle length control by the spinal cord. (D) Muscle force control by the spinal cord. (E) Diagram showing the relationship between muscle length and bend along the x-axis of the spinal joint.

movement velocity (Kim et al., 2014). These findings are in agreement with the transition control model of the basal ganglia, and suggest that striatal output signals represent velocity errors for particular directions of movement, which are integrated by SNr GABA neurons as a mechanism to specify position--in an integrator, the rate of change of output is proportional to the magnitude of input. Integrators are common in analog computing and used in the output function of closed loop control systems to achieve stability and accuracy in control.

Despite baseline firing rates that range considerably within a particular type of cell, correlation with x or y-axis head position remains high. As shown in Figure 14, this can be explained by how a change in firing rate during a given movement is *proportional* to the baseline firing rate of each individual cell. Thus, the method by which different SNr cells can transduce similar striatal outputs into a change proportional to baseline must be multiplicative or divisive (Silver, 2010). An alternative possibility is that this proportionality is due in some way to the properties of signal integration, which remains largely unknown for this class of cells. These neurons are known to have a voltage-gated persistent sodium current, which contributes to the fast rise of the action potentials, allowing persistent and high firing rates; they also express type 3 transient receptor potential channels (TRPC3) that can depolarize the cell at hyperpolarized membrane potentials (Atherton and Bevan, 2005; Zhou and Lee, 2011). How such intrinsic properties or recurrent circuit properties contribute to the relevant computations *in vivo*

remains to be elucidated. In a control hierarchy, normalization to a common scale is important for effective communication between levels; errors from higher controllers must be scaled correctly as a reference signal for lower level controllers or else the reference signal changes may produce too much or not enough output to reduce the higher errors. Such normalization becomes even more important as the complexity of inter-level communication increases, such as when efference or perceptual copies are combined or sent to distant systems. Utilization of a common percentage scale between levels is an elegant solution to this problem.

#### **3.4.5. Significance**

Our results have implications for understanding the clinical symptoms associated with movement disorders. According to our model, Parkinsonian symptoms like bradykinesia (slowed movement) and akinesia (inability to move)(Albin et al., 1989; DeLong, 1990) can be explained by a reduction in *the rate of change* in the firing rate of GABA cells in BG output nuclei, owing to the failure of dopamine neurons to modulate the velocity-related signals entering the integrator circuit, which generates changes in the reference signals for body configuration position control systems. Dopamine depletion, found in Parkinson's disease, is predicted to reduce the magnitude of the signal entering the integrator, thus reducing the rate of change in the output (Yin, 2014b).

## 4. Beyond Reward Prediction Errors: the Role of Dopamine in Movement Kinematics<sup>1</sup>

### 4.1. Introduction

The role of dopamine (DA) in behavior has remained controversial despite decades of research (Cannon and Palmiter, 2003; Cagniard et al., 2006; Jin and Costa, 2010; Leblois et al., 2010; Rossi et al., 2013a). Loss of DA neurons in Parkinson's disease is associated with severe motor deficits, suggesting that dopaminergic signaling is important for movement. Studies have also shown that DA activity is correlated with initiation and termination of instrumental behaviors, locomotion, and postural control (Jin and Costa, 2010; Wang and Tsien, 2011a; Fan et al., 2012; Barter et al., 2014). However, other researchers have found no clear relationship between DA activity and movement (Schultz et al., 1983; Romo and Schultz, 1990) and instead conclude that phasic DA signaling encodes reward prediction error, the difference between the expected reward and the actual reward, which can serve as a teaching signal in reinforcement learning (Schultz et al., 1997; Bayer and Glimcher, 2005; Glimcher, 2011; Fiorillo, 2013).

One major limitation of all previous work is a lack of detailed and continuous recording of movement parameters. The experiments performed in this chapter were

---

<sup>1</sup> This chapter is a modified version of a previously published article: Barter JW, Li S, Lu D, Bartholomew RA, Rossi MA, Shoemaker CT, Salas-Meza D, Gaidis E, Yin HH (2015a) Beyond reward prediction errors: the role of dopamine in movement kinematics. *Front Integr Neurosci*.

designed to address this limitation and shed light on the gap in understanding between the role of DA in controlling movement and in reward processing, by combining video tracking and wireless in vivo recording of DA activity during a cued reward task. As described in the chapter 2, these same experimental techniques were previously used by us to investigate the role of SNr GABA neurons, and by other researchers to investigate the role of striatal medium spiny projection neurons in the sensorimotor striatum, in generating free behavior. It was found that the activity of SNr output neurons reflected horizontal and vertical vector components of position (Barter et al., 2015a), while the activity of striatal projection neurons correlated with horizontal and vertical vector components of velocity (Kim et al., 2014). These findings support a new model of BG function, according to which the nuclei of the BG collectively function as a transition control system situated in a hierarchy of negative feedback perceptual control systems (Yin, 2014b). We hypothesized that the role of DA in this system is to perform gain modulation for the transition controller in the BG (Yin, 2014b); together with glutamatergic inputs, DA signals can determine the magnitude of the descending signal from the striatum, and thus the rate of change in BG outputs from the SNr (Kim et al., 2014; Barter et al., 2015a).

To test this hypothesis, we used a combination of video tracking and wireless in-vivo neural recording during a cued reward task in mice to investigate the continuous relationship between DA activity and movement. We found that the phasic activity of SNc DA neurons reflected distinct vector components of movement velocity and

acceleration. Using a transgenic mouse line in which channelrhodopsin 2 is expressed selectively in DA neurons, we also found that photo-stimulation of DA neurons in the SNc could reliably generate movements.

## **4.2. Methods**

### **4.2.1. Subjects**

Eleven male C57BL6/J mice (25-35g) were used in the electrophysiology experiments. Seven mice (2 males, and 5 females) were used in the optogenetics experiments. All procedures were approved by the Duke University Institutional Animal Care and Use Committee. To make mice perform movements repeatedly, we gave them limited access to water. After the recording session each day, mice had free access to water for 1 hour. Each mouse received about 0.5ml to 1ml of 10% sucrose during the experimental session. When they had free access to water afterwards, they consumed ~2 ml. The health of all mice was monitored daily.

### **4.2.2. Behavior**

We used a simple Pavlovian trace conditioning task to study the phasic DA responses in relation to rewards (unconditional stimulus, US) and cues predicting rewards (conditional stimulus, CS). In this task, the mouse stands on an elevated platform (4x5cm, elevated 40cm) and its movement can be monitored with a camera

facing it at 30frames/s (Figure 24). An auditory cue predicted the delivery of a sucrose reward, and the mouse reliably moved following the cue and following the reward. The experimental apparatus and procedures are the same as what we used in two recent studies (Kim et al., 2014; Barter et al., 2015a). This design allows us to record from DA neurons while monitoring movement kinematics, using a small LED light positioned on the headstage. It also minimizes z-axis movements.

Each trial began with the presentation of a tone (100ms, 21.6dB) followed by the delivery of 13 $\mu$ l 10% sucrose solution dispensed by a Valvelink 8.2 (AutoMate Scientific) and delivered through a spout fixed to the platform. The sucrose solution was delivered ~2s after the termination of the tone. Each session contained 50-150 trials, with a variable inter-trial-interval of 20-50s. Each session lasted approximately 1hr.

For sucrose/air puff sessions, either an ABAB design was used, in which reward trials and air puff trials were presented in blocks, or an AB design was used, in which sucrose trials were followed by air puff trials. The same auditory cue was used (duration =100ms). Air puffs were 200ms in duration and delivered from a computer-controlled 1500 series dispenser (EFD, 12PSI).

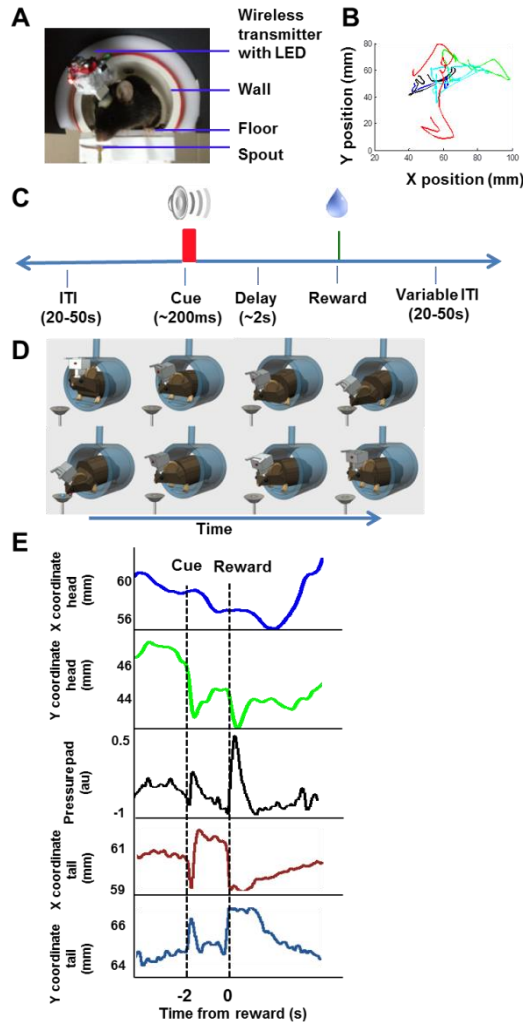


Figure 24. Behavior and video tracking in unrestrained mice. (A) Mice perched on an elevated platform housed in a tube, wearing a miniaturized 16 channel wireless headstage (~3.8g). The camera (not shown) is facing the animal. (B) Illustration of movement trajectory. The mouse starts to move following presentation of the cue (CS), and moves again following the presentation of the reward (US, 13 $\mu$ l 20% sucrose solution). Each color illustrates the path on a single trial, showing variability from trial to trial. (C) Illustration of the Pavlovian trace conditioning task used (Barter et al., 2015). (D) Cartoon illustration of the movements. Top row illustrates movement toward the spout; bottom row illustrates movement back to the starting position. (E) Illustration of movement tracked by the head LED. Pressure pads were placed underneath the animal, so that changes in pressure exerted by the hind paws can be measured. Pressure pad measures as well as video tracking of the tail demonstrate that the movements were not restricted to the head. Position coordinates are mm from frame edge.

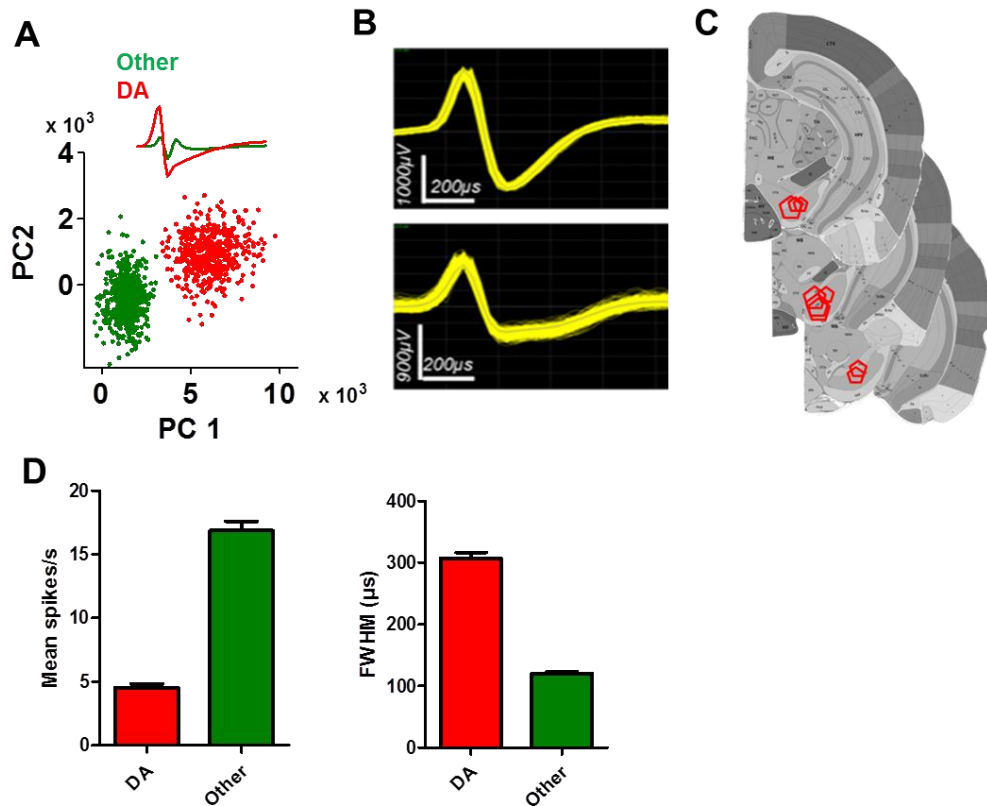


Figure 25. Identification of DA neurons in the substantia nigra. (A) Classification of a putative DA neuron and a non-DA neuron using principal component analysis (PCA). (B) Representative waveforms of putative DA neurons. (C) Summary of electrode placements shown in coronal brain sections taken from the Allen Brain Atlas (Lein et al., 2006). (D) Average firing rate and spike width (FWHM, full width at half maximum) of putative DA neurons and non-DA neurons. DA neurons are characterized by lower firing rates and wider spike widths (unpaired t-tests,  $p < 0.0001$ ).

#### 4.2.3. Neural recording and data analysis

Sixteen-channel electrode arrays (Innovative Neurophysiology) were lowered at the following stereotaxic coordinates in relation to bregma: 2.9-3mm posterior, 1.2mm

lateral, and 4.6mm below brain surface. Six mice were implanted in left nigra and the other six were implanted in the right nigra. The arrays consisted of 16 tungsten wires, 35 $\mu$ m in diameter and 7mm in length, arranged in a 4 by 4 configuration, attached to an Omnetics connector. Row spacing was 200 $\mu$ m and electrode spacing was 150 $\mu$ m. Electrode arrays were fixed to the skull with dental acrylic. Following the completion of the experiments, all mice were perfused and their brains sliced with a Vibratome and examined under a microscope to verify electrode placement.

The behavioral and electrophysiological data were recorded with a Cerebus data acquisition system (Blackrock) and analyzed with Matlab, Neuroexplorer, and Graphpad Prism. Single unit activity was recorded with miniaturized wireless headstages (Triangle BioSystems International), as described previously (Fan et al., 2011). Attached to the front end are miniature LEDs (2mm, Osram). Single units were selected using online sorting algorithms and then re-sorted offline (Fan et al., 2011; Rossi et al., 2013a). Only single-unit activity with a clear separation from noise (at least 5 to 1 compared to the noise band) was used for data analysis.

#### **4.2.4. Kinematic variables**

Position, velocity, and acceleration are vector quantities with both magnitude and direction. For movement measured with video tracking, this vector has two components (x and y). X and y head position vectors were differentiated to get x and y-

velocity, and the second derivative was taken to obtain acceleration. X and y-velocity and x and y-acceleration were then split into positive and negative components to yield a total of 8 kinematic variables: up and down velocity and acceleration, left and right velocity and acceleration.

We then compared the neural activity to the movement kinematics. To assess the correlation between neural activity between firing rate and movement kinematics, we analyzed data from the entire session. A complete record of neural activity and the continuous kinematic variables for each session was analyzed in Matlab with a bin size of 30ms. The analysis consisted of two steps: first, for each session, cross-correlation was performed between the firing rate of each neuron and each of the 8 kinematic variables to determine the shift required for the highest correlation between the two signals. Second, the neural signal and the kinematic signal were shifted accordingly and a Pearson correlation was then performed to determine the correlation between the two signals. Classification of different functional classes of neurons was determined by the strength of the correlation between the kinematic variable and neural activity ( $p < 0.05$ ).

#### **4.2.5. Optogenetic stimulation**

By crossing *Th-cre* mice, which express Cre recombinase in tyrosine hydroxylase positive neurons, with a knockin line (Ai32, ChR2-EYFP) for Cre-dependent expression of

channelrhodopsin (Madisen et al., 2012), we generated *Th::Ai32* mice for selective activation of DA neurons.

Custom-made optic fibers (5mm length below ferrule, 105µm core diameter, 1.25mm-OD ceramic zirconia ferrule; Precision Fiber Products) were lowered into the brain and secured in place with dental acrylic and skull screws (Sparta et al., 2012). Mice were allowed to recover for 2-3 weeks before testing began.

Photo-stimulation was always bilateral. A custom-made commutator was used to split a single laser beam into two beams for bilateral stimulation. During stimulation sessions, mice were connected to a 473nm wavelength laser by two sheathed fibers (62-µm core diameter, connected by ceramic sleeves, Precision Fiber Products). The total output of the laser was adjusted each day, to obtain ~636 mW/mm<sup>2</sup> transmittance.

Following completion of experiments, mice were anesthetized with isoflurane and perfused with ice-cold 4% paraformaldehyde. Brains were post fixed for ~24hours at 4°C, cryoprotected in sucrose solution, and then sliced at 60µm on a Vibratome. Slices were incubated with primary chicken anti-GFP (1:1000, AbCam) and TH primary rabbit anti-TH (1:1000, Millipore) with 10% goat serum and 0.25% Triton X-100 overnight at 4°C. Secondary antibodies (Alexa Fluor 594 goat anti-rabbit and Alexa Fluor 488 Goat anti-Chicken) were used to visualize TH and GFP, respectively (1:250, Molecular Probes). Slices were imaged with an Axio Zoom.V16 (Zeiss) microscope and processed using Zen software (Zeiss).

### **4.3. Results**

#### **4.3.1. Video tracking**

The sucrose spout was located low and offset from the center of the perch platform, requiring the animal to lower and move its head to one side to obtain sucrose reward. A typical cued movement is illustrated in Figure 24E: following the cue, the mouse initiated a movement towards the sucrose spout, adjusting its body so that its mouth was near to the spout. Once the sucrose solution was delivered, the mouse made another movement to consume the sucrose before returning to a neutral posture. Because the mice were not restrained and allowed to move freely within the confines of the small platform, the movement trajectories varied considerably between animals, sessions, and even individual trials within the same session. Although we tracked movements using a single LED placed on the head to track movements, this does not mean that the mouse only moved its head. As can be seen in Figure 24E, reward-directed movements involved clear movement of the whole body, as confirmed by pressure pads placed underneath the mouse, and video tracking of tail movements at the time of cue or reward.

#### **4.3.2. Classification of DA neurons**

We recorded activity of DA neurons in the SNc, the largest DA cell group targeted by classic studies of phasic DA activity (Ljungberg et al., 1992; Schultz, 1998a).

As shown in Figure 25, putative DA neurons recorded from the SNc are identified by their firing rate and waveform properties (Grace and Bunney, 1984; Rossi et al., 2013a; Rossi et al., 2013b). DA neurons have considerably wider spike waveforms and lower firing rates compared to GABAergic neurons in this area (Figure 25D, unpaired t-tests,  $p < 0.0001$ ). We recorded from 106 putative DA neurons over a period of 1-6 months depending on the animal.

#### **4.3.3. Correlation between DA activity and kinematics**

We observed phasic activity in DA neurons following the auditory cue and sucrose reward delivery (Figures 26), similar to what has been observed in previous studies in monkeys (Schultz et al., 1997) and in mice (Cohen et al., 2012). However, we also found a strong correlation between these patterns of neural activity and kinematics (Figures 26-28). As shown in Figures 26-28, the firing rates of individual dopamine neurons were found to correlate with head velocity and acceleration during a 1s window surrounding cue and reward. These same correlations were confirmed using a session-wide correlation analysis.

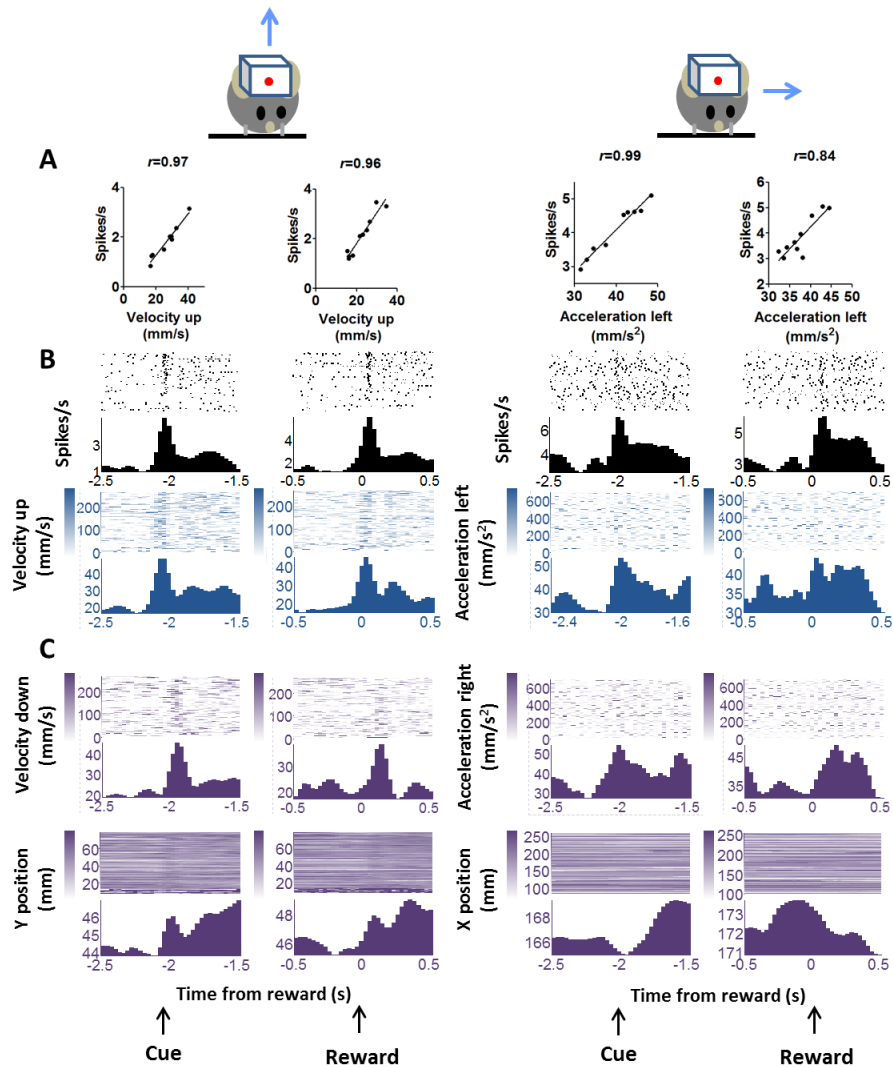


Figure 26. “Burst” DA neurons show positive correlation with kinematic variables. (A) Firing rate of representative neuron showing positive correlation with vector components of velocity and acceleration. Two major movements are detected during the trial, one in response to the cue and the other in response to reward delivery. These are displayed separately. “Velocity up” means velocity in the upward direction. Blue arrows indicate movement direction, but note that only the vector components are indicated. Actual movements would consist of both x and y-components. The correlation analysis uses data displayed in the raster plots below. A 1s peri-event window (either cue or reward) was used. (B) Peri-event raster plots of the neurons and the correlated kinematic variables. (C). The major alternative kinematic variables are shown. These are not highly correlated with neural activity as determined by our unbiased cross-correlation analysis.

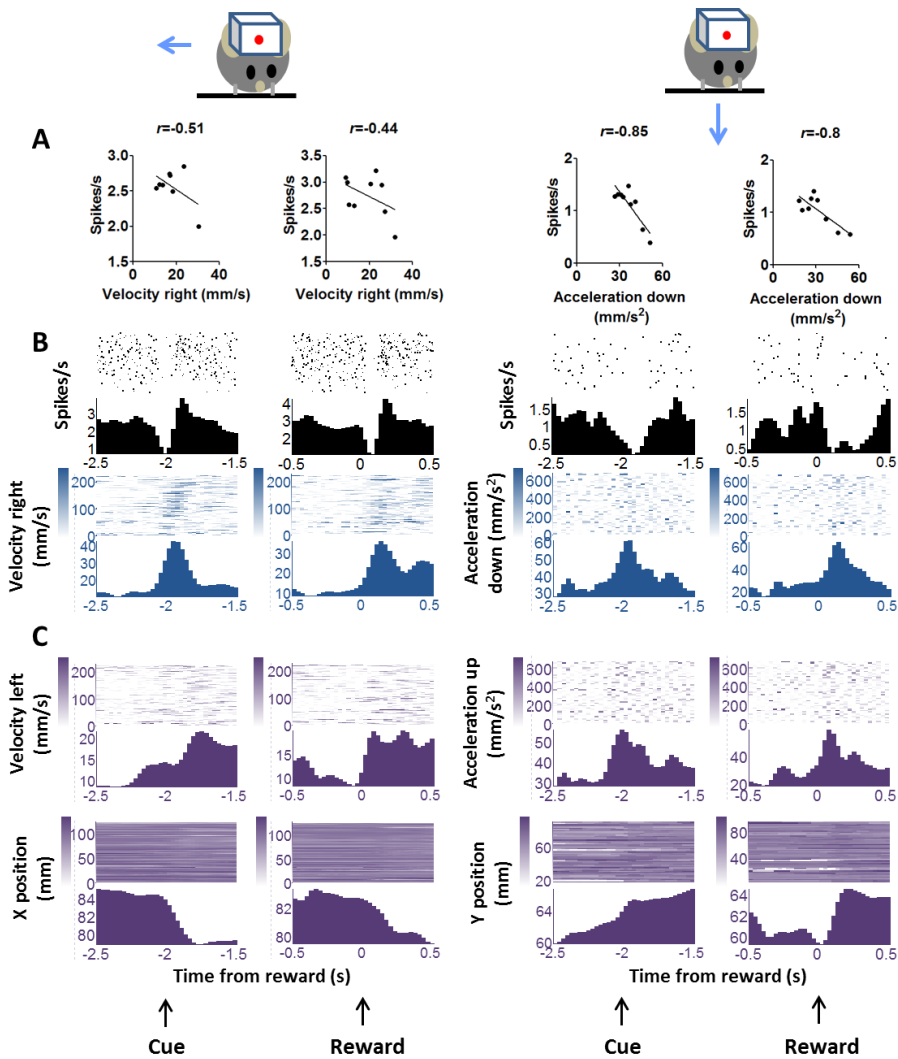


Figure 27. “Pause” DA neurons is negative correlated with kinematic variables. (A) Firing rate of representative neuron showing negative correlation with vector components of velocity and acceleration. Two major movements are detected during the trial, one in response to the cue and the other in response to reward delivery. These are displayed separately. (B) Peri-event raster plots of the neurons and the correlated kinematic variables. (C) The major alternative kinematic variables are shown

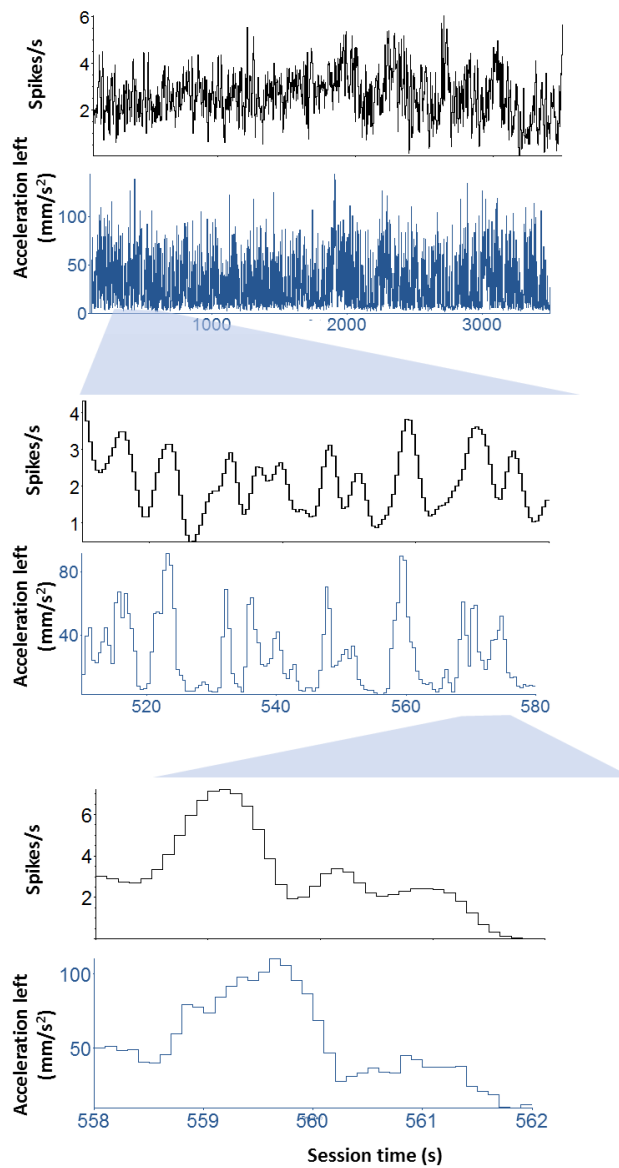


Figure 28. Continuous correlation between neural activity and kinematics. Illustration of a representative neuron and its correlation with kinematics independent of task-related events such as cue and reward. To dissociate kinematic variables from these task events. Rather than selecting only data from the trial, we performed an unbiased correlation between firing rate and the kinematic variables for the entire session, including inter-trial-intervals. This unbiased analysis was used to classify the neurons.

Correlations between neural activity and movement kinematics were identified using an unbiased correlation for the entire session, including inter-trial intervals (Figure 28). In this analysis, the strength of overall correlation does not depend on the high correlation during the trials; the majority of the data come from inter-trial-intervals (20-50s per trial) whereas only a minor fraction come from active trial periods (~2s per trial). The results of this analysis show significant correlations between DA activity and kinematics. These results were used to classify neurons (Table 1). It is important to note that different vector components of velocity and acceleration variables are often necessarily correlated, and thus there are often statistically significant correlations between DA activity and multiple vector components. In the current analysis the kinematic variable with the highest absolute value of correlation coefficient was used to classify neurons. This classification method is in agreement with the observation of strong correlation between DA firing and movement at the time of cue and reward; a given neuron shows similar correlation during the trial period (around cue and reward) and during the inter-trial-interval, during which spontaneous movements were observed.

Cross-correlation analysis allows us to examine the direction specificity of the relationship between neural activity and movements. If a neuron is positively correlated with velocity in a particular direction, it will often show the opposite correlation with velocity in the opposite direction (Figure 26). Thus, not only do DA neurons show direction selectivity, there also appears to be a reciprocal inhibition organization, with

opponent signals generated for different movement directions. This pattern was not common in neurons that are negatively correlated with movement in a particular direction.

#### **4.3.4. Appetitive vs. aversive behavioral tasks**

Because we used an appetitive behavioral task, it is unclear whether the observed correlation between neural activity and movement kinematics is in some way due to the presence of a reward. To address this question, we performed additional experiments in which sucrose reward was switched with an aversive air puff to the face during the same recording session. In these experiments, the experimental setup and trace conditioning procedure remained unchanged except for the switching of sucrose reward for air puff delivered from the same location ( $n=3$  mice). Behavior in these experiments around the air puff trials was markedly different from that observed during sucrose rewarded trials, as can be clearly seen in the movement trajectories. A typical behavior consisted of moving away from the air puff, both during anticipatory ‘bracing’ movements at the cue and again at the time of air puff delivery. Despite these major differences in both movement kinematics and behavioral goals, the correlation between neural activity and kinematics was still robust during these air-puff trials and comparable to the correlation seen during reward trials (Figure 30).

#### 4.3.5. Summary of correlation analysis

Based on data from all recording sessions (appetitive as well as appetitive/aversive), we identified neurons that are correlated with velocity and acceleration in 4 directions (Table 1). Neurons associated with different directions have comparable firing rates (one-way ANOVA,  $F_{3,97}=0.63$ ,  $p=0.6$ ). Of all recorded neurons, 10 neurons were not significantly correlated with any of the kinematic variables. The firing rates of most recorded DA neurons (96/106, 91%) were correlated with either movement acceleration or velocity. Both positive and negative correlations were found, but the positive correlation is far more common (78% vs. 22% of correlated neurons).

The DA neurons with positive correlation with velocity or acceleration (Figure 26) are the burst neurons that transiently increase firing at the time of salient events (cue or reward). This pattern of response has been well documented in previous studies (Schultz, 1998a). The less common neurons with negative correlations tend to pause at the time of cue or reward (Figure 27). Both types usually precede the kinematic variables, but the lag between neural activity and kinematics is much longer in negatively correlated neurons (Figure 31B,  $158\pm 25.7$ ms, compared with  $20.0\pm 10.5$ ms for positively correlated neurons, unpaired test,  $p<0.0001$ ).

#### 4.3.6. Lateralization of the DA response

The electrode arrays were always implanted unilaterally; 6 mice were implanted in the left nigra, and in 5 mice in the right nigra. Of movement-correlated neurons, 40 were recorded from the left nigra and 57 from the right nigra. Since many neurons recorded were correlated with either leftward or rightward movements, we examined the distribution of these neurons to see if there is any lateralization of leftward and rightward neurons. As shown in Figure 32, among velocity-correlated neurons, the majority of DA neurons correlated with rightward movements are found in the left nigra, whereas the majority of DA neurons correlated with leftward movements are found in the right nigra (Chi-square=5.99,  $p=0.01$ ). There was no significant difference between the two sides for acceleration related neurons (Chi-square=3.6,  $p=0.06$ ).

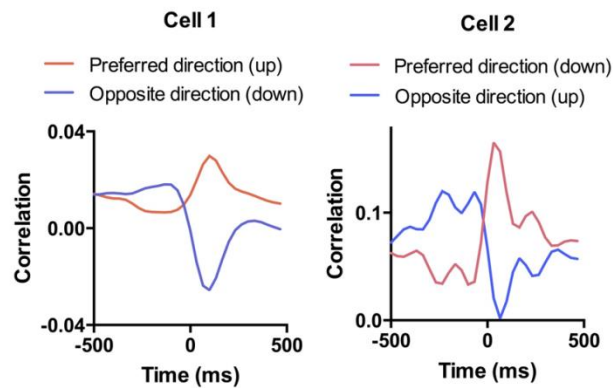


Figure 29. Selectivity of DA responses. To illustrate the direction selectivity of DA neurons, we compared the session-wide cross-correlation between neural activity and velocity in opposite directions. Shown are two examples in which the cell is positive correlated with movement in one direction and negatively correlated with movement in the opposite direction. This pattern is similar to what we observed previously in SNr GABAergic output neurons (Barter et al., 2015a).

#### 4.3.7. Optogenetic stimulation of DA neurons

Although our electrophysiological experiments show strong correlations between dopamine firing rates and movement kinematics, such results do not tell us whether DA activity is directly involved in generating these properties of movement. To investigate the 'causal' role of dopamine, we selectively stimulated dopamine neurons while measuring movement kinematics. To accomplish this we developed a transgenic mouse line in which channelrhodopsin, which depolarizes neurons upon exposure to blue light (Boyden et al., 2005), is expressed selectively in DA neurons. This was accomplished by crossing *Th-cre* (expressing Cre recombinase in tyrosine hydroxylase positive neurons) with the *Ai32* line, which has a floxed stop cassette at the *Rosa26* locus, allowing Cre-inducible ChR2 expression (Madisen et al., 2012). Representative pattern of ChR2 expression is shown in Figure 33.

We used a blue laser (473nm) to stimulate two groups of mice, one group with ChR2 expressed in Th-positive neurons (*Th::Ai32*), and a control group with only Th-Cre expression but no ChR2. We found that optogenetic stimulation of DA neurons could induce movements. Although these movements were sometimes very subtle, they could be clearly detected with our tracking method. It is important to note that because this stimulation procedure presumably activated multiple functional subtypes of dopamine neurons simultaneously, its net effect on individual movement vector components cannot be known. We therefore used distance and speed to quantify the movements as a way to combine these unknown vector components. Distance is defined as the

distance travelled between the location of the LED at the onset of stimulation train and its location at the termination of the train. Speed is defined as the derivative of the distance.

As shown in Figure 34, we first mimicked the phasic burst of activity by high frequency stimulation (40Hz, 5 pulses, 3ms pulse width, power  $\sim 636\text{mW}/\text{mm}^2$ ). This stimulation parameter generated movements that are similar to what we observed during our recording experiments (2 *Th-Cre* control mice, 8 sessions, 3 *Th::Ai32* mice, 14 sessions, 40 stimulation trials per session, variable inter-trial-interval: 6-18 s with a mean of 12s, unpaired t-test,  $p=0.025$  for peak speed, and  $p=0.028$  for distance).

We then systematically varied stimulation frequency (each train lasted  $\sim 1\text{s}$ ) and examined the effects on movement kinematics (3 *Th-Cre* control mice, 12 sessions, 4 *Th:: Ai32* mice, 9 sessions, 8-20 stimulation trials per session, inter-trial-interval=9s). To analyze the movement kinematics, we used a repeated-measures 2-way ANOVA with genotype and stimulation frequency as factors. For peak speed during stimulation, we found a main effect of genotype ( $F_{1,38}=6.44$ ,  $p=0.02$ ), no main effect of frequency ( $F_{2,38}=0.2$ ,  $p=0.82$ ), and no interaction between genotype and frequency ( $F_{2, 38}= 0.41$ ,  $p=0.67$ ). For distance moved, we found a main effect of genotype ( $F_{1,38} =6.06$ ,  $p=0.02$ ), no main effect of frequency ( $F_{2,38}= 0.90$ ,  $p=0.41$ ), and no interaction between genotype and frequency ( $F_{2, 38}=0.92$ ,  $p=0.41$ ). These results demonstrate that stimulation of DA neurons is sufficient to generate movements. The distinct horizontal and vertical components of the kinematic variables produced by stimulation are shown in Figure 35.

This example showed that movements induced by photo-stimulation had both x and y-components, in agreement with our prediction that stimulation should affect multiple types of DA neurons.

#### **4.3.8. Comparing DA and GABA neurons**

SNr GABA output neurons are known to inhibit DA neurons. Some have argued that the firing of DA neurons is largely due to disinhibition: bursting is observed during a pause in GABA output neurons (Tepper and Lee, 2007). This view is supported by our data. Figure 36 illustrates a putative DA neuron compared with a putative GABA output neuron recorded from the electrode array. The GABA output reflects the positive component of the y-position vector; it increases when the mouse moves upwards.

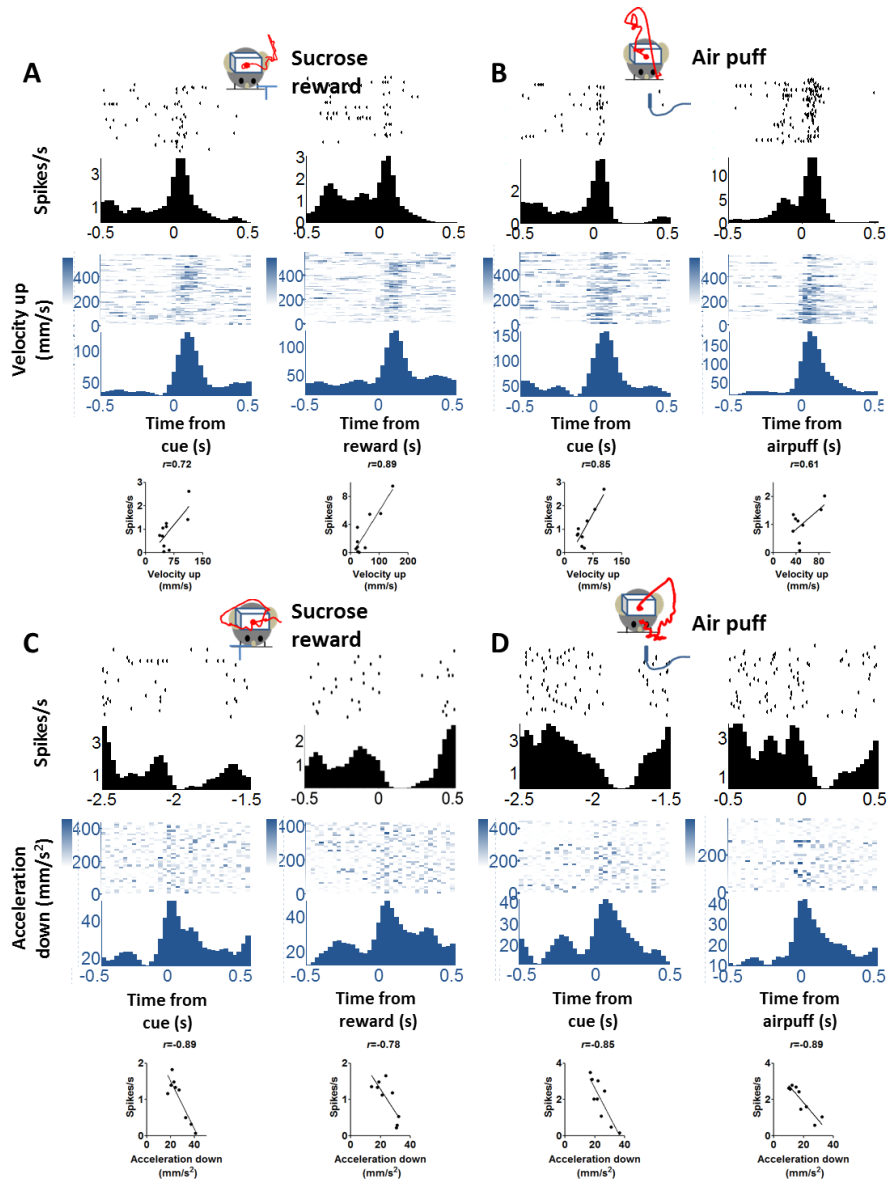


Figure 30. Correlation between firing rate and acceleration is similar on appetitive (sucrose reward) and aversive (air puff) trials. (A) An example of a positively correlated DA neuron on reward trials. The red line represents average movement trajectory from the session. (B) The same neuron on air puff trials. Note that the actual trajectories differed significantly between reward and air puff trials, but the upward components of velocity are similar, as shown here. (C) An example of a negatively correlated DA neuron on reward trials. (D) The same neuron on air puff trials

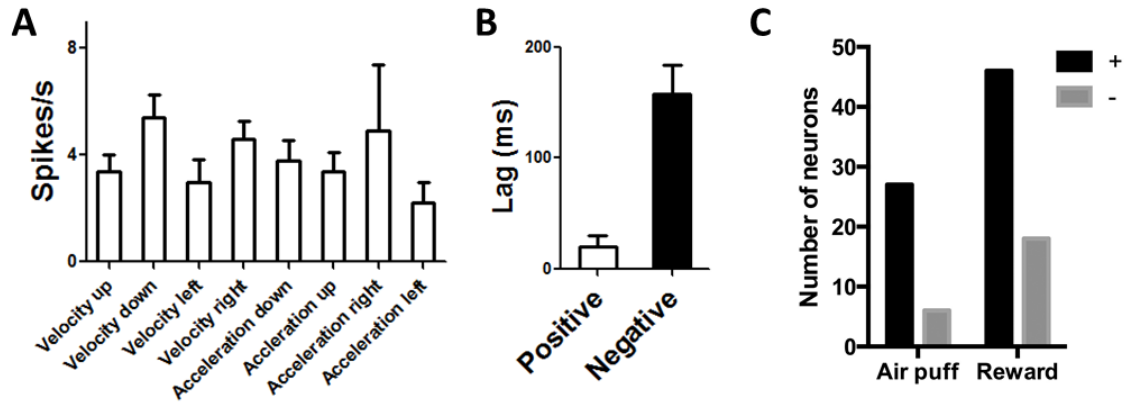


Figure 31. Population data for DA neurons on rewarded and air puff trials. (A) Different classes of DA neurons show comparable firing rates. (B) Using cross correlation analysis, we also found the lag is much longer for negatively correlated neurons, suggesting that, in these neurons, a pause in firing precedes some movement. (C) The proportion of positively and negatively correlated neurons is similar for aversive and rewarding sessions.

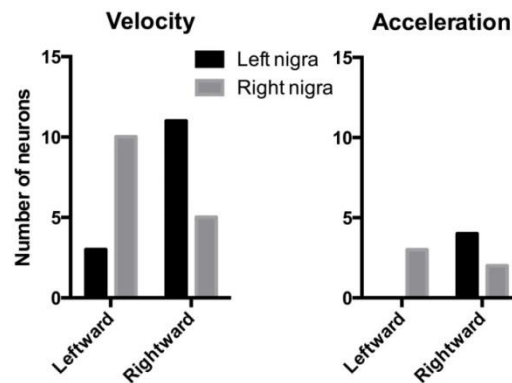


Figure 32. Lateralization of direction-specific neurons. Among velocity-related DA neurons, there are more rightward neurons in the left nigra, and more leftward neurons in the right nigra. There was no significant lateralization among acceleration-related neurons, though the sample size is much smaller

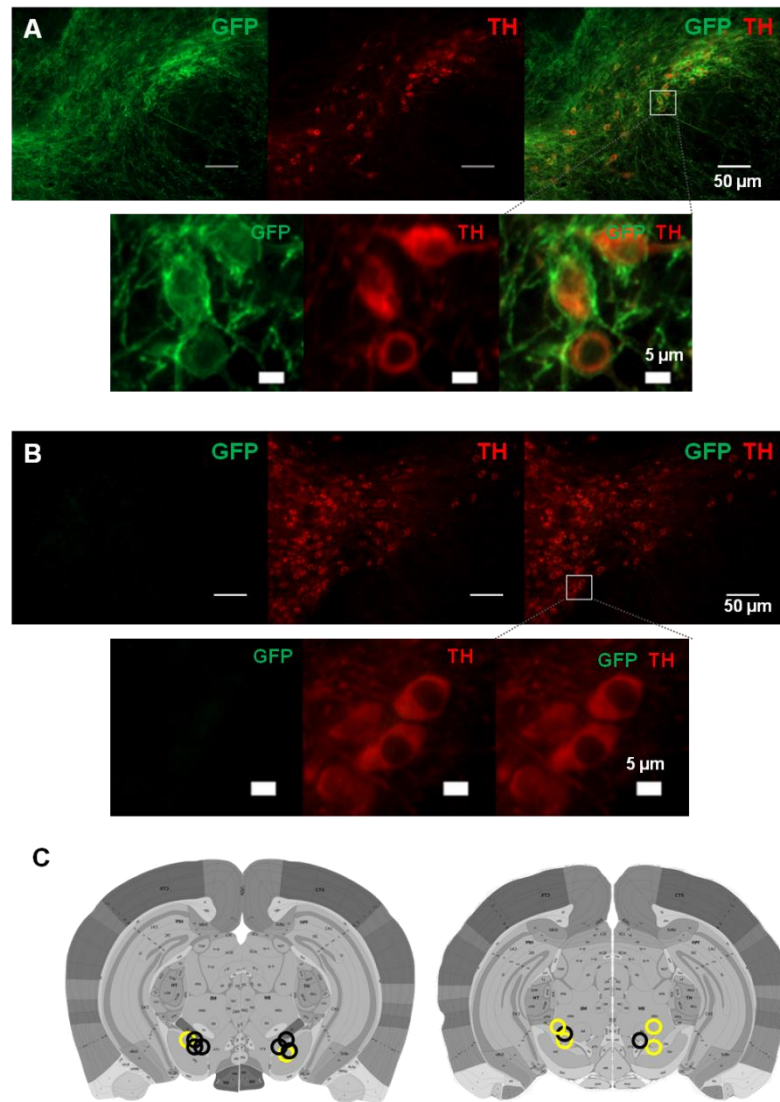


Figure 33. Expression of channelrhodopsin 2 in dopamine neurons in Th::Ai32 mice. (A) Locations of bilateral optic fibers based on histological verification of coronal brain slices. Representative GFP fluorescence, indicating ChR2 expression, is co localized with TH in the substantia nigra of Th::Ai32 transgenic mice. Scale bar is 50  $\mu\text{m}$  (upper panels). Lower panels are zoomed in images from the box shown in the upper right panel (scale bar 5  $\mu\text{m}$ ). (B) GFP fluorescence is absent in Th-Cre control mice. Same conventions as A. (C) Optic fiber placements for Th::Ai32 (n=4; black circles) or Th-Cre (n=3; yellow circles) mice. Atlas images are from the Allen Brain Atlas (Lein et al., 2006). Available from: <http://mouse.brain-map.org/>.

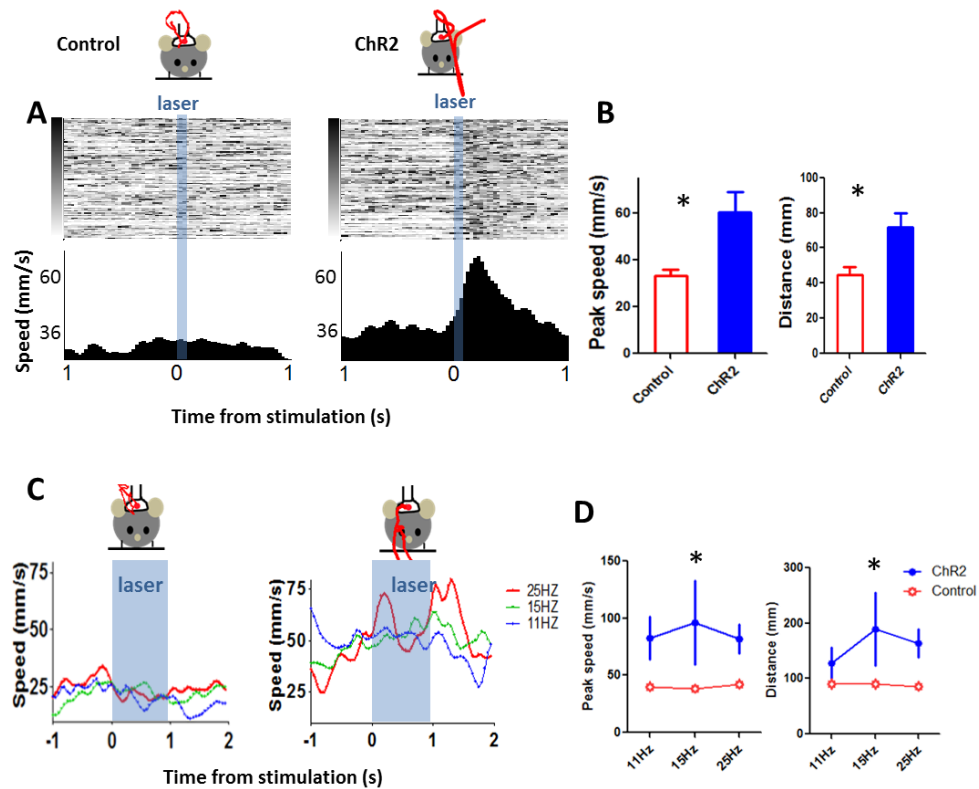


Figure 34. Optogenetic stimulation of DA neurons can elicit movements. (A) To mimic burst firing of DA neurons, we selectively stimulated DA neurons using optogenetics. We generated a transgenic mouse line (Th-Cre $\times$ Ai32) to selectively express ChR2 in DA (tyrosine hydroxylase-positive) neurons. A brief stimulation at 40Hz (3ms pulse width, 5 pulses) generated movement, in the ChR2 (Th::Ai32) mouse but not in a control mouse (Th-Cre) that also received the same light stimulation. Control mice were implanted with fibers and stimulated using identical procedures. Red trace represents movement trajectory. (B) Peak speed and distance for ChR2 (Th::Ai32) and control (Th-Cre) mice. \* $p < 0.05$ . (C) Left, movement kinematics plotted for different stimulation frequencies (11, 15, and 25Hz, 3ms pulse width, 1 s duration). (D) Peak speed during stimulation train and distance traveled (at the end of the train) at different stimulation frequencies. \* $p < 0.05$

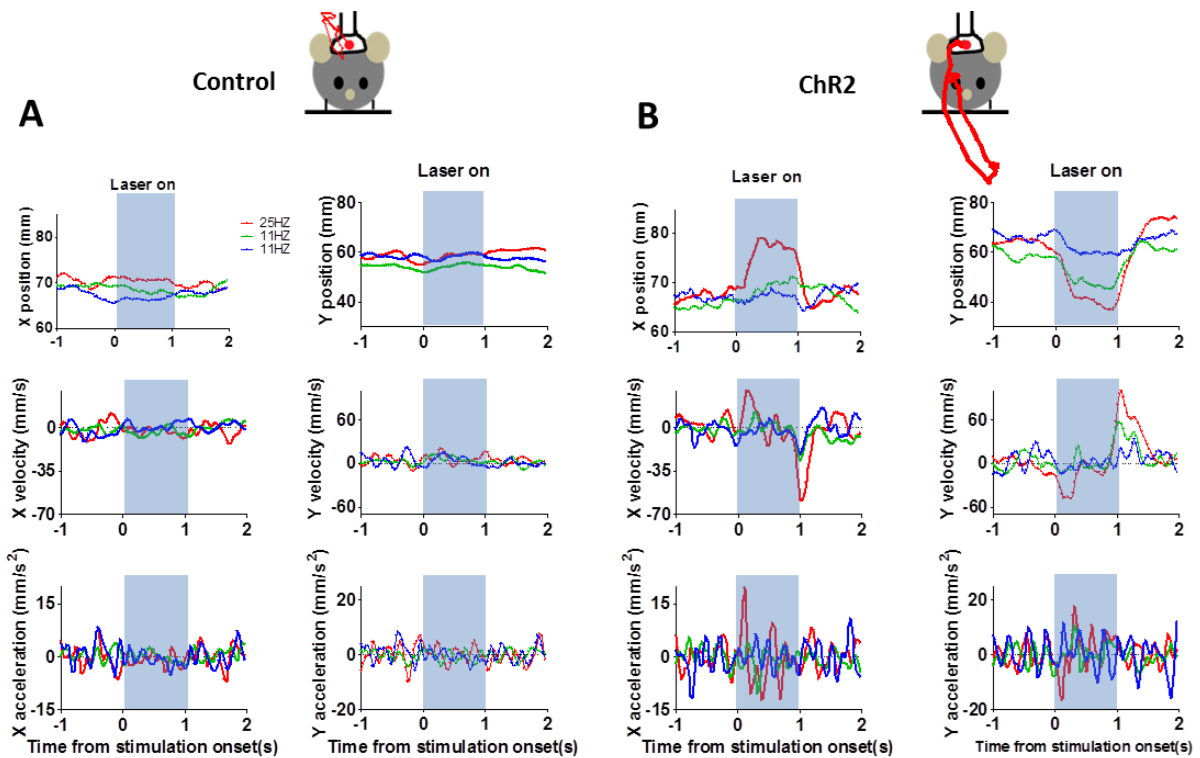


Figure 35. Detailed movement kinematics during optogenetic stimulation. (A) Representative horizontal (x) and vertical (y) components of the movements in a control mouse (Th-Cre). Position, velocity, and acceleration are plotted separately. Red traces show movement trajectories produced by the stimulation. (B) Representative data from a Th::Ai32 mouse.

#### 4.4. Discussion

##### 4.4.1. Summary

In the current study we employed a Pavlovian trace conditioning task in parallel with motion tracking to investigate the phasic responses of dopamine neurons to cue presentation and reward delivery in relation to movements. Our results show similar patterns to those previously reported in monkeys (Schultz, 1998b), rats (Roesch et al.,

2007) and mice (Cohen et al., 2012). In these studies, the patterns of neural activity were interpreted within the framework of the reward prediction error hypothesis (Schultz et al., 1997). In the current study, such an interpretation of neural data in relation to task events is also possible. However, a careful analysis of motion tracking data revealed for the first time a continuous relationship between neural activity and motor output which is at odds with the reward prediction error hypothesis, and implies the possibility of a much simpler interpretation of the role of dopamine in behavior.

The use here of continuous video-based motion tracking allowed us to precisely quantify the behavior of animals. This technique is a key difference separating the current study from previous work, which has historically interpreted neural data in relation to experimenter-defined task events rather than in relation to continuous behavior. As shown in Figure 24, at the time of cue presentation the animal initiates a movement to bring its head closer to the reward spout, and then at the time of reward delivery the animal initiates consumption behavior. When quantified these two movements register as changes in head velocity and acceleration vector components occurring at the time of cue and reward delivery. The phasic responses of DA neurons were highly correlated with these velocity and acceleration components of movement. Thus, even though DA neurons do exhibit typical phasic responses to cue and reward presentation, these responses may be entirely explained by their relationship to task-elicited movements.

The correlations found between DA firing and movement kinematics were not restricted only to changes occurring around cue and reward but existed during the entire experimental session, including inter-trial interval (Figure 28). DA neurons correlating with different vector components of movement were identified using an unbiased session-wide correlation analysis between firing rate and all candidate variables. As shown in Figures 30, these correlations were also independent of the presence of reward; similar high correlations were found in the same neuron between trials in which an aversive airpuff followed the cue and trials in the same session in which the cue predicted a sucrose reward. DA neurons thus represent movement kinematics independently of whether the movement is directed to approach a reward or to avoid an unpleasant stimulus. To investigate the 'causal' role of DA neurons in movement, we mimicked phasic DA activity through optogenetic stimulation of dopamine neurons. Using brief pulse-trains of stimulation at physiological frequencies (Pan et al., 2013; Rossi et al., 2013b), we were able to elicit similar movements to those seen in response to task events during recording sessions (Figure 34).

The correlation between firing rate of dopamine neurons and specific vector components of velocity and acceleration reported here has also been observed in striatal neurons (Kim et al., 2014). Combined, these results suggest that nigrostriatal projections may be organized into a number of distinct vector-component controllers, in which DA neurons project to striatal neurons controlling the same direction of movement. For example, DA neurons that fire during leftward movement are

hypothesized to project to striatal neurons that fire during leftwards movements. Given that unilateral stimulation of striatum or application of DA agonists after depletion-induced receptor supersensitivity can produce contraversive turning or circling behavior (Ferrier, 1876; Hefti et al., 1980), we expect that striatal-DA modules are asymmetrically distributed across the two sides of the brain. This prediction is supported by our results, which show that the left nigra contains more rightward neurons and the right nigra contains more leftward neurons (Figure 32).

**TABLE 1 | Summary of different types of DA neurons.**

	<b>Velocity</b>	<b>Acceleration</b>	<b>Total</b>
Up	18	9	31
Down	19	13	28
Left	13	4	18
Right	16	5	20
Total	66	31	97

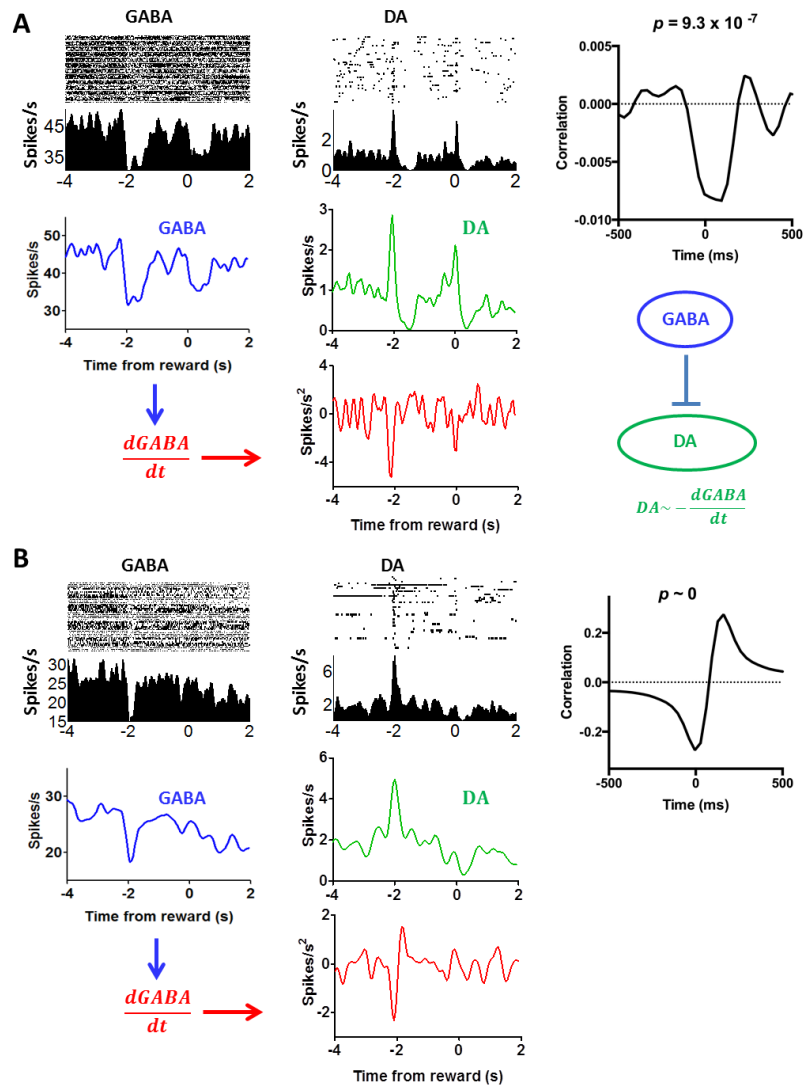


Figure 36. Comparison of putative nigral GABA and DA neurons from the same electrode array. (A) The activity of the GABA neuron reflects y-position coordinates, an example of representation of instantaneous position coordinates reported in our recent study (Barter et al., 2015). The activity of DA neuron reflects velocity in the upward direction. If we take the derivative of the GABA output, we can generate a mirror image of the DA activity. This result, then, is in support of disinhibition: the reduction in GABA output is accompanied by an increase in DA firing. Note that these projections are mostly collaterals of fibers terminating in other areas such as the tectum and thalamus. Cross-correlogram shows the relationship between DA firing and the derivative of the GABA output from the entire session. (B) Another example illustrating the relationship between DA and GABA neurons from a different mouse

#### 4.4.2. Caveats

The results of this study suggest that DA plays a direct role in generating movement kinematics, rather than encoding reward prediction error, and support the hypothesis that nigrostriatal DA modulates the gain of a closed loop movement velocity controller. They have important implications for our understanding of BG function. But before discussing these implications, a few caveats must be mentioned.

First, we only recorded the activity of DA neurons in the SNc, which contains the largest group of DA neurons forming the nigrostriatal pathway, which mainly targets the dorsal striatum. We did not record from the ventral tegmental area (VTA), which gives rise to the mesolimbic pathway projecting to ventral striatum, prefrontal cortex, and other limbic regions. It is possible that VTA DA neurons have different properties in responding to rewards. However, it should be pointed out that SNc and VTA neurons are known to have similar patterns of phasic activity in response to task events (Schultz, 1998a). The activity of VTA neurons has also been shown to correlate highly with movement (Puryear et al., 2010; Wang and Tsien, 2011b; Wang et al., 2013). Thus, the role of VTA DA in reward processing and kinematic control remains an open question.

A second caveat is the possibility that the Cre driver line used for generating the *Th::Ai32* mice may express Cre recombinase in some non-DA neurons as well (Lammel et al., 2015). Although the main evidence showing Cre expression in non-DA neurons comes from the VTA rather than the SNc, we cannot rule out the possibility that photo-stimulation activated a small number of non-DA neurons as well. Although our

histological analysis showed that ChR2 expression is confined to tyrosine hydroxylase positive neurons, cell counts using confocaimages would be required to confirm this conclusion.

A recent study reported the existence of a subset of optogenetically identified SNr GABAergic neurons exhibiting short latency burst responses to salient cues during a trace conditioning task (Pan et al., 2013), thus raising the possibility that the putative DA neurons reported here just a subset of GABA neurons with phasic responses. In the absence of cell type identification in each recorded neuron, we cannot rule out this possibility. However, it is unlikely that the putative dopamine neurons reported here are GABAergic for several reasons. First, we identified DA neurons based on waveform and firing rate (Figure 25). The low average firing rates of putative DA neurons (~ 5 Hz) in our study are comparable to those of identified DA neurons reported in Pan et al. The high tonic firing rates of GABA neurons in their study are also comparable to what we observed, indicating similar cell type classification criteria. In support of this claim, similar short latency phasic responses in SNr GABA neurons have been reported in recent studies employing the same cell-identification criteria as used here (Fan et al., 2012; Rossi et al., 2013a).

#### **4.4.3. Reward prediction error**

Previous work has found phasic firing of DA neurons after reward delivery early in training, and after presentation of reward-predicting cues later in training (Schultz, 1998a). This finding has been taken as evidence in support of influential models of learning that use prediction errors as teaching signals in learning (Rescorla and Wagner, 1972; Sutton and Barto, 1981; Schultz et al., 1997; Schultz, 1998a; Fiorillo, 2013). Although it is beyond the scope of the current discussion to address the technical limitations of these models, the findings presented here provide clear evidence against the role of dopamine in reward prediction.

Previous studies rarely quantified movements even though reward-related task variables were not dissociated from movement. Most studies also recorded from restrained animals, so even if the animals attempted to move by generating the requisite neural signal they were prevented from actually doing so (Bayer and Glimcher, 2005). But inability to move does not mean that the neural signals involved in the control of movement properties are absent. Thus, in all previous studies of the role of dopamine signaling in reward processing, movement is an important confound.

Our results suggest that shifts in DA responses to task events over time could reflect changes in movement properties over time. For example, a naïve mouse will run to obtain a reward only at the sight of a reward but not at the sound of a reward-predicting tone. A well-trained mouse, on the other hand, may begin reward-directed movement at the sound of the tone. Our results also suggest a way to reconcile the role

of dopamine in responding to both rewards, and 'salient' stimuli; they all elicit movement. None of the experimental manipulations (reward size, probability, violations of reward prediction) used in traditional studies are free of this movement confound, since in all of these cases the manipulation could result in subtle changes in movement which would be impossible to detect without motion tracking. However, in order to directly test these hypotheses would require that we employ an identical experimental apparatus to those used in the original studies, with the addition of motion tracking.

None of the following findings can be accounted for by the RPE hypothesis: the selectivity of DA neurons for different directions of motion (Figure 26-27), the linear relationship between DA activity and kinematic variables independent of reward (Figures 28, 30), the high correlation between DA activity and movement on appetitive and aversive trials (Figure 30), the lateralization of leftward and rightward selective neurons on the two sides of the brain (Figure 32), or the observation that DA activity reflects the mathematical derivative of the GABAergic SNr output (Figure 36). Nor can it explain previous observations on locomotion (Wang et al., 2013), posture control (Wang and Tsien, 2011a; Barter et al., 2014), motivational modulation (Rossi et al., 2013a), or instrumental behaviors (Jin and Costa, 2010; Fan et al., 2012). Yet, all these results can be explained by the crucial role of DA in shaping movement kinematics.

#### **4.4.4. Nigrostriatal DA and direction specificity**

The correlation reported here between DA activity and velocity components of movement is similar to what has been reported in striatal neurons (Kim et al., 2014). Given that the striatum is a major target for DA neurons, and that stimulation of DA neurons or their targets in the striatum can elicit movement (Kravitz et al., 2010), this is unsurprising.

The directional specificity observed in both DA and striatal neurons suggests a scenario in which DA neurons whose activity correlates with a particular direction of movement project to striatal neurons whose activity correlates with the same direction of movement. For example, DA neurons that fire during leftward movements are hypothesized to project to striatal cells that also fire during leftward movements. Given that unilateral dopamine depletion is well known to elicit contraversive turning in mice (Hefti et al., 1980), we predict a scenario in which DA neurons controlling leftward movements are located on the right side of the brain and vice versa. This prediction is supported by our results which show that the left nigra contains more right-movement correlating dopamine neurons and the right nigra contains more left-movement dopamine neurons.

Unlike traditional accounts of movement which assume that movement direction is encoded by a population vector of differently tuned cortical neurons (Georgopoulos et al., 1986), the current data support a model in which tuning properties of different neurons reflect membership to different position controllers for a particular axis of

orientation or joint angle. By combining the outputs of these controllers, position along multiple dimensions can be controlled in parallel. This hypothesis is supported by previous work suggesting distinct controllers in the brainstem for horizontal and vertical movements (Masino, 1992).

#### **4.4.5. Transition control**

The role of dopamine in scaling aspects of behavior is well known by a number of different terms. For example, DA is thought to reduce sensorimotor threshold (White, 1986), or increase “response vigor” (Niv et al., 2007), or bias action selection (McClure et al., 2003; Roesch et al., 2007). However, these accounts are purely descriptive, and offer no explanation of the underlying functions actually responsible for generating behavior, or the specific role of dopamine in modulating these functions.

The present findings support a model of the BG as a transition control system (Yin, 2014b) in which DA acts as the output gain or ‘throttle’. According to this model, the basal ganglia constitute a level in a perceptual control hierarchy, and as such are thought to receive reference signals from higher systems, and to correct their own errors by sending reference signals to lower systems capable of reducing them. The key variable being controlled by the basal ganglia in this model is the velocity of various types of perceptual signals. According to this model, there are different classes of neurons in the basal ganglia actively controlling different vector components of body

movement. Neurons that fire preferentially when the animal moves a body part in a particular direction send descending reference signals to position controllers utilizing the same body part located in the midbrain, diencephalon and cortex, which in turn command muscle length and joint angle controllers in the reticulospinal pathway (Yin, 2014b). This model also predicts that a similar process occurs for adjusting the reference signals of various self-contained motor programs such as locomotor rhythm control by the MLR, so that the BG control the desired speed of locomotion, for example, in the same way that they control the desired position of a body part. However because the present data describe only correlations with body geometry, we will focus our discussion on body configuration transition control as a prototype for all forms of transition control.

The body configuration of an animal can be described as a set of joint angles. These angles can be perceived as the difference in muscle length between extensors and flexors at a joint, and controlled by continuously sending reciprocal muscle length reference signals of opposite signs to those muscles. Joints can also be combined through a similar process into unified multi-joint configurations such as 'extend/retract' or 'sway', and controlled as such. Such systems are position control systems, since the reference signal specifies a desired position and not a desired movement or torque; speed is determined by the loop gain of the system and cannot be regulated. To actively regulate movement speed between different body configurations, velocity itself must be a controlled variable; perceived as the derivative of the position of a particular

configuration variable and controlled by adjusting the reference signal of the position controller for the same variable.

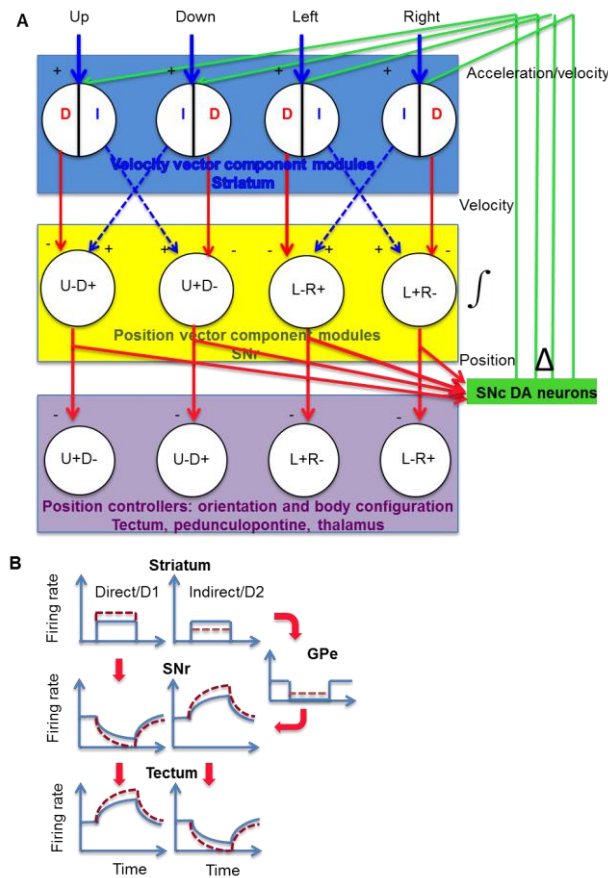


Figure 37. Proposed model for DA modulation of striatal outputs . (A) SNr neurons receive projections from the striatum and external globus pallidus, via the direct (D, striatonigral) and indirect (I, striatopallidal) pathways. The net effect on the SNr could be either inhibitory (minus sign) or excitatory (disinhibitory, plus sign). Both types of signals represent velocity error signals from the velocity controller. The dorsal striatum is hypothesized to contain at least four different modules, each responsible for movement in a specific direction. Striatal neurons can signal velocity error signals (Kim et al.,2014), which is integrated by the SNr and converted into position reference signal to position controllers in the midbrain and diencephalon (Barter et al.,2015). Using the outputs from the different modules, this circuit can perform vector addition to generate the actual movement vector. The magnitude of the signal entering the integrator is proportional to the rate of change in the integrator output. (B) Illustration of activity in the BG circuit, using a square pulse to represent a transient burst of action potentials

with constant firing rate from striatal projection neurons. Dotted lines indicate altered firing rates as a result of DA modulation. DA is known to exert opposite effects on striatonigral neurons and striatopallidal neurons. Striatonigral neurons, which express D1 receptors, are increased by D1 activation, whereas striatopallidal neurons are inhibited by D2 activation (Gerfen and Surmeier, 2011). Moreover, activation of D1 receptors can also potentiate GABA release at the striatonigral terminals (Chuhma et al., 2011), whereas activation of D2 receptors can reduce GABA release at the pallidonigral terminals (Connelly et al., 2010; de Jesús Aceves et al., 2011). The net effect is consistent for the targets of SNr output. DA modulation has the net effect of potentiating the firing rate in a given position vector component, and further suppressing the antagonistic component. By increasing the rate of change in the position reference, the actual movement velocity is increased. As shown, both movement amplitude and speed are altered, but these variables can be independently controlled.

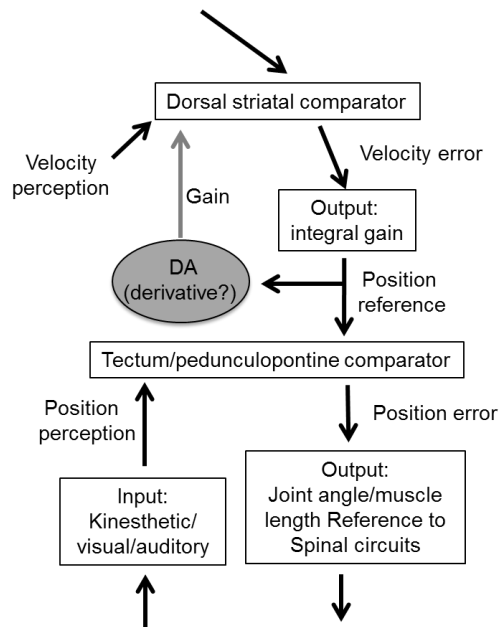


Figure 38. Model of cascade control hierarchy for velocity and position control of a single joint angle. The velocity control system is hierarchically higher than the position control system. There are multiple position controllers, including those for orientation and body configuration, which can command hierarchically lower controllers for joint angle, muscle length, and muscle tension (not shown here). The lowest level is the tension or force controller, with alpha motor neurons acting as the comparator and muscles as the output function (Yin, 2014a).

As discussed in the previous chapter, evidence suggests that body configuration and orientation are variables controlled at the level of the midbrain, brainstem and motor cortex, and that reference signals representing the desired states of these systems are issued from SNr neurons (Barter et al., 2015a). These SNr neurons, in turn, are believed to integrate inputs from striatal neurons representing the velocity of movement of the same controllers (Kim et al., 2014). Although direct evidence has so far only implicated this process in controlling head position along the frontal plane, striatal neurons are known to show diverse body part representation (Carelli and West, 1991; Alexander et al., 1986), suggesting that position control occurs in parallel for all of the controllers involved in voluntary movement, with each controller having a dedicated set of neurons in the striatum, SNr and brainstem or motor cortex. It is proposed here that striatal neurons convert a hierarchically higher error signal into a set of signals specifying movement directions and relative speeds for the set of body configuration variables required to reduce that error. These signals are thought to be represented by striatal firing rate in different configuration control modules, and the magnitude of these signals is thought to be determined by DA, which acts as the output gain of this system. These striatal signals are sent to the SNr where they are integrated. By integrating these signals, the firing rate of SNr neurons, and thus desired position, can change. In this way, striatal neurons control the movement of a body part through SNr neurons, which themselves control the position of the same body part.

The exact function of DA neurons as gain control in this process is still not fully clear. One possibility is that DA neurons actively control signal velocity by comparing the velocity of GABA cell firing to a reference velocity specified from elsewhere in the brain, and sending the velocity error to the striatum in the form of output gain adjustment. In this way, if the GABA signals—and thus body configuration—are changing too fast, DA neurons will turn down the gain, and if they are changing too slowly DA neurons will turn up the gain. An alternate possibility is that DA neurons act as a part of a more complex open-loop adaptive control mechanism. In either case, it should be pointed out that outputs from the BG can vary continuously in the absence of a changing reference signal as a neutral posture is defended against environmental disturbances.

#### **4.4.6. Above transition control**

According to the model presented here, the comparator for the transition controller resides in the striatum. Thus, each striatal module for controlling the movement of a particular configuration variable must receive perceptual inputs representing that quantity, as well as a reference signal from a hierarchically higher control system. These signals are likely to arrive at the striatum from thalamic and cortical projections. This arrangement allows for the velocity controller to be used as a common output function for controlling any number of higher perceptual variables,

such as proximity to a target. Control of such higher-level perceptual variables is often termed 'goal directed' or 'voluntary' behavior.

For example, the mice in the current task must reduce proximity between mouth and sucrose spout to zero, given any starting head position. In this scenario, head movement is hypothesized to be guided by at least 3 target position controllers; one perceiving and controlling each of the three dimensions of target position in Cartesian XYZ coordinate space. For each of these three control systems, the input is a single value representing the position of the spout along a spatial dimension and the output, which represents current error, is converted into a set of velocity command signals for configuration controllers capable of reducing that error. For example, control of x-axis position relative to the target is likely to involve reference velocity commands to 'left-right bend' spine configuration controllers, while control of z-axis position is likely to involve velocity commands to 'extend-retract' spine position controllers. According to this model, as the proximity error is reduced the velocity reference signals will also be proportionately reduced, resulting in a deceleration as the mouth approaches the spout. The same basic principles are expected to apply in any proximity control task, such as locomotor pursuit or arm reaching.

#### **4.4.7. Control of input**

To understand the hierarchical control model presented here, it is important to point out the fundamental difference between this model and traditional models that purport to use closed loop control (Todorov and Jordan, 2002). Attempts to apply control theory in neuroscience have largely been hampered by a key misunderstanding introduced by engineering terminology. In the engineering tradition, controllers are typically said to control their outputs, because the output value can match the desired value (from the perspective of the engineer). The controller is thus described as an input/output device: error in, behavior out.

Thus according to the traditional view, feedback control is the process of computing the commands (or “control signals”) required to produce a particular position given a particular error. Such systems are known as servos. But the prescribed reference value in any living organism does not come from outside of the organism, as with a user adjusting the temperature setting of a thermostat, but from within (Powers et al., 1960). Consequently, in living control systems, the reference signal is never an input command from the environment. The true input always comes from perceptual representations, the desired values of which are dictated by reference signals within the organism. The key operation, then, is the control of sensory inputs through variation in motor outputs. Whenever feedback control is viewed as the control of output, the control loop cannot be analyzed correctly, because the inside and outside of the system are reversed. In the model described here, only perceptual inputs are controlled;

outputs vary as needed to control input at a desired level. Command signals in a control system are not sensory or motor; they are the result of a comparison between the two.

#### **4.4.8. DA and adaptive gain control**

As mentioned above, we hypothesize that the sensorimotor striatum is organized into topographically mapped modules, each dedicated to controlling a specific velocity vector component of a specific configuration controller (i.e. left/right bending of the spine). DA is hypothesized to serve as the output gain in these velocity controllers. As a neuromodulator, DA does not directly cause firing of target neurons, but alters the responsiveness of these neurons to inputs (Gerfen and Surmeier, 2011). Thus DA can determine the magnitude of the velocity command signal, and consequently the rate of change in body configurations. The lack of DA is therefore expected to reduce movement speed. Indeed, slowness of movement or bradykinesia is a major symptom of Parkinson's disease, due to degeneration of DA neurons.

DA can have different effects on striatonigral (D1-expressing) and striatopallidal (D2-expressing) neurons giving rise to the direct and indirect pathways, respectively, but the ultimate effect is to proportionally modulate opponent output signals for downstream controllers (Figure 37). The organization of direct and indirect pathways implements a phase splitter that takes a common input to the striatum and generates antiphase output signals for commanding antagonistic controllers. For example, to move

a configuration in one direction may depend on signaling from the direct pathway while moving it in the opposite direction may depend on signaling from the indirect pathway. If this antiphase organization did not exist then configurations could only move quickly in one direction from neutral, because to move in the other direction would depend entirely on integrator leak. The facilitating properties of the striatonigral synapse suggests that nigral integration of the inhibitory input is possible, whereas the depressing property of the pallidonigral synapse means that integration of the excitatory (disinhibitory) input is also possible (Connelly et al., 2010; Zhou and Lee, 2011). This ‘antiphase integrator’ hypothesis is supported by findings that neurons from both pathways are simultaneously activated during behavior (Cui et al., 2013; Isomura et al., 2013), and by the observed opponent BG outputs from the SNr projection neurons (Fan et al., 2012; Rossi et al., 2013a; Barter et al., 2014; Barter et al., 2015a).

#### **4.4.9. Relationship between BG output and DA activity**

A major source of input to SNr DA neurons is neighboring SNr GABA neurons, which inhibit DA neurons directly. These inhibitory projections come from collaterals of the GABAergic fibers which presumably synapse on other targets such as the tectum and thalamus (Tepper and Lee, 2007). SNc DA neurons can fire tonically at a low rate by calcium entry through voltage-gated calcium channels. Burst firing in DA neurons, on the other hand, appears to require NMDA currents produced by glutamatergic inputs.

However, due to tonic GABAergic inhibition from SNr outputs, reduced GABA release can also generate burst firing (Kang and Kitai, 1993; Tepper et al., 1995; Paladini et al., 1999). Local blockade of nigral GABA-A receptors causes bursting in DA neurons, which suggests tonic activation of GABA-A receptors on DA neurons. Thus disinhibition is a major contributor to burst firing in DA neurons recorded here. On the other hand, excitatory inputs from other sources, such as the tectum and pedunculo-pontine nucleus, can also drive DA neurons, but their effects can be reduced by the inhibitory nigral output. Bursting is prevented by GABA-A inhibition even in the presence of glutamatergic inputs (Tepper and Lee, 2007; Paladini and Roeper, 2014).

Whereas activity in most DA neurons is correlated with velocity or acceleration, activity in GABA neurons is correlated with instantaneous position (Barter et al., 2015a). This pattern suggests that the DA neurons could take the derivative of GABA outputs from the BG. Our results support this hypothesis (Figure 36), showing simultaneously recorded GABA and DA neurons in which the derivative of the GABA output is subtracted from the output of the DA neurons. Although these results are preliminary, they suggest a scenario in which there are paired sets of GABA and DA neurons that are part of the same controller modules. In this way, a derivative of BG output can be fed back into the striatum as the velocity control output gain. The functional significance of this feature is in dynamically adjusting the sensitivity of the control loop to facilitate fast movements when the reference signal is changing quickly and stable movements when the reference signal is changing slowly. If the gain of velocity control were fixed then

there would exist a constant tradeoff between speed and stability in movement. The lack of such gain control may explain common symptoms in movement disorders such as Parkinson's disease, which is characterized by tremor and neural oscillations as a result of DA depletion (Brown, 2006; Costa et al., 2006).

As mentioned earlier, an alternative possibility is that DA signaling constitutes the error signal in a signal-velocity control system. According to this perspective, DA neurons monitor the derivative of GABA cell firing and thus the velocity of position reference signals, continuously comparing the perceived velocity against a reference velocity signal coming from elsewhere in the brain. If GABA signals change faster than the velocity reference signal, then DA firing will go down and thus turn down the gain of striatal output responsible for GABA signal change; if GABA signals change too slowly, then DA firing will go up and thus turn up the gain of the same striatal outputs. In this scheme, DA activity would also closely mirror the derivative of GABA cells. According to this model, DA output controls signal velocity by turning up or down the gain of striatal neurons--like turning the knob on a faucet to achieve desired flow. Although such signal-velocity control by DA could occur in parallel with perceptual velocity control in the striatum, it could also conceivably replace perceptual velocity control altogether since signal-velocity of GABA neurons should closely mirror actual movement velocity. In this scenario, the striatum does not need to perform a velocity comparison but must only convert a higher error signal into a set of 'direction' signals which are integrated in the SNr. Thus the exact organization of the velocity control system, whether it be signal-

velocity control, perceptual-velocity control or a combination of the two, remains an open question.

Regardless whether it constitutes a closed loop signal-velocity controller or occurs in parallel with perceptual velocity control, the ability of DA to modulate velocity independently of the higher error signals is an important one, especially in the context of sequenced behaviors. In a sequence, when a new step in a sequence is initiated, the initial error going to be large and then shrink as the animal approaches the goal of that step. If this error is translated directly into velocity command signals, then this pattern will result in very fast movements towards the beginning of a step and very slow movements towards the end of a step. However, if DA is able to modulate the velocity of GABA outputs, then the speed of behavior should be relatively constant as DA turns up and down the gain as needed to hold GABA velocity constant and drive reasonably paced movements despite large changes in the intensity of cortical inputs. This hypothesized function may explain the 'start/stop' activity of dopamine neurons during a sequence task (Jin and Costa, 2010), and the 'ramping' activity in dopamine neurons which has been reported as animals near a target (Howe et al., 2013).

#### **4.4.10. Clinical implications**

According to our model, because DA adjusts the gain of the transition controller, it affects the rate of change of perceptual variables. This feature could explain the role

of DA in certain movement disorders including Parkinson's disease and Tourette syndrome which are characterized by low and high concentrations of DA, respectively. The model supported by the current findings also provides a rough computational explanation of hypokinetic and hyperkinetic movement disorders, according to which hypokinetic disorders can be caused by decreased DA activity or decreased striatal output, and hyperkinetic disorders can be caused by the opposite changes.

As already mentioned, we propose that a reduction in DA simply reduces the magnitude of striatal output, in spikes/s. Because there is hypothesized to be a neural integrator in the SNr receiving these outputs, then a reduced magnitude of striatal outputs results in reduced rate of change in SNr output, and thus a reduced rate of change in body configurations and motor functions. If the integrator in the SNr is leaky and always slowly returning to neutral at a constant rate, then if the total number of spikes entering the integrator is reduced, the overall signal-range will also be reduced—resulting in a reduced range of motion. The reduction in both range and speed of movements in Parkinson's disease is well known. Indeed, it was this observation that led to the proposal that BG output firing rate could encode both variables (DeLong, 1990).

The choreoform movements observed in Huntington's, caused by widespread damage to striatal neurons (Reiner et al., 1988), may also be accounted for by the same model. According to this account, striatal neurons are largely responsible for converting a hierarchically higher error signal, such as proximity error between mouth and sucrose spout, into a precise set of lower velocity or 'direction' reference signals which are

integrated at the SNr to move the body in a way that reduces the error. This process can be likened in some ways to a prism splitting a single beam of light (proximity error) into an array of component beams (movement directions). However, if striatal cells are damaged in a non-uniform way then, like a broken prism, the conversion between proximity error and movement directions will be fractured, and the movements and their relative speeds produced to accomplish a desired proximity will be irregular and likely occur at different speeds ranging from slow to extremely fast. As with any control system with a faulty output function, the outputs are expected to oscillate rapidly around neutral as the higher system works through a faulty output to defend its reference settings; a pattern of output that can be clearly observed in HD patients (Albin et al., 1989).

#### **4.4.11. Implications for motor control**

In previous studies attempting to relate neural activity with movement kinematics, the observed correlation between kinematic variables and single unit activity is typically very low (Paninski et al., 2004). When movement-related signals are used to move some external device, as in brain-machine-interface applications, extensive transformation of the neural data is needed (Hochberg et al., 2006). It is necessary to design a “decoder” to get the signal needed to drive the effector (Taylor et al., 2002). By contrast, here we have shown a strong linear relationship between neural

activity and kinematics. However this is not due to any coding of movement to be used by a decoder; rather the signals recorded are the actual signals used in neural circuits that generate the movements.

#### **4.4.12. Rewards and other goals**

As previously outlined, control of body velocity is driven by a still higher level of control. For example, an animal may alter body velocity to reach for a target, or to center a target in visual space. Perception of such hierarchically higher variables is likely performed in cortical circuits, which are well known to compute such abstract perceptual representations and thus a large pool of potential controlled variables. Many reference signals at the higher levels are acquired perceptual representations, i.e. memories (Mountcastle et al., 1975). By comparing such representations--also traditionally called goals--against incoming perceptions, cortical circuits may calculate the errors required to drive the appropriate goal-seeking movements through basal ganglia circuits. The transition controller can thus be viewed as the final common path for behaviors that are traditionally called 'voluntary'. Such behaviors originate from error signals in controllers above the level of transition control. These error signals can become the reference signals for the central movement controller in the BG. This arrangement allows the velocity controller to be commanded by any number of

systems. A particular action can be performed for any number of purposes, e.g. turning left to reach a reward or to avoid an air puff (Kim et al., 2014).

The term ‘reward’ may thus be more clearly defined as the control of such higher variables; if your goal is to reach for a cup then you might call it ‘rewarding’ to succeed, or if you are hungry they you might call it ‘rewarding’ to eat. In both of these examples it would said that the degree of ‘reward’ experienced is proportionate to how badly the goal is desired, and in proportion to the capacity of an event or object to meet that need. For example, a very hungry animal would be said to find one pellet of food more rewarding than a sated animal, and to find two pellets more rewarding still (Keramati and Gutkin, 2011). Another way to state this is that ‘reward’ is simply a way of describing error reduction in a control system; a hungry animal is by definition experiencing a higher error than a full animal, and pellets are ‘valued’ in proportion to their capacity to reduce that error.

Thus, according to our model, what is often called “reward expectancy” can be viewed as an error signal in a higher-order controller (Yin, 2014a). Because this error is transformed into a transition command signal, then it is proportional to output movement velocity of the animal as long as such velocity is physically possible. In food deprived animals, an increase in the size of the expected reward is known to be associated with faster movements (Hikosaka, 2007). Of course, such a mechanism is not restricted to pursuit of food, but would equally apply to retreat from danger. This correlation between output velocity and value manipulations may thus account for

experimental findings regarding 'value coding' in dopamine neurons and other BG nuclei (Sato and Hikosaka, 2002; Atallah et al., 2014; Cohen et al., 2012; McClure et al., 2003; Roesch et al., 2007; Schultz et al., 1997; Schultz, 2015).

The control of movement velocity is just one type of transition control. The input nucleus of the BG, the striatum, receives inputs from multiple cortical regions, and there are multiple parallel cortico-BG-thalamic loop networks (Alexander et al., 1986). These thalamic loops are topographically organized, with the sensorimotor striatum receiving inputs from primary motor and somatosensory cortices. According to our model, this sensorimotor network contains the transition controller for movement, while the other networks would constitute different transition controllers with different controlled variables based on their sensory representations. The controlled variables for the associative and limbic networks are not well defined, but they are presumably related to exteroceptive and interoceptive inputs, respectively (Yin, 2014b). The rate of change in these perceptual transitions can also be controlled in much the same way, though using a different set of effectors. Indeed, for orofacial consummatory behaviors, DA has been implicated in the control of reward rate (Rossi and Yin, 2015).

It is also important to note that certain perceptual transitions, such as pellet delivery in an FR operant task, cannot be controlled through a single motor transition but must instead be controlled through a sequence of other perceptual transitions, which are themselves controlled through motor transitions. In these cases, it is likely that the error signal of the highest system is sent not to motor regions but instead back

up to cortical regions via thalamic projections, where it is used as a new reference signal for other high-level controllers. In this way, the same mechanism used for motor transitions may be used to generate complex hierarchical sequenced behaviors. This arrangement would explain the apparent role of DA in modulating 'motivation' (Berridge, 2006), which is arguably just another way of describing the velocity of higher-order behavioral transitions.

#### **4.4.13. Conclusions**

Given the known movement deficits following degeneration of DA neurons, it is unsurprising that phasic DA activity is related to movement kinematics. What is surprising is how long it took for this relationship to be uncovered. The failure of previous studies to identify the role of DA in shaping movement kinematics could be explained by the lack of continuous behavioral measurements in unrestrained animals (Romo and Schultz, 1990).

There is a fundamental difference between our approach and that taken in most previous studies. In traditional experimental designs, neural and behavioral data are typically analyzed around a series of discrete time stamps that are meant to represent specific task events as labeled by the experimenter, creating the impression that behavior consists of a series of pulse-like events. Although this approach may provide the appearance of rigor, it also leads the experimenter to ignore any behavior that is not

described by task labels, which often reflect his own perception of the experimental events and theoretical biases in the first place.

As shown in the present study, however, behavior is a continuous process and must be analyzed as such. Although this may seem a daunting task, the underlying relationships between neural activity and behavioral output may actually be quite straightforward.

## **5. General Discussion**

### **5.1. Summary**

#### **5.1.1. Summary, Chapter 2**

In this set of experiments, mice stood on a small covered perch which was continuously tipped left and right along the roll plane while neural activity was recorded wirelessly. During each recording session, mice were exposed to slow and fast speeds of postural disturbance. Pressure pads were mounted in the left and right floor of the perch to monitor mouse movement. In both dopamine and GABA neurons, we found two basic patterns of neural activity; one class of cell increased firing with tip to the left and decreased with tip to the right while the other class decreased firing with tip to the left and increased with tip to right. This correlation between neural firing rate and instantaneous postural disturbance is continuous and very high. The correlation is seen for both slow and fast disturbances. The majority of cells recorded fell into one of these two categories. Pressure pad readout, as expected, revealed paw forces on the left pad to increase with tilt to the left and decrease with tilt to the right while the opposite pattern was observed on the right pad.

These results show continuous and graded modulation of activity in the substantia nigra during performance of an ongoing motor task. GABAergic outputs, which are known to project to the PPN and tectum, in this case may function to continually adjust the reference settings of these motor systems as a means of defending neutral body position against continuous disturbance. Dopamine signaling in

this case may reflect the continuous modulation of some internal property of BG signaling involved in motor control, such as the output gain of a higher level control system. Combined, these results move us beyond a simple 'gate' model of basal ganglia function by suggesting that BG outputs, rather than monolithically disinhibiting brainstem motor structures, instead coordinate behavior by continuously specifying desired states of lower systems.

### **5.1.2. Summary, Chapter 3**

In the previous set of experiments we demonstrated continuous and graded modulation of substantia nigra activity by a postural control task. However, because we did not record motor outputs in this study, the exact relationship between neural and motor outputs remained an open question. The experiments in this chapter were designed to address this question through use of continuous motion tracking of the head in parallel with neural recording from the substantia nigra during a simple goal-directed task. In this study, mice were water deprived and then positioned in the same perch used during the previous set of experiments. However, in this study, the perch was kept stationary and modified with the addition of a movable drinking spout. During each session, mice performed a simple reward-guided task in which sucrose solution was delivered in small quantities after the presentation a cue. The purpose of this task

was to elicit voluntary head movements and to investigate the relationship between these continuous movements and the activity of GABA output neurons in the SNr.

A typical reward-directed behavior involved the movement of the whole head and body to collect the sucrose solution following its delivery. However, movements during each individual trial were unique. For all movements, the majority of GABA cells were found to either positively or negatively correlate with either x or y-axis head position vector components. These correlations were very high, and not due to averaging artifacts as trial-by-trial correlation between movement and neural activity can be clearly observed. These correlations were also independent of the presence of a reward.

These data show for the first time a continuous and quantitative relationship between basal ganglia output and body posture. One attractive possibility is that these signals represent reference signals sent to downstream postural and orientation controllers. In this case a baseline level of GABA activity would represent neutral reference position, and changes in activity above and below this level represent increased or decreased reference positions. Thus, during free behavior it is a transition in GABA output from baseline that constitutes a movement while the signal itself specifies a position. This model represents an important revision of classical models of BG function, according to which output signals are thought to discretely release the initiation of a monolithic action.

### 5.1.3. Summary, Chapter 4

In the set of experiments outlined in chapter 3 we demonstrated a continuous and quantitative relationship between the activity of individual GABA neurons and the x or y-axis position of the head. However, the relationship between SNc dopamine activity and head movement during the performance of the same task was not analyzed. The set of experiments in chapter 4 were designed to address this by investigating the correlation between DA activity and kinematic properties of head movement during the same task.

Analyses of behavioral data show that animals produce movements at the onset of the cue and also at reward delivery. Dopamine-classified cells show phasic firing or pausing at the onset of each of these movements. When compared to head movement kinematics, these patterns of neural activity correlate highly with different vector components of head acceleration and velocity; up, down, left and right. Importantly, these correlations are continuous and exist throughout the entire recording session. These correlations are also independent of the presence of reward.

We also employed optogenetics to stimulate SNc DA neurons expressing channelrhodopsin 2 (ChR2) while head movements were recorded and quantified. We found that stimulation of ChR2-expressing animals could elicit head movement while stimulation of control animals had no effect. Combined, these data suggest the interesting possibility that dopamine is responsible for controlling the velocity of transitions between different body postures.

## **5.2. The role of BG in behavior**

Combined, the results of the studies described in the previous three chapters support a new model for the function of the BG in coordinating motor behavior (Yin, 2014; Powers, 1973). According to this model, the SNr does not inhibit or disinhibit motor functions or ‘actions’, but instead continuously specifies reference settings for lower control systems, such as desired body configuration or orientation along a particular axis. Dopamine neurons in the SNc, on the other hand, are thought to be responsible not for reinforcing ‘actions’ or controlling ‘vigor’ as traditionally believed, but for modulating the gain of transitions between different reference states.

## **5.3. Control of sensory input**

Before the model described here—or the role in it of BG outputs—can be fully understood, it is necessary to first highlight a key principle so ubiquitous that it is often invisible: negative feedback control in behavior. Take the example of an animal that has been trained to walk in a ‘figure 8’ pattern; while the observer sees a consistent pattern from trial to trial, it is actually brought about by a constantly changing set of motor outputs, which may change even more dramatically if the walking platform is tipped (Powers, 1973; Powers, 1989; Yin, 2013). The key feature of behavior in this case, as is the case in all motor behavior (Bernstein, 1967), is that variable acts produce consistent results. Another way to state this is that in a continuously changing environment, the

outputs of the animal vary in precisely the manner required to defend certain perceptual variables against change; a mouse standing on a tipping platform will extend its limbs as needed to keep its body upright, while a thirsty mouse will move its head from any starting position in exactly the pattern required to bring it close to a drinking spout.

When the outputs of a system have the effect of continuously holding a sensed variable constant against environmental change, then that system is by definition exhibiting negative feedback control (Powers, 1973). Negative feedback control is the only known mechanism capable of reliably producing this effect. As mentioned in a previous chapter, negative feedback control was first discovered in the 1930s and used by engineers to design systems to replace human operators. The engineers had thus, by definition, created a working model of human behavior as surely as if they had set out to do exactly that (Powers, 1992). Originally popularized by Norbert Wiener and his *Cybernetics*, the analysis of negative feedback in behavior has, however, been handicapped by a small number of key errors in its original description which have limited its usefulness (Barter et al., 2015b; Powers, 1992; Yin, 2013). When viewed correctly, negative feedback is an extremely elegant principle that can account for the majority of animal behavior.

### **5.3.1. Motor control as control of sensory input**

Motor control by lower levels in the nervous system, such as control of locomotion and posture by brainstem and spinal systems, is thought to be relatively straightforward and to depend on local network dynamics (Grillner et al., 2008). However, at higher levels involving complex sensory goals, such as target reaching, motor control is thought to represent the solution to a significantly more difficult set of problems; namely the problems involved in calculating the patterns of muscle output that will be required to achieve a sensory goal state (Franklin and Wolpert, 2011; Krakauer et al., 1999; Shadmehar et al., 2010; Shadmehar and Krakauer, 2008).

To be able to accurately perform these calculations, the brain must have extensive knowledge of the masses of various body parts, spring constants and properties of muscle contraction, variations in mechanical advantage with changes in joint angle, and physical properties of external objects, among other things (Yin, 2013). These measures must then be applied to an internal physical model of the body and world used to compute a required movement backwards from the goal state while also taking into account the effects changing environmental conditions. This is an extremely difficult computational problem which is made even more so by imperfect sensors, nonstationarity of muscle properties over time, a high level of redundancy in effectors, and a constant high level of uncertainty of environmental conditions (Franklin and Wolpart, 2011). The difficulty of this problem has led researchers to propose a number of computationally intense mechanisms by which the brain may solve it, including

Bayesian decision theory, optimal feedback control and predictive control (Franklin and Wolpert, 2011). However, there is little information on how the brain may actually carry out these computations.

Alternately, when motor control is viewed as the control of sensory input, then feedforward calculation of inverse kinematics is no longer required (Powers, 1992; Yin, 2013); Instead the motor system operates as a hierarchical cascade control system with spinal circuits controlling muscle length and tension, brainstem circuits controlling orienting and highly patterned sequences of movement such as locomotion, and basal ganglia circuits controlling transitions in the states of brainstem and motor systems for the sake of accomplishing still higher perceptual goal states defined by cortical and thalamic circuits.

### **5.3.2. Goal directed behavior as control of sensory input**

It is currently common practice to equate a behavioral goal with a 'reward' or a 'reinforcer' (Schultz, 2015; Howe et al., 2013; Steinberg et al., 2013; Atallah et al., 2014). From this perspective, the probability of certain actions in response to certain patterns of sensory input is altered through exposure to reinforcing events in such a way as to maximize net reward over time (Schultz, 2015; Glimcher, 2011; Keramati & Gutkin, 2011). However, the exact nature of the 'actions' being reinforced is rarely clearly defined—and when it is, as in the more rigorous computational models (Hong and

Hikosaka, 2011), it is defined as a pattern of motor output. Although this framework succeeds in accounting for certain properties of behavior in highly controlled laboratory environments, it fails as soon as the motor requirements change; according to this perspective a mouse that has learned to press a lever in an operant chamber should fail dramatically if the lever is moved to a different position on the wall, or if the cage is slightly tipped. Obviously, this is not the case.

When behavior is viewed as the control of sensory input, on the other hand, the high variability of motor output and the adaptability of behavior are no longer puzzling. According to this perspective, a goal is just another term for a reference signal in a control system. The only difference between reference signals controlling low-level motor variables and those that would commonly be considered 'goals', is that goals tend to correspond to hierarchically higher controlled variables which are easily observed, such as proximity to food. Computationally, all reference signals are used in the exact same way regardless of their position in the hierarchy (Powers, 1973).

For example, if it is the goal of a mouse to obtain a food pellet, then the control system for that behavior can be described as some form of food proximity control, where the reference signal for proximity is close to zero. However food proximity is represented perceptually—visual size of food, whisker detection of food—the system will continuously compare its incoming perceptual signal to its reference state for that perception, and the difference between these two values will drive error-correcting behavioral systems, such as locomotion and orientation towards the food target. Unlike

'action selection' models of behavior, perceptual control systems continue to work in the face of unpredictable environmental change. As long as locomotion towards a target reliably brings the target closer, then such a target proximity control system will work regardless of the terrain, the starting positions of the mouse or food, or even if the food is actively moving.

#### **5.4. Model of the motor control hierarchy**

As discussed in previous chapters, the experimental data presented here support a model of BG function in which the SNr is responsible for setting the reference states of lower control systems, and in which SNc dopamine neurons are responsible for modulating the gain of striatal output, which is itself integrated to generate SNr output as a means of smoothly transitioning the reference states of lower systems (Barter et al., 2015b; Yin, 2014b). However, in order for these proposed functions to make complete sense, it is necessary to explain them in their full context. We will thus use the following section to sketch a complete outline of the model control hierarchy, starting at the bottom and working our way up level by level. Although it is important to stress that this is an early-stage and incomplete model of the motor system that will likely require revision in the future, it is equally important to stress that this is a true model in the tradition of physics; operating strictly by its own rules and without any direct reference to the real world, this model is capable of generating behavior (Powers, 1992).

#### **5.4.1. Muscle force control**

The lowest level of control in this model is muscle force control (Figure 23D; Yin, 2014b; Powers, 1973). This level is traditionally referred to as the 'tendon reflex'. The circuits at this level receive inputs from type 1b fibers located in the golgi tendon organ, which represent increasing tendon force with increasing firing rate (Nicholls et al., 1992). These signals terminate on inhibitory 1b interneurons, which connect directly to alpha motor neurons (Nicholls et al., 1992). Alpha motor neurons make direct muscle contact and are responsible for muscle contraction. Thus, when a muscle contracts above a threshold the type 1b output increases, which feeds back to decrease the output of alpha motor neurons and thus muscle contraction. When the same muscle relaxes below a threshold, feedback works in the opposite direction to increase contraction. While this form of negative feedback has long been recognized as important in adapting muscle contraction to changing loads and in preventing muscles from producing dangerous levels of force, its exact computational role in movement has remained disputed (Mann, 1981).

According to the model presented here, this circuit operates as a negative feedback perceptual control system in which the circuit continuously senses force and continuously adjusts muscle output through alpha motoneurons to maintain force at a reference level specified by descending inputs. The importance of having force as the

lowest level of a control hierarchy is at least twofold; first, if force control is normalized to occur within a safe range then it is protective. Second; it is highly energetically efficient since force will only be applied as much as is required to achieve a desired muscle length and no more.

#### **5.4.2. Muscle length control**

The second level of control in our model is muscle length control (Figure 23C; Yin, 2014b; Powers, 1973). Muscle length is controlled through a combination of stretch velocity and position sensors located in muscle spindles. Length velocity is perceived by type 1a sensory fibers. These fibers represent velocity of stretch, and synapse directly onto the dendrites of motor neurons. Length position is perceived by type 2 sensory fibers, which are also located in the spindle, but they are non-adapting and thus represent muscle length directly. Both type 1a and type 2 fibers are excitatory and terminate on alpha motor neurons. Because the spindle itself contains muscle fibers which can be controlled through descending spinal influences, the sensitivity of 1a and 2 fibers can be adjusted by contracting these muscles and consequently adjusting the mechanical properties of the spindle (Mann, 1981; Nicholls et al., 1992). In this way, by contacting the spindle to different degrees, the outputs of the spindle fibers at different muscle lengths can be made similar.

Because they receive both inhibitory inputs from force sensors and excitatory inputs from length sensors, alpha motor neurons can be viewed as the comparator in a negative feedback system in which force is the controlled variable, and in which muscle length error specifies the reference force (Powers, 1973). According to this perspective, the difference (force error) between length input (reference signal) and force input (perceptual signal) is directly responsible for muscle contraction. If muscle force input becomes greater than muscle length input, then there will be decreased contraction until the two signals match. Likewise, if outputs of the spindle fiber increase or decrease because the muscle length increased or decreased at a given spindle sensitivity (length error), then the muscle will contract or relax, respectively, until the perceived force matches reference force issued by the spindle fiber. In this way, muscle length can be controlled through muscle force in a two-level control hierarchy. The reference signal for muscle length can be altered by adjusting the sensitivity of the spindle, which is accomplished by gamma motor neurons (Mann, 1981).

Interestingly, by combining type 1a and type 2 perceptions the control system becomes a variation of a 'PD controller' in which the output of the controller is a function not only of the position of the sensed signal, but a combination of the position and the derivative of that signal. When position and velocity signals are combined to influence controller output, you have a system that responds more quickly to disturbances than a simple proportional control system but still retains a high degree of

stability. PD controllers are known in engineering to have performance gains over simple proportional controllers (Boyd and Barret, 1991).

### **5.4.3. Body configuration control**

The third level of control in our model is body configuration control (Figure 23B; Yin, 2014b). The circuits at this level are traditionally referred to as being responsible for reciprocal inhibition, central pattern generation, and various postural and joint reflexes. Body configuration is also likely controlled by motor cortical effects on brainstem and spinal networks via the pyramidal tract. In its simplest form, configuration can be perceived as the difference between extensor and flexor group muscle lengths for a given axis of joint movement, and controlled by sending errors as appropriately-scaled length reference signals of opposite signs to muscles across a joint. For example, in the knee joint the configuration may be perceived as the average difference between the anterior and posterior thigh muscles. If this joint is perceived to be too flexed then the joint angle error will be split and transformed into two sets of muscle length reference signal changes; the length reference signals of the anterior muscles will be decreased while those of the posterior muscles will be increased in the correct proportions to allow for geometrical cooperation between them, given the relative angles, points of attachment and mechanical properties of the muscles involved.

In a complex joint having more than one axis, such as the shoulder or spine, the same muscle groups can participate simultaneously in multiple joints. For example, the muscles of the trunk perform both dorsal and lateral bend angle control; dorsal bending is controlled as the difference between abdominal and back muscles, while lateral bending is controlled as the difference between the left and right muscles of the entire trunk. In this way, a group of left abdominal muscles may participate simultaneously in both dorsal and lateral bend control as it integrates error signals from both controllers. It is also likely the case that groups of muscles are combined through a similar process to generate even more complex postural variables incorporating multiple joints, such as 'limb extension/retraction' seen in the spinal flexor reflex (Mann, 1981), or the hip sway seen during postural control (Massion, 1994).

Reference signals for body configuration controllers are hypothesized to descend, in large part, from reticulospinal cells in the brainstem and terminate on specialized reciprocally innervating circuits in the spinal cord, such as the burst generators that comprise CPGs (Grillner and Wallen, 2002). These reticulospinal cells are in turn commanded and further patterned by hierarchically higher body configuration controllers in the brainstem and midbrain including PPN, MLR and tectum. Body configurations are also likely controlled at multiple levels by direct motor cortical influences on spinal and brainstem circuits via the pyramidal motor system.

#### 5.4.4. Transition control

The fourth level of control in our model is the level of transition control (Figure 23A; Yin, 2014b). This level is traditionally described in terms of ‘action selection’ or ‘goal directedness’, and is responsible for continuously adjusting the reference levels of downstream controllers as a means of reducing still higher errors. According to the current model, transition control is the primary function of the basal ganglia, which receive higher reference signals from cortical and thalamic inputs and send errors as moving reference signals from SNr neurons to midbrain and brainstem motor regions. As outlined in previous chapters, the basal ganglia are thought to accomplish transition control by converting inputs to the striatum from higher systems into a set of ‘direction’ or velocity error signals which are sent to SNr, where they are continuously integrated to determine SNr firing rate and thus reference signal position for specific lower systems capable of reducing the higher error. DA neurons in the SNc are hypothesized to be responsible for modulating the velocity of these transitions by continuously adjusting the gain of striatal output signals if SNr position signals change too quickly or too slowly—much like adjusting the knob on a faucet to control the speed of water-level change in a sink.

The importance of the transition system is in being able to convert a monolithic error signal, such as the perceived x-axis visual proximity of head to food, into a dynamically controlled set of body movements capable of reducing that error to zero. In principle the transition system can perform this process in parallel for a large number of

higher control systems as long as their outputs do not cancel one another. For example, it should be possible to control, in parallel, x,y, and z-axis visual proximity of head to food simply by adding those errors together in the striatum.

#### **5.4.5. Control of higher sensory variables**

The fifth level of control in our model is the level at which perceptions from other sensory modalities, such as visual or auditory, are controlled by sending errors to the transition control system in the BG. The variables that can be controlled at this level can be as complex as an animal's ability to perceive them, as long as it is physically possible to control those variables through transitions in body postures. For example, a mouse might use this level of control to regulate visual or olfactory proximity to a food cup, while a high-ranking monkey might use it to regulate the social posture of one of his subordinates. In both of these cases, a relatively elaborate sensory variable is controlled by converting errors into a motor transition; the mouse might reduce proximity error by moving his head in the appropriate direction, while the monkey might control the social signaling of a conspecific by producing an aggressive movement or facial expression. Perceptions and errors at this level of control are likely generated by cortical and thalamic sensory systems, which can represent a wide array of abstract sensory variables and thus report their presence (no error) or absence (error) to striatal regions.

Although certain perceptions can be controlled through a single transition step, certain other perceptions can only be controlled through a sequence of transitions, each with its own controlled sensory variable. To control the perception of 'food pellet delivery', for example, a mouse on an FR1 schedule must perform a sequence of at least 2 steps in order to control for food delivery: 1) close body proximity to operant lever, 2) 'lever click' sound. Depending on the operant task, such a sequence can easily grow to involve a large nested hierarchy of steps, such as if the animal is required to achieve a fixed number of light blinks in order for a single pellet to be delivered, and if achieving single light blink requires a fixed number of alternating left-right lever presses. As the size and sophistication of the required sequence control hierarchy grows, an animal's continued ability to successfully control the highest variable is said to be its intelligence.

Given the hierarchical nature of thalamic loops from BG to cortex (Alexander et al., 1986), one attractive possibility is that such sequences are assembled by connecting the output of one loop to the input of another loop via thalamic projections. In this way, rather than commanding a motor reference by projecting to the brainstem, the BG could command a perceptual reference by projecting to another cortical system. For example, if a mouse is required to press a lever in order for a food pellet to be delivered, then the 'food-pellet control' system will only work if its error signals are sent to the 'lever click control' system via thalamic projections. The 'lever click' control systems, however, can be controlled through motor transitions.

#### 5.4.6. Learning

When a mouse learns to press a lever for food, the majority of the motor functions involved are innate and common to all mice; locomotion, orienting, and postural control are sufficient to reliably bring the mouse close to the lever from any starting point and across almost any terrain, and rearing is sufficient to depress a lever. The main difficulties in acquiring this behavior are in learning the perceptual goals involved, and in learning the proper sequence in which to control them. According to the model presented here, learning is thought to depend on a process of random variation and selective retention, in which system parameters change randomly in response to increasing or constant error, but hold their trajectory of change in response to decreasing error (Powers, 2008). This type of learning is likely proportionate to the degree of failure in an active control system.

For example, a mouse first learning to press a lever for food may randomly approach different perceptual targets and produce different postural transitions until a food pellet happens to be delivered, at which point its behavior will become less random. Underlying this behavior is a 'food control' system which is failing and thus shuffling the components and settings of its output function as a means of establishing control. If error is reduced in this reorganizing system—a food pellet is delivered—then this shuffling will slow as a means of preserving elements of a working output function. However, if the error fails to be reduced or increases then this shuffling is expected to speed up as a means of dismantling a failed output function and exploring new

configurations. Over time, as successes slow the reorganization and failures speed it up, this process is expected to converge on a working output function capable of reliably and quickly reducing errors, thus slowing reorganization to the point that it becomes negligible. The aim of learning in this model is thus to achieve performance in a closed loop control system, rather than to maximize 'rewards' in an open loop behavioral system as is commonly assumed to form the basis of learning (Todorov and Jordan, 2002; McClure et al., 2003 ). Very similar algorithms are widely and successfully used in machine learning and to train neural networks (Finkel et al., 2008).

### **5.5. The role of SN in behavior**

As with any system-component, the function of the SN can only be explained with respect to the function of the system as a whole. According to the model presented here, the function of the motor system is to control a hierarchy of perceptual variables, with muscle force at the lowest level of controlled variable and complex sensory goal states at the highest level. Within this hierarchy, the BG is proposed to function as a system for continuously orchestrating the reference signals of lower control systems as a means of controlling still higher perceptual variables. Within the BG, the function of the SNr is proposed be directly responsible for specifying the reference states of lower systems, while SNc DA neurons are proposed to be responsible for modulating the gain of transition control and thus the velocity of SNr output signals.

The continuous correlations between postural disturbance and neural activity in the SN shown in chapter 2, and the continuous correlations between head position and BG output demonstrated in chapter 3 stand in strong support this model system. Such results cannot be explained by classical accounts of BG function, which assume that BG outputs act as a gate for action selection (Hikosaka et al., 2000; Grillner et al., 2013). Critically, classical accounts of BG function also fail in explaining the continuous, dynamic and adaptive nature of free animal behavior, whereas the model presented here succeeds in a number of important ways.

The continuous correlations between DA activity and motor outputs shown in chapter 4 also stand in support of the model outlined above. Classical accounts DA function in scaling 'vigor' (Niv et al., 2007) or 'wanting' (Berridge, 2006), on the other hand, do not constitute working models in that they do not explain how behavior is actually generated; these are simply verbal descriptions and cannot be formally tested. Classical accounts of the role of DA in reinforcement learning, while testable, fail badly in accounting for the simple variability and adaptability of animal behavior. All such accounts are also based on data gathered from experimental tasks that neglected to measure motor output during task performance, which as we have seen is an important confounding variable.

## 5.6. Limitations and future directions

The neural and behavioral findings presented here shed important new light on the role of the BG in generating behavior, and on the functions of the nervous system in general. However, the experiments used to generate these findings were improvised and employed relatively crude methods compared with what will be possible in the future. For example, commercially available 3D motion capture systems can be used to precisely measure whole-body kinematic outputs at over 200HZ, allowing us to investigate and possibly define the exact set of body controllers used in a mouse. These behavioral measurement systems could also be used in real-time in combination with various motorized behavioral tasks to ‘clamp’ aspects of behavior, such as body postures or target proximities, by setting them as controlled variables by an external high-gain control system. In much the same way that the voltage clamp was used by physiologists to investigate voltage-dependent membrane properties that would have otherwise been obscured by the closed-loop nature of the system (Hodgkin and Huxley, 1952), such ‘behavioral clamps’ are expected to allow for the investigation of nervous system properties that are typically obscured by the closed-loop nature of behavior.

A major open question regarding the function of SN outputs in behavior is the destination of the recorded signals. While it is reasonable to speculate that SNr GABA neurons control head position largely through projections to brainstem and midbrain motor regions, it is also likely that these movements are influenced in important ways by motor cortex via thalamic projections. Likewise, the exact striatal targets of DA

neurons, and their relationship to different categories of SNr GABA neurons remains unknown. Future experiments must therefore be designed to address the functional connectivity of SN neurons during a variety of different behaviors requiring the contribution of different motor systems.

Finally, the model of the BG and the motor hierarchy presented here is unique in that it represents the rough sketch of a system that can be built and tested against experimental observations. In the same way the behavior of a model in physics (force=mass x acceleration, for example) can be compared with the behavior of physical reality, the behavior of this model, once assembled, can be compared to that of the nervous system and animal. In both cases, the comparison is necessary to test the model so that it can be revised and made more accurate over time. A testable version of the model proposed here will help to guide and interpret future empirical research, which will in turn provide observations against which to test and refine the model. Although it is impossible to predict how long this process will take, or the exact set of experiments or model-revisions that will be required, a complete and refined working model of this kind is one of the ultimate goals of neuroscience.

## References

- Albin RL, Young AB, Penney JB (1989) The functional anatomy of basal ganglia disorders. *Trends in Neurosciences* 12:366–375.
- Alexander GE, Crutcher MD (1990) Functional architecture of basal ganglia circuits: neural substrates of parallel processing. *Trends in Neurosciences* 13:266–271.
- Alexander GE, DeLong MR, Strick PL (1986) Parallel organization of functionally segregated circuits linking basal ganglia and cortex. *Annual review of neuroscience* 9:357–381.
- Alexander RM (2013) *Principles of Animal Locomotion*. Princeton University Press.
- Anon (1966) *The Functions of the Brain*. London, Smith, Elder, 1876.
- Atallah HE, McCool AD, Howe MW, Graybiel AM (2014) Neurons in the Ventral Striatum Exhibit Cell-Type-Specific Representations of Outcome during Learning. *Neuron* 82:1145–1156.
- Atherton JF, Bevan MD (2005) Ionic Mechanisms Underlying Autonomous Action Potential Generation in the Somata and Dendrites of GABAergic Substantia Nigra Pars Reticulata Neurons In Vitro. *J Neurosci* 25:8272–8281.
- Barter JW, Castro S, Sukharnikova T, Rossi MA, Yin HH (2014) The role of the substantia nigra in posture control. *Eur J Neurosci* 39:1465–1473.
- Barter JW, Li S, Lu D, Bartholomew RA, Rossi MA, Shoemaker CT, Salas-Meza D, Gaidis E, Yin HH (2015a) Beyond reward prediction errors: the role of dopamine in movement kinematics. *Front Integr Neurosci* 9 Available at: <http://www.ncbi.nlm.nih.gov/pmc/articles/PMC4444742/> [Accessed July 1, 2015].
- Barter JW, Li S, Sukharnikova T, Rossi MA, Bartholomew RA, Yin HH (2015b) Basal ganglia outputs map instantaneous position coordinates during behavior. *J Neurosci* 35:2703–2716.
- Basso MA, Wurtz RH (2002) Neuronal Activity in Substantia Nigra Pars Reticulata during Target Selection. *J Neurosci* 22:1883–1894.
- Bayer HM, Glimcher PW (2005) Midbrain dopamine neurons encode a quantitative reward prediction error signal. *Neuron* 47:129–141.
- Beckstead RM, Domesick VB, Nauta WJH (1979) Efferent connections of the substantia nigra and ventral tegmental area in the rat. *Brain Research* 175:191–217.
- Bernshtein NA (1967) *The co-ordination and regulation of movements*. Pergamon Press.

- Berridge KC (2006) The debate over dopamine's role in reward: the case for incentive salience. *Psychopharmacology* 191:391–431.
- Bjursten LM, Norrsell K, Norrsell U (1976) Behavioural repertory of cats without cerebral cortex from infancy. *Exp Brain Res* 25:115–130.
- Black HS (1934) Stabilized Feedback Amplifiers\*. *Bell System Technical Journal* 13:1–18.
- Bloem BR, Beckley DJ, Remler MP, Roos RAC, van Dijk JG (1995) Postural reflexes in Parkinson's disease during "resist" and "yield" tasks. *Journal of the Neurological Sciences* 129:109–119.
- Bolam JP, Smith Y, Ingham CA, von Krosigk M, Smith AD (1993) Convergence of synaptic terminals from the striatum and the globus pallidus onto single neurones in the substantia nigra and the entopeduncular nucleus. *Prog Brain Res* 99:73–88.
- Boyd SP, Barratt CH (1991) *Linear controller design: limits of performance*. Prentice Hall PTR.
- Bretzner F, Drew T (2005) Motor cortical modulation of cutaneous reflex responses in the hindlimb of the intact cat. *J Neurophysiol* 94:673–687.
- Brocard F (2003) Differential Contribution of Reticulospinal Cells to the Control of Locomotion Induced By the Mesencephalic Locomotor Region. *Journal of Neurophysiology* 90:1714–1727.
- Brocard F, Ryczko D, Fenelon K, Hatem R, Gonzales D, Auclair F, Dubuc R (2010) The Transformation of a Unilateral Locomotor Command into a Symmetrical Bilateral Activation in the Brainstem. *Journal of Neuroscience* 30:523–533.
- Brown MTC, Henny P, Bolam JP, Magill PJ (2009) Activity of Neurochemically Heterogeneous Dopaminergic Neurons in the Substantia Nigra during Spontaneous and Driven Changes in Brain State. *J Neurosci* 29:2915–2925.
- Brown P (2006) Bad oscillations in Parkinson's disease. In: *Parkinson's Disease and Related Disorders*, pp 27–30. Springer. Available at: [http://link.springer.com/chapter/10.1007/978-3-211-45295-0\\_6](http://link.springer.com/chapter/10.1007/978-3-211-45295-0_6) [Accessed July 2, 2015].
- Cabelguen J-M, Bourcier-Lucas C, Dubuc R (2003) Bimodal locomotion elicited by electrical stimulation of the midbrain in the salamander *Notophthalmus viridescens*. *J Neurosci* 23:2434–2439.
- Cagniard B, Beeler JA, Britt JP, McGehee DS, Marinelli M, Zhuang X (2006) Dopamine Scales Performance in the Absence of New Learning. *Neuron* 51:541–547.

- Cannon CM, Palmiter RD (2003) Reward without Dopamine. *J Neurosci* 23:10827–10831.
- Cannon WB (1935) STRESSES AND STRAINS OF HOMEOSTASIS. *Journal of the Medical Sciences* 189:13–14.
- Carelli RM, West MO (1991) Representation of the body by single neurons in the dorsolateral striatum of the awake, unrestrained rat. *J Comp Neurol* 309:231–249.
- Carter DA, Fibiger HC (1978) The projections of the entopeduncular nucleus and globus pallidus in rat as demonstrated by autoradiography and horseradish peroxidase histochemistry. *J Comp Neurol* 177:113–123.
- Chevalier G, Deniau JM (1990) Disinhibition as a basic process in the expression of striatal functions. *Trends Neurosci* 13:277–280.
- Chevalier G, Vacher S, Deniau JM (1984) Inhibitory nigral influence on tectospinal neurons, a possible implication of basal ganglia in orienting behavior. *Exp Brain Res* 53:320–326.
- Cohen JY, Haesler S, Vong L, Lowell BB, Uchida N (2012) Neuron-type-specific signals for reward and punishment in the ventral tegmental area. *Nature* 482:85–88.
- Connelly WM, Schulz JM, Lees G, Reynolds JNJ (2010) Differential Short-Term Plasticity at Convergent Inhibitory Synapses to the Substantia Nigra Pars Reticulata. *J Neurosci* 30:14854–14861.
- Costa RM, Lin S-C, Sotnikova TD, Cyr M, Gainetdinov RR, Caron MG, Nicolelis MAL (2006) Rapid Alterations in Corticostriatal Ensemble Coordination during Acute Dopamine-Dependent Motor Dysfunction. *Neuron* 52:359–369.
- Cui G, Jun SB, Jin X, Pham MD, Vogel SS, Lovinger DM, Costa RM (2013) Concurrent activation of striatal direct and indirect pathways during action initiation. *Nature* 494:238–242.
- Deliagina TG (2006) Neural Bases of Postural Control. *Physiology* 21:216–225.
- Deliagina TG, Arshavsky YI, Orlovsky GN (1998) Control of spatial orientation in a mollusc. *Nature* 393:172–175.
- Deliagina TG, Sirota MG, Zelenin PV, Orlovsky GN, Beloozerova IN (2006) Interlimb postural coordination in the standing cat. *The Journal of Physiology* 573:211–224.
- Deliagina TG, Zelenin PV, Beloozerova IN, Orlovsky GN (2007) Nervous mechanisms controlling body posture. *Physiology & Behavior* 92:148–154.
- Deliagina TG, Zelenin PV, Orlovsky GN (2012) Physiological and circuit mechanisms of postural control. *Current Opinion in Neurobiology* 22:646–652.

- DeLong MR (1990) Primate models of movement disorders of basal ganglia origin. *Trends in Neurosciences* 13:281–285.
- DeLong MR, Georgopoulos AP (2011) Motor Functions of the Basal Ganglia. In: *Comprehensive Physiology*. John Wiley & Sons, Inc. Available at: <http://onlinelibrary.wiley.com/doi/10.1002/cphy.cp010221/abstract> [Accessed August 25, 2015].
- Dimitrova D (2003) Postural Muscle Responses to Multidirectional Translations in Patients With Parkinson's Disease. *Journal of Neurophysiology* 91:489–501.
- Drew T, Dubuc R, Rossignol S (1986) Discharge patterns of reticulospinal and other reticular neurons in chronic, unrestrained cats walking on a treadmill. *Journal of Neurophysiology* 55:375–401.
- Drew T, Rossignol S (1990) Functional organization within the medullary reticular formation of intact unanesthetized cat. I. Movements evoked by microstimulation. *Journal of Neurophysiology* 64:767–781.
- Dubuc R, Brocard F, Antri M, Fénelon K, Gariépy J-F, Smetana R, Ménard A, Le Ray D, Viana Di Prisco G, Pearlstein É, Sirota MG, Derjean D, St-Pierre M, Zielinski B, Auclair F, Veilleux D (2008) Initiation of locomotion in lampreys. *Brain Research Reviews* 57:172–182.
- Eidelberg E (1981) Consequences of spinal cord lesions upon motor function, with special reference to locomotor activity. *Prog Neurobiol* 17:185–202.
- Ekeberg Ö, Grillner S (1999) Simulations of neuromuscular control in lamprey swimming. *Philosophical Transactions of the Royal Society of London Series B: Biological Sciences* 354:895–902.
- Fagerstedt P, Ullén F (2001) Lateral turns in the lamprey. I. Patterns of motoneuron activity. *Journal of neurophysiology* 86:2246–2256.
- Fagerstedt P, Zelenin PV, Deliagina TG, Orlovsky GN, Grillner S (2000) Crossed reciprocal inhibition evoked by electrical stimulation of the lamprey spinal cord. *Exp Brain Res* 134:147–154.
- Fallon JH, Moore RY (1978) Catecholamine innervation of the basal forebrain. IV. Topography of the dopamine projection to the basal forebrain and neostriatum. *J Comp Neurol* 180:545–580.
- Fan D, Rossi MA, Yin HH (2012) Mechanisms of Action Selection and Timing in Substantia Nigra Neurons. *Journal of Neuroscience* 32:5534–5548.

- Finkel JR, Kleeman A, Manning CD (2008) Efficient, Feature-based, Conditional Random Field Parsing. In: ACL, pp 959–967 Available at: <http://anthology.aclweb.org/P/P08/P08-1.pdf#page=1003> [Accessed September 27, 2015].
- Fiorillo CD (2013) Two dimensions of value: dopamine neurons represent reward but not aversiveness. *Science* 341:546–549.
- Franklin DW, Wolpert DM (2011) Computational Mechanisms of Sensorimotor Control. *Neuron* 72:425–442.
- Freeze BS, Kravitz AV, Hammack N, Berke JD, Kreitzer AC (2013) Control of Basal Ganglia Output by Direct and Indirect Pathway Projection Neurons. *J Neurosci* 33:18531–18539.
- Freund HJ, Hummelsheim H (1984) Premotor cortex in man: Evidence for innervation of proximal limb muscles. *Exp Brain Res* 53:479–482.
- Garcia-Rill E (1986) The basal ganglia and the locomotor regions. *Brain Research Reviews* 11:47–63.
- Georgopoulos AP, Schwartz AB, Kettner RE (1986) Neuronal population coding of movement direction. *Science* 233:1416–1419.
- Gerfen CR, Engber TM, Mahan LC, Susel Z, Chase TN, Monsma FJ, Sibley DR (1990) D1 and D2 dopamine receptor-regulated gene expression of striatonigral and striatopallidal neurons. *Science* 250:1429–1432.
- Gerfen CR, Surmeier DJ (2011) Modulation of striatal projection systems by dopamine. *Annu Rev Neurosci* 34:441–466.
- Glickstein M, Stein J (1991) Paradoxical movement in Parkinson's disease. *Trends in neurosciences* 14:480–482.
- Glimcher PW (2011) Understanding dopamine and reinforcement learning: The dopamine reward prediction error hypothesis. *PNAS* 108:15647–15654.
- Goodale MA, Murison RCC (1975) The effects of lesions of the superior colliculus on locomotor orientation and the orienting reflex in the rat. *Brain Research* 88:243–261.
- Grace AA, Bunney BS (1983) Intracellular and extracellular electrophysiology of nigral dopaminergic neurons—1. Identification and characterization. *Neuroscience* 10:301–315.
- Grace AA, Bunney BS (1984) The control of firing pattern in nigral dopamine neurons: single spike firing. *J Neurosci* 4:2866–2876.

- Graybiel AM (1998) The Basal Ganglia and Chunking of Action Repertoires. *Neurobiology of Learning and Memory* 70:119–136.
- Grillner S (2006) Biological Pattern Generation: The Cellular and Computational Logic of Networks in Motion. *Neuron* 52:751–766.
- Grillner S (2011) Control of Locomotion in Bipeds, Tetrapods, and Fish. In: *Comprehensive Physiology*. John Wiley & Sons, Inc. Available at: <http://onlinelibrary.wiley.com/doi/10.1002/cphy.cp010226/abstract> [Accessed September 27, 2015].
- Grillner S, Deliagina T, Manira A El, Hill RH, Orlovsky GN, Wallén P, Ekeberg Ö, Lansner A (1995) Neural networks that co-ordinate locomotion and body orientation in lamprey. *Trends in Neurosciences* 18:270–279.
- Grillner S, Ekeberg Ö, Manira A El, Lansner A, Parker D, Tegnér J, Wallén P (1998) Intrinsic function of a neuronal network — a vertebrate central pattern generator<sup>1</sup>. *Brain Research Reviews* 26:184–197.
- Grillner S, Robertson B, Stephenson-Jones M (2013) The evolutionary origin of the vertebrate basal ganglia and its role in action selection. *J Physiol* 591:5425–5431.
- Grillner S, Wallén P (2002) Cellular bases of a vertebrate locomotor system—steering, intersegmental and segmental co-ordination and sensory control. *Brain research reviews* 40:92–106.
- Grillner S, Wallén P, Brodin L, Lansner A (1991) Neuronal network generating locomotor behavior in lamprey: circuitry, transmitters, membrane properties, and simulation. *Annu Rev Neurosci* 14:169–199.
- Grillner S, Wallén P, Saitoh K, Kozlov A, Robertson B (2008) Neural bases of goal-directed locomotion in vertebrates—An overview. *Brain Research Reviews* 57:2–12.
- Guertin PA (2009) The mammalian central pattern generator for locomotion. *Brain Research Reviews* 62:45–56.
- Gulley JM, Kuwajima M, Mayhill E, Rebec GV (1999) Behavior-related changes in the activity of substantia nigra pars reticulata neurons in freely moving rats. *Brain Research* 845:68–76.
- Hefti F, Melamed E, Sahakian BJ, Wurtman RJ (1980) Circling behavior in rats with partial, unilateral nigro-striatal lesions: Effect of amphetamine, apomorphine, and DOPA. *Pharmacology Biochemistry and Behavior* 12:185–188.

- Henny P, Brown MTC, Northrop A, Faunes M, Ungless MA, Magill PJ, Bolam JP (2012) Structural correlates of heterogeneous in vivo activity of midbrain dopaminergic neurons. *Nat Neurosci* 15:613–619.
- Hikosaka O (2007) Basal Ganglia Mechanisms of Reward-Oriented Eye Movement. *Annals of the New York Academy of Sciences* 1104:229–249.
- Hikosaka O, Takikawa Y, Kawagoe R (2000) Role of the basal ganglia in the control of purposive saccadic eye movements. *Physiological reviews* 80:953–978.
- Hikosaka O, Wurtz RH (1983) Visual and oculomotor functions of monkey substantia nigra pars reticulata: I. Relation of visual and auditory responses to saccades. *Journal of Neurophysiology* 49:1230–1253.
- Hochberg LR, Serruya MD, Friehs GM, Mukand JA, Saleh M, Caplan AH, Branner A, Chen D, Penn RD, Donoghue JP (2006) Neuronal ensemble control of prosthetic devices by a human with tetraplegia. *Nature* 442:164–171.
- Hodgkin AL, Huxley AF (1952) A quantitative description of membrane current and its application to conduction and excitation in nerve. *J Physiol* 117:500–544.
- Hong S, Hikosaka O (2011) Dopamine-mediated learning and switching in cortico-striatal circuit explain behavioral changes in reinforcement learning. *Front Behav Neurosci* 5:15.
- Horvitz JC (2000) Mesolimbocortical and nigrostriatal dopamine responses to salient non-reward events. *Neuroscience* 96:651–656.
- Howe MW, Tierney PL, Sandberg SG, Phillips PEM, Graybiel AM (2013) Prolonged dopamine signalling in striatum signals proximity and value of distant rewards. *Nature* 500:575–579.
- Isa T, Sasaki S (2002) Brainstem control of head movements during orienting; organization of the premotor circuits. *Progress in neurobiology* 66:205–241.
- Isomura Y, Takekawa T, Harukuni R, Handa T, Aizawa H, Takada M, Fukai T (2013) Reward-Modulated Motor Information in Identified Striatum Neurons. *J Neurosci* 33:10209–10220.
- Jin X, Costa RM (2010) Start/stop signals emerge in nigrostriatal circuits during sequence learning. *Nature* 466:457–462.
- Kakei S, Hoffman DS, Strick PL (2003) Sensorimotor transformations in cortical motor areas. *Neuroscience Research* 46:1–10.

- Kaneda K, Isa K, Yanagawa Y, Isa T (2008) Nigral Inhibition of GABAergic Neurons in Mouse Superior Colliculus. *J Neurosci* 28:11071–11078.
- Kang Y, Kitai ST (1993) A whole cell patch-clamp study on the pacemaker potential in dopaminergic neurons of rat substantia nigra compacta. *Neuroscience Research* 18:209–221.
- Karayannidou A, Beloozerova IN, Zelenin PV, Stout EE, Sirota MG, Orlovsky GN, Deliagina TG (2009) Activity of pyramidal tract neurons in the cat during standing and walking on an inclined plane. *The Journal of Physiology* 587:3795–3811.
- Kawagoe R, Takikawa Y, Hikosaka O (1998) Expectation of reward modulates cognitive signals in the basal ganglia. *Nat Neurosci* 1:411–416.
- Keramati M, Gutkin BS (2011) A reinforcement learning theory for homeostatic regulation. In: *Advances in neural information processing systems*, pp 82–90 Available at: <http://papers.nips.cc/paper/4437-a-reinforcement> [Accessed July 31, 2015].
- Kermadi I, Joseph JP (1995) Activity in the caudate nucleus of monkey during spatial sequencing. *Journal of Neurophysiology* 74:911–911.
- Kim N, Barter JW, Sukharnikova T, Yin HH (2014) Striatal firing rate reflects head movement velocity. *Eur J Neurosci* 40:3481–3490.
- Kinjo N, Atsuta Y, Webber M, Kyle R, Skinner RD, Garcia-Rill E (1990) Medioventral medulla-induced locomotion. *Brain Res Bull* 24:509–516.
- Knutson B, Adams CM, Fong GW, Hommer D (2001) Anticipation of increasing monetary reward selectively recruits nucleus accumbens. *J Neurosci* 21:RC159.
- Krakauer JW, Ghilardi M-F, Ghez C (1999) Independent learning of internal models for kinematic and dynamic control of reaching. *Nat Neurosci* 2:1026–1031.
- Kravitz AV, Freeze BS, Parker PRL, Kay K, Thwin MT, Deisseroth K, Kreitzer AC (2010) Regulation of parkinsonian motor behaviours by optogenetic control of basal ganglia circuitry. *Nature* 466:622–626.
- Kreitzer AC (2009) Physiology and Pharmacology of Striatal Neurons. *Annual Review of Neuroscience* 32:127–147.
- Lacquaniti F, Maioli C (1994) Coordinate transformations in the control of cat posture. *Journal of Neurophysiology* 72:1496–1515.

- Leblois A, Wendel BJ, Perkel DJ (2010) Striatal Dopamine Modulates Basal Ganglia Output and Regulates Social Context-Dependent Behavioral Variability through D1 Receptors. *J Neurosci* 30:5730–5743.
- Ljungberg T, Apicella P, Schultz W (1992) Responses of monkey dopamine neurons during learning of behavioral reactions. *Journal of Neurophysiology* 67:145–163.
- Madisen L et al. (2012) A toolbox of Cre-dependent optogenetic transgenic mice for light-induced activation and silencing. *Nat Neurosci* 15:793–802.
- Magoun HW (1950) Caudal and cephalic influences of brainstem reticular formation. *Physiological reviews* 30:459–474.
- Manira A El, Pombal MA, Grillner S (1997) Diencephalic projection to reticulospinal neurons involved in the initiation of locomotion in adult lampreys *Lampetra fluviatilis*. *J Comp Neurol* 389:603–616.
- Mann MD (1981) *The nervous system and behavior*. Harper & Row Limited.
- Manson MD, Armitage JP, Hoch JA, Macnab RM (1998) Bacterial locomotion and signal transduction. *Journal of bacteriology* 180:1009–1022.
- Masino T (1992) Brainstem control of orienting movements: intrinsic coordinate systems and underlying circuitry. *Brain Behav Evol* 40:98–111.
- Massion J (1994) Postural control system. *Current opinion in neurobiology* 4:877–887.
- Matsumoto M, Hikosaka O (2007) Lateral habenula as a source of negative reward signals in dopamine neurons. *Nature* 447:1111–1115.
- Matsuyama K, Drew T (2000) Vestibulospinal and reticulospinal neuronal activity during locomotion in the intact cat. II. Walking on an inclined plane. *J Neurophysiol* 84:2257–2276.
- McClure SM, Daw ND, Read Montague P (2003) A computational substrate for incentive salience. *Trends in Neurosciences* 26:423–428.
- Menard A, Grillner S (2008) Diencephalic Locomotor Region in the Lamprey--Afferents and Efferent Control. *Journal of Neurophysiology* 100:1343–1353.
- Miller H (1968) The Basal Ganglia and Posture. *Proc R Soc Med* 61:434–435.
- MINK JW (1996) THE BASAL GANGLIA: FOCUSED SELECTION AND INHIBITION OF COMPETING MOTOR PROGRAMS. *Progress in Neurobiology* 50:381–425.

- Miri A, Azim E, Jessell TM (2013) Edging toward Entelechy in Motor Control. *Neuron* 80:827–834.
- Mori S (1987) Integration of posture and locomotion in acute decerebrate cats and in awake, freely moving cats. *Progress in Neurobiology* 28:161–195.
- Mori S, Kawahara K, Sakamoto T, Aoki M, Tomiyama T (1982) Setting and resetting of level of postural muscle tone in decerebrate cat by stimulation of brain stem. *Journal of Neurophysiology* 48:737–748.
- Mountcastle VB, Lynch JC, Georgopoulos A, Sakata H, Acuna C (1975) Posterior parietal association cortex of the monkey: command functions for operations within extrapersonal space. *Journal of Neurophysiology* 38:871–908.
- Naitoh Y (1974) Bioelectric basis of behavior in protozoa. *American Zoologist* 14:883–893.
- Nash JF, others (1950) Equilibrium points in n-person games. *Proc Nat Acad Sci USA* 36:48–49.
- Nicholls JG, Martin AR, Wallace BG, Kuffler SW (1992) From neuron to brain: a cellular and molecular approach to the function of the nervous system. Sinauer Associates.
- Nicolelis MAL (2007) *Methods for Neural Ensemble Recordings*, Second Edition. CRC Press.
- Niv Y, Daw ND, Joel D, Dayan P (2006) Tonic dopamine: opportunity costs and the control of response vigor. *Psychopharmacology* 191:507–520.
- O’Donnell P (2003) Dopamine gating of forebrain neural ensembles. *European Journal of Neuroscience* 17:429–435.
- Paladini CA, Iribe Y, Tepper JM (1999) GABAA receptor stimulation blocks NMDA-induced bursting of dopaminergic neurons in vitro by decreasing input resistance. *Brain Research* 832:145–151.
- Paladini CA, Roeper J (2014) Generating bursts (and pauses) in the dopamine midbrain neurons. *Neuroscience* 282:109–121.
- Paninski L, Fellows MR, Hatsopoulos NG, Donoghue JP (2004) Spatiotemporal Tuning of Motor Cortical Neurons for Hand Position and Velocity. *Journal of Neurophysiology* 91:515–532.
- Pan W-X, Brown J, Dudman JT (2013) Neural signals of extinction in the inhibitory microcircuit of the ventral midbrain. *Nat Neurosci* 16:71–78.

- Parent A, Bouchard C, Smith Y (1984) The striatopallidal and striatonigral projections: two distinct fiber systems in primate. *Brain Res* 303:385–390.
- Parent A, Hazrati L-N (1995) Functional anatomy of the basal ganglia. I. The cortico-basal ganglia-thalamo-cortical loop. *Brain Research Reviews* 20:91–127.
- Pavlova EL (2004) Vestibular compensation in lampreys: restoration of symmetry in reticulospinal commands. *Journal of Experimental Biology* 207:4595–4603.
- Pavlova EL, Deliagina TG (2002) Responses of Reticulospinal Neurons in Intact Lamprey to Pitch Tilt. *Journal of Neurophysiology* 88:1136–1146.
- Peterson BW (1979) Reticulospinal Projections to Spinal Motor Nuclei. *Annual Review of Physiology* 41:127–140.
- Peterson DBW, Pitts NG, Fukushima K (1979) Reticulospinal connections with limb and axial motoneurons. *Exp Brain Res* 36:1–20.
- Powers WT, Clark RK, Mc Farland RL (1960) A general feedback theory of human behavior: Part I. Perceptual and motor skills 11:71–88.
- Powers WT (1973) *Behavior: the Control of Perception*. Aldine Publishing Company.
- Powers WT (1998) *Living Control Systems*. Benchmark Publications.
- Powers WT (1992) *Living Control Systems II*. Benchmark Publications.
- Powers WT (2008) *Living Control Systems III: The Fact of Control*. Control Systems Group.
- Puryear CB, Kim MJ, Mizumori SJY (2010) Conjunctive encoding of movement and reward by ventral tegmental area neurons in the freely navigating rodent. *Behavioral Neuroscience* 124:234–247.
- Rauscent A, Le Ray D, Cabirol-Pol M-J, Sillar KT, Simmers J, Combes D (2006) Development and neuromodulation of spinal locomotor networks in the metamorphosing frog. *J Physiol Paris* 100:317–327.
- Redgrave P, Gurney K (2006) The short-latency dopamine signal: a role in discovering novel actions? *Nat Rev Neurosci* 7:967–975.
- Reiner A, Albin RL, Anderson KD, D'Amato CJ, Penney JB, Young AB (1988) Differential loss of striatal projection neurons in Huntington disease. *PNAS* 85:5733–5737.
- Robinson DA (1972) Eye movements evoked by collicular stimulation in the alert monkey. *Vision Research* 12:1795–1808.

- Roesch MR, Calu DJ, Schoenbaum G (2007) Dopamine neurons encode the better option in rats deciding between differently delayed or sized rewards. *Nat Neurosci* 10:1615–1624.
- Romo R, Schultz W (1990) Dopamine neurons of the monkey midbrain: contingencies of responses to active touch during self-initiated arm movements. *Journal of Neurophysiology* 63:592–606.
- Rossi MA, Fan D, Barter JW, Yin HH (2013a) Bidirectional Modulation of Substantia Nigra Activity by Motivational State. *PLoS ONE* 8:e71598.
- Rossi MA, Sukharnikova T, Hayrapetyan VY, Yang L, Yin HH (2013b) Operant Self-Stimulation of Dopamine Neurons in the Substantia Nigra. *PLoS ONE* 8:e65799.
- Rossi MA, Yin HH (2015) Elevated dopamine alters consummatory pattern generation and increases behavioral variability during learning. *Front Integr Neurosci* 9 Available at: <http://www.ncbi.nlm.nih.gov/pmc/articles/PMC4432675/> [Accessed July 2, 2015].
- Saitoh K, Menard A, Grillner S (2007) Tectal Control of Locomotion, Steering, and Eye Movements in Lamprey. *Journal of Neurophysiology* 97:3093–3108.
- Sato M, Hikosaka O (2002) Role of primate substantia nigra pars reticulata in reward-oriented saccadic eye movement. *J Neurosci* 22:2363–2373.
- Schultz DW, Ruffieux A, Aebischer P (1983) The activity of pars compacta neurons of the monkey substantia nigra in relation to motor activation. *Exp Brain Res* 51:377–387.
- Schultz W (1998a) The phasic reward signal of primate dopamine neurons. *Adv Pharmacol* 42:686–690.
- Schultz W (1998b) Predictive reward signal of dopamine neurons. *J Neurophysiol* 80:1–27.
- Schultz W (2015) Neuronal Reward and Decision Signals: From Theories to Data. *Physiological Reviews* 95:853–951.
- Schultz W, Dayan P, Montague PR (1997) A Neural Substrate of Prediction and Reward. *Science* 275:1593–1599.
- Shadmehr R, Krakauer JW (2008) A computational neuroanatomy for motor control. *Exp Brain Res* 185:359–381.
- Shadmehr R, Smith MA, Krakauer JW (2010) Error Correction, Sensory Prediction, and Adaptation in Motor Control. *Annual Review of Neuroscience* 33:89–108.
- Silver RA (2010) Neuronal arithmetic. *Nat Rev Neurosci* 11:474–489.

- Skinner RD, Garcia-Rill E (1984) The mesencephalic locomotor region (MLR) in the rat. *Brain Res* 323:385–389.
- Sparks DL (2002) The brainstem control of saccadic eye movements. *Nature Reviews Neuroscience* 3:952–964.
- Sparta DR, Stamatakis AM, Phillips JL, Hovelsø N, van Zessen R, Stuber GD (2012) Construction of implantable optical fibers for long-term optogenetic manipulation of neural circuits. *Nat Protocols* 7:12–23.
- Squire LR (2013) *Fundamental Neuroscience*. Academic Press.
- Steinberg EE, Keiflin R, Boivin JR, Witten IB, Deisseroth K, Janak PH (2013) A causal link between prediction errors, dopamine neurons and learning. *Nat Neurosci* 16:966–973.
- Stern Y, Mayeux R, Rosen J, Ilson J (1983) Perceptual motor dysfunction in Parkinson's disease: a deficit in sequential and predictive voluntary movement. *Journal of Neurology, Neurosurgery & Psychiatry* 46:145–151.
- Stoof JC, Keibian JW (1981) Opposing roles for D-1 and D-2 dopamine receptors in efflux of cyclic AMP from rat neostriatum. *Nature* 294:366–368.
- Surmeier DJ, Song W-J, Yan Z (1996) Coordinated Expression of Dopamine Receptors in Neostriatal Medium Spiny Neurons. *J Neurosci* 16:6579–6591.
- Swanson LW (2012) *Brain Architecture: Understanding the Basic Plan*. OUP USA.
- Takakusaki K, Habaguchi T, Ohtinata-Sugimoto J, Saitoh K, Sakamoto T (2003) Basal ganglia efferents to the brainstem centers controlling postural muscle tone and locomotion: a new concept for understanding motor disorders in basal ganglia dysfunction. *Neuroscience* 119:293–308.
- Takakusaki K, Saitoh K, Harada H, Kashiwayanagi M (2004) Role of basal ganglia–brainstem pathways in the control of motor behaviors. *Neuroscience Research* 50:137–151.
- Takakusaki K, Tomita N, Yano M (2008) Substrates for normal gait and pathophysiology of gait disturbances with respect to the basal ganglia dysfunction. *J Neurol* 255:19–29.
- Taylor DM, Tillery SIH, Schwartz AB (2002) Direct Cortical Control of 3D Neuroprosthetic Devices. *Science* 296:1829–1832.
- Tepper JM, Lee CR (2007) GABAergic control of substantia nigra dopaminergic neurons. In: *Progress in Brain Research*, pp 189–208. Elsevier. Available at: <http://linkinghub.elsevier.com/retrieve/pii/S0079612306600113> [Accessed July 2, 2015].

- Tepper JM, Martin LP, Anderson DR (1995) GABAA receptor-mediated inhibition of rat substantia nigra dopaminergic neurons by pars reticulata projection neurons. *J Neurosci* 15:3092–3103.
- Thompson RF, Thompson JK, Kim JJ, Krupa DJ, Shinkman PG (1998) The Nature of Reinforcement in Cerebellar Learning. *Neurobiology of Learning and Memory* 70:150–176.
- Todorov E, Jordan MI (2002) Optimal feedback control as a theory of motor coordination. *Nat Neurosci* 5:1226–1235.
- Tresch MC, Kiehn O (2000) Motor coordination without action potentials in the mammalian spinal cord. *Nat Neurosci* 3:593–599.
- Ungless MA, Grace AA (2012) Are you or aren't you? Challenges associated with physiologically identifying dopamine neurons. *Trends Neurosci* 35:422–430.
- Visser JE, Bloem BR (2005) Role of the basal ganglia in balance control. *Neural Plast* 12:161–174; discussion 263–272.
- Waitzman DM, Ma TP, Optican LM, Wurtz RH (1991) Superior colliculus neurons mediate the dynamic characteristics of saccades. *J Neurophysiol* 66:1716–1737.
- Wang DV, Tsien JZ (2011a) Conjunctive Processing of Locomotor Signals by the Ventral Tegmental Area Neuronal Population. *PLoS ONE* 6:e16528.
- Wang DV, Tsien JZ (2011b) Convergent Processing of Both Positive and Negative Motivational Signals by the VTA Dopamine Neuronal Populations. *PLoS ONE* 6:e17047.
- Wang S, Tan Y, Zhang J-E, Luo M (2013) Pharmacogenetic activation of midbrain dopaminergic neurons induces hyperactivity. *Neurosci Bull* 29:517–524.
- White NM (1986) Control of sensorimotor function by dopaminergic nigrostriatal neurons: Influence on eating and drinking. *Neuroscience & Biobehavioral Reviews* 10:15–36.
- Wise SP, Murray EA, Gerfen CR (1996) The frontal cortex-basal ganglia system in primates. *Crit Rev Neurobiol* 10:317–356.
- Woods SC, Seeley RJ, Porte D, Schwartz MW (1998) Signals That Regulate Food Intake and Energy Homeostasis. *Science* 280:1378–1383.
- Yin HH (2013) Restoring Purpose in Behavior. In: *Computational and Robotic Models of the Hierarchical Organization of Behavior* (Baldassarre G, Mirolli M, eds), pp 319–347. Springer Berlin Heidelberg. Available at: [http://link.springer.com/chapter/10.1007/978-3-642-39875-9\\_14](http://link.springer.com/chapter/10.1007/978-3-642-39875-9_14) [Accessed July 2, 2015].

- Yin HH (2014a) Action, time and the basal ganglia. *Philosophical Transactions of the Royal Society of London B: Biological Sciences* 369:20120473.
- Yin HH (2014b) How Basal Ganglia Outputs Generate Behavior. *Advances in Neuroscience* 2014:e768313.
- Zelenin PV, Grillner S, Orlovsky GN, Deliagina TG (2001) Heterogeneity of the population of command neurons in the lamprey. *J Neurosci* 21:7793–7803.
- Zelenin PV, Orlovsky GN, Deliagina TG (2007) Sensory-Motor Transformation by Individual Command Neurons. *Journal of Neuroscience* 27:1024–1032.
- Zhou F-M (2010) A transient receptor potential channel regulates basal ganglia output. *Rev Neurosci* 21:95–118.
- Zhou F-M, Lee CR (2011) Intrinsic and integrative properties of substantia nigra pars reticulata neurons. *Neuroscience* 198:69–94.
- Zink CF, Pagnoni G, Martin ME, Dhamala M, Berns GS (2003) Human striatal response to salient nonrewarding stimuli. *J Neurosci* 23:8092–8097.
- Zink CF, Tong Y, Chen Q, Bassett DS, Stein JL, Meyer-Lindenberg A (2008) Know your place: neural processing of social hierarchy in humans. *Neuron* 58:273–283.

## Biography

Joseph William Barter was born on November, 8, 1985 in Bar Harbor, Maine. He attended Macalester College in Saint Paul, Minnesota where he graduated in 2008 with majors in Biology and Neuroscience Studies. He attended Duke University in Durham, NC, USA and received his Doctor of Philosophy in Psychology and Neuroscience in December 2015. During his time at Duke he was a National Science Foundation Graduate Research Fellow. While at Duke, he published the following articles:

Barter JW, Castro S, Sukharnikova T, Rossi MA, Yin HH (2014) The role of the substantia nigra in posture control. *Eur J Neurosci* 39:1465–1473.

Barter JW, Li S, Lu D, Bartholomew RA, Rossi MA, Shoemaker CT, Salas-Meza D, Gaidis E, Yin HH (2015a) Beyond reward prediction errors: the role of dopamine in movement kinematics. *Front Integr Neurosci* 9

Barter JW, Li S, Sukharnikova T, Rossi MA, Bartholomew RA, Yin HH (2015b) Basal ganglia outputs map instantaneous position coordinates during behavior. *J Neurosci* 35:2703–2716.